Journal
of
The Franklin Institute
Devoted to Science and the Mechanic Arts

Vol. 271 APRIL, 1961 No. 4

STATISTICAL DESIGN OF LINEAR DISCRETE-DATA CONTROL SYSTEMS VIA THE MODIFIED z-TRANSFORM METHOD*

BY

JULIUS T. TOU[1]

ABSTRACT

A solution is presented for the analytical design of digital controller in accordance with a specified optimum criterion. This approach makes use of the modified z-transform technique. The analytical design procedure for systems with random noise occurring in the input channel and for those with random noise occurring at a point in the control loop is developed via modified z-transformation. Much attention is centered upon stationary random functions because of their frequent occurrence in control systems and their being amenable to mathematical treatment. In this paper, physical realizability and system constraints are considered, general design equations for both cases of noise occurrence are derived, and systems with deterministic inputs are discussed.

Linear discrete-data control theory has been the subject of considerable interest (1–3).[2] Various methods of analysis and synthesis have been developed. Among the most commonly used techniques are the z-transform method (4) and the modified z-transform method (5). More recently, the discrete-data control problems have been analyzed by the state-transition method (6–9). With the exception of several papers (10–15), most of the work published in the literature (16) is concerned primarily with the design of control systems based upon deterministic inputs. Systems are usually designed to have optimum or satisfactory performance in response to a test input.

However, in common practice the particular form of the inputs to a control system is not known analytically. In fact, the inputs can generally be described only statistically. Thus, optimum synthesis of

* The work reported here was supported in part by the Office of Naval Research under Contract Nonr-1100(18), through the Information Systems Branch.

[1] Control and Information Systems Laboratory, School of Electrical Engineering, Purdue University, Lafayette, Ind.

[2] The boldface numbers in parentheses refer to the references appended to this paper.

(Note—The Franklin Institute is not responsible for the statements and opinions advanced by contributors in the JOURNAL.)

control systems often necessitates a statistical approach. During the past few years, several procedures for the optimum design of linear discrete-data control systems subjected to stochastic inputs have been proposed (10–15). However, all of them have limited their discussion to linear systems with random noise occurring in the input channel only. Little attention has been paid to discrete-data systems with random noise or disturbance occurring at other points of the control loop than in the input channel.

GENERAL SYNTHESIS PRINCIPLES

Shown in Fig. 1 is the block diagram of a basic discrete-data feedback control system, which is to be optimized in the sense of minimum

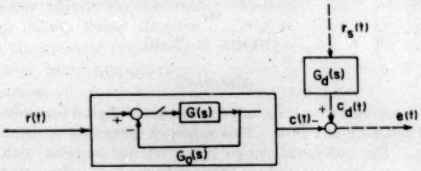

FIG. 1.

mean-square error. The input signal and noise are assumed to be functions of stationary random processes. The system error is measured by the difference between the desired output $c_d(t)$ and the actual output $c(t)$; that is,

$$e(t) = c_d(t) - c(t). \tag{1}$$

The sampled values of the system output and error are related by

$$e(nT, m) = c_d(nT, m) - c(nT, m), \tag{2}$$

where n is an integer and m lies between 0 and 1. It can readily be shown that the mean-square error $\overline{e^2(t)}$ is related to the mean-square value of error samples by the following integral (1)

$$\overline{e^2(t)} = \int_0^1 \overline{e^2(nT, m)}dm. \tag{3}$$

When the minimization of mean-square error is chosen as the performance criterion, the design of linear discrete-data control systems is usually initiated with the description of the signals by correlation sequences and pulse-spectral densities (1). It has been shown that for a given value of m, the mean-square value of error samples can be evaluated from

$$\overline{e^2(nT, m)} = \frac{1}{2\pi j}\oint_\Gamma \phi_{ee}(z, m)z^{-1}dz, \tag{4}$$

where the contour Γ is the unit circle of the z plane, and $\phi_{ee}(z, m)$ is the z transform associated with the autocorrelation sequence for $e(nT, m)$. With the complex variable z replaced by $e^{j\omega T}$, $\phi_{ee}(z, m)$ becomes a function of frequency, and it may be referred to as the *modified pulse-spectral density* for the error signal (15).

Combining Eqs. 3 and 4 yields

$$\overline{e^2(t)} = \frac{1}{2\pi j} \oint_\Gamma \left[\int_0^1 \phi_{ee}(z, m) dm \right] z^{-1} dz. \tag{5}$$

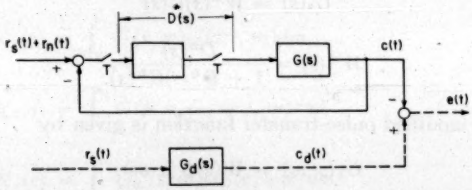

FIG. 2.

The system is said to be optimum if the mean-square error is minimum. Then the design objective is to determine the transfer function of a pulsed-data compensator for the system so that the mean-square error given by the above equation is reduced to a minimum. The *modified pulse-spectral density* $\phi_{ee}(z, m)$ can readily be determined in terms of the pulse-spectral densities for the input signals and noise, and the modified z-transform associated with the transfer function of the system, if certain properties of correlation sequences and pulse-spectral densities are utilized. Once the expression for $\phi_{ee}(z, m)$ is so determined, the minimization process can be carried out by applying the calculus of variations (17, 18) to the integral given in Eq. 5. Thus, the general synthesis procedure involves three major steps: (1) determination of $\phi_{ee}(z, m)$, (2) application of the calculus of variations to the integral of Eq. 5; and (3) evaluation of the pulse-transfer function of the optimum compensator. Based upon this general procedure, the optimum synthesis of linear discrete-data control systems via the modified z-transform method is carried out in the following sections.

SYSTEMS WITH NOISE IN THE INPUT CHANNEL

Referring to Fig. 2, $G(s)$ is the transfer function of the continuous data portion of the system, $D^*(s)$ is the transfer function of the pulsed-data compensator, and $G_d(s)$ is the desired system transfer function. The input and output of this linear discrete-data control system are assumed to be $r(t) = r_s(t) + r_n(t)$ and $c(t) = c_s(t) + c_n(t)$, respectively, and the desired output signal is $c_d(t)$. These signals are assumed to be stationary random functions.

It can be shown that $\phi_{ee}(z, m)$ is given by (15)

$$\phi_{ee}(z, m) = \phi_{c_dc_d}(z, m) + \phi_{c_sc_s}(z, m) + \phi_{c_nc_n}(z, m) + \phi_{c_sc_n}(z, m) + \phi_{c_nc_s}(z, m) - \phi_{c_dc_s}(z, m) - \phi_{c_sc_d}(z, m) - \phi_{c_dc_n}(z, m) - \phi_{c_nc_d}(z, m). \quad (6)$$

Assume that the over-all modified pulse-transfer function of the discrete-data feedback control system be $G_0(z, m)$. Since, from Fig. 2,

$$G_0(s) = W^*(s)G(s) \quad (7)$$

where

$$W^*(s) = \frac{D^*(s)}{1 + D^*(s)G^*(s)} \quad (8)$$

the over-all modified pulse-transfer function is given by

$$G_0(z, m) = W(z)G(z, m). \quad (9)$$

The block diagram of Fig. 2 is redrawn as shown in Fig. 3, with the feedback system represented by its open-loop equivalent and the desired transfer function $G_d(s)$ preceded by a sampler and an ideal desampler. In order for the signal input to $G_d(s)$ to have the same statistical properties, it can be shown that the transfer function $H_s(s)$ of the ideal desampler is given by

$$H_s(s) = \frac{\phi_{r_sr_s}(s)}{\phi_{r_sr_s}{}^*(s)}. \quad (10)$$

This artifice greatly simplifies the system synthesis.

Making use of the properties of pulse-spectral densities (15) reduces Eq. (6) to

$$\begin{aligned}\phi_{ee}(z, m) = {} & [W(z)W(z^{-1})G(z, m)G(z^{-1}, m) \\ & - W(z)G(z, m)G_d'(z^{-1}, m) \\ & - W(z^{-1})G(z^{-1}, m)G_d'(z, m) \\ & - G_d'(z, m)G_d'(z^{-1}, m)]\phi_{r_sr_s}(z) \\ & + [W(z)W(z^{-1})G(z, m)G(z^{-1}, m) \\ & - W(z)G(z, m)G_d'(z^{-1}, m)]\phi_{r_sr_n}(z) \\ & + [W(z)W(z^{-1})G(z, m)G(z^{-1}, m) \\ & - W(z^{-1})G(z^{-1}, m)G_d'(z, m)]\phi_{r_nr_s}(z) \\ & + W(z)W(z^{-1})G(z, m)G(z^{-1}, m)\phi_{r_nr_n}(z), \end{aligned} \quad (11)$$

where $G_d'(z, m)$ is the modified z-transform associated with $G_d'(s) = H_s(s)G_d(s)$; and $\phi_{r_sr_s}(z)$, $\phi_{r_nr_n}(z)$, $\phi_{r_sr_n}$ and $\phi_{r_nr_s}(z)$ denote the pulse-

spectral densities and the cross pulse-spectral densities for the input signal $r_s(t)$ and the input noise $r_n(t)$. Then

$$\begin{aligned}\int_0^1 \phi_{ee}(z, m)dm = {} & W(z)W(z^{-1})K_1(z)\phi_{rr}(z) \\ & - W(z)K_2(z)[\phi_{r_s r_s}(z) + \phi_{r_s r_n}(z)] \\ & - W(z^{-1})K_2(z^{-1})[\phi_{r_s r_s}(z) + \phi_{r_n r_s}(z)] \\ & + K_3(z)\phi_{r_s r_s}(z) \qquad (12)\end{aligned}$$

in which

$$K_1(z) = \int_0^1 G(z, m)G(z^{-1}, m)dm \qquad (13)$$

$$K_2(z) = \int_0^1 G(z, m)G_d'(z^{-1}, m)dm \qquad (14)$$

$$K_3(z) = \int_0^1 G_d'(z, m)G_d'(z^{-1}, m)dm \qquad (15)$$

$$\phi_{rr}(z) = \phi_{r_s r_s}(z) + \phi_{r_n r_n}(z) + \phi_{r_s r_n}(z) + \phi_{r_n r_s}(z). \qquad (16)$$

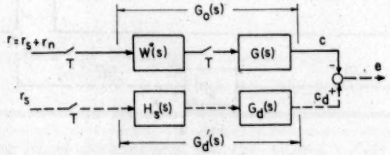

FIG. 3.

Application of the calculus of variations to the integral of Eq. 5 with the integrand given in Eq. 11 yields the optimum pulse-transfer function

$$W(z) = \frac{\left\{\dfrac{K_2(z^{-1})[\phi_{r_s r_s}(z) + \phi_{r_n r_s}(z)]}{K_1^-(z)\phi_{rr}^-(z)}\right\}_+}{K_1^+(z)\phi_{rr}^+(z)}. \qquad (17)$$

The derivation of Eq. 17 is presented in Appendix I.

When the pulse-transfer function $W(z)$ of the optimum system is determined, the pulse-transfer function of the required compensator $D(z)$ can readily be derived from Eq. 18.

$$D(z) = \frac{W(z)}{1 - G(z)W(z)} = \frac{W(z)}{1 - G_0(z)}. \qquad (18)$$

The above discussions reveal that the determination of $W(z)$ and $D(z)$ simply involves the evaluation of z-transforms and modified z-transforms, ordinary integration and simple algebraic manipulations. Consequently, by using the results derived above, optimum design of discrete-data control systems with noise in the input channel can be done systematically in a simple manner.

SYSTEMS WITH NOISE IN THE CONTROL LOOP

Quite frequently random noise or disturbance occurs in the controlled system or process. The optimum design theory fails to be conclusive, if this problem is not studied. As far as the author has been able to determine, the statistical design of linear discrete-data feedback systems with noise or disturbance occurring in the control loop has not been extensively studied in the literature. This section attempts to present a solution to this design problem.

In the basic linear discrete-data feedback control system shown in Fig. 4, the random noise or disturbance $n(t)$ is assumed to occur at a

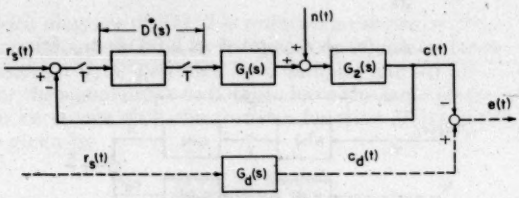

FIG. 4.

point in the control loop. The input signal is $r_s(t)$ and the output of this system in the presence of the noise $n(t)$ is $c(t) = c_s(t) + c_n(t)$. The system error is then given by

$$e(t) = c_d(t) - c_s(t) - c_n(t), \tag{19}$$

where $c_d(t)$ is the desired output signal. In terms of the error samples,

$$e(nT, m) = c_d(nT, m) - c_s(nT, m) - c_n(nT, m). \tag{20}$$

Case I

If the input signal $r_s(t)$ and the noise $n(t)$ are uncorrelated, the mean-square value of the error samples is equal to

$$\overline{e^2(nT, m)} = \overline{e_d^2(nT, m)} + \overline{c_s^2(nT, m)} + \overline{c_n^2(nT, m)} - \overline{c_s(nT, m)c_d(nT, m)} - \overline{c_d(nT, m)c_s(nT, m)}. \tag{21}$$

The mean-square value of the error samples may be written as (1)

$$\overline{e^2(nT, m)} = \frac{1}{2\pi j} \oint_\Gamma \phi_{ee}(z, m) z^{-1} dz \tag{22}$$

where

$$\phi_{ee}(z, m) = \phi_{c_d c_d}(z, m) + \phi_{c_s c_s}(z, m) + \phi_{c_n c_n}(z, m) - \phi_{c_s c_d}(z, m) - \phi_{c_d c_s}(z, m). \tag{23}$$

To simplify the evaluation of $\phi_{ee}(z, m)$, the block diagram of Fig. 4 is redrawn as shown in Fig. 5, where $H_s(s)$ and $H_n(s)$ are the transfer

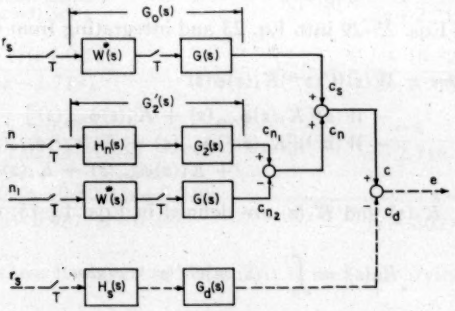

FIG. 5.

functions of the ideal desamplers for the signal $r_s^*(t)$ and the noise $n^*(t)$. The transfer function $H_s(s)$ is given in Eq. 10, and it can be shown that the transfer function $H_n(s)$ is

$$H_n(s) = \frac{\phi_{nn}(s)}{\phi_{nn}^*(s)}. \tag{24}$$

Making use of the properties of pulse-spectral densities (15), one readily derives the *modified pulse-spectral densities* given in the right-hand side of Eq. 23. They are found to be

$$\phi_{c_s c_s}(z, m) = W(z)W(z^{-1})G(z, m)G(z^{-1}, m)\phi_{r_s r_s}(z) \tag{25}$$

$$\phi_{c_d c_d}(z, m) = G_d'(z, m)G_d'(z^{-1}, m)\phi_{r_s r_s}(z) \tag{26}$$

$$\phi_{c_s c_d}(z, m) = W(z^{-1}, m)G(z^{-1}, m)G_d'(z, m)\phi_{r_s r_s}(z) \tag{27}$$

$$\phi_{c_d c_s}(z, m) = W(z, m)G(z, m)G_d'(z^{-1}, m)\phi_{r_s r_s}(z) \tag{28}$$

$$\phi_{c_nc_n}(z, m) = W(z)W(z^{-1})G(z, m)G(z^{-1}, m)\phi_{n_1n_1}(z) - W(z)G(z, m)G_2'(z^{-1}, m)\phi_{nn_1}(z) - W(z^{-1})G(z^{-1}, m)G_2'(z, m)\phi_{n_1n}(z) + G_2'(z, m)G_2'(z^{-1}, m)\phi_{nn}(z). \quad (29)$$

In Eq. 29, $G_2'(z, m)$ is the modified z-transform associated with

$$G_2'(s) = H_n(s)G_2(s) \quad (30)$$

and

$$N_1(s) = C_{n_1}(s). \quad (31)$$

In Fig. 4,

$$G(s) = G_1(s)G_2(s). \quad (32)$$

Substituting Eqs. 25–29 into Eq. 23 and integrating from 0 to 1 yields

$$\int_0^1 \phi_{ee}(z, m)dm = W(z)W(z^{-1})K_1(z)\phi(z) - W(z)[K_3(z)\phi_{r_sr_s}(z) + K_4(z)\phi_{nn_1}(z)] - W(z^{-1})[K_2(z^{-1})\phi_{r_sr_s}(z) + K_4(z^{-1})\phi_{n_1n}(z)] + K_5(z)\phi_{r_sr_s}(z) + K_5(z)\phi_{nn}(z) \quad (33)$$

where $K_1(z)$, $K_2(z)$ and $K_3(z)$ are defined in Eqs. 13–15, respectively, and

$$K_4(z) = \int_0^1 G(z, m)G_2'(z^{-1}, m)dm \quad (34)$$

$$K_5(z) = \int_0^1 G_2'(z, m)G_2'(z^{-1}, m)dm \quad (35)$$

$$\phi(z) = \phi_{r_sr_s}(z) + \phi_{n_1n_1}(z). \quad (36)$$

Equation 33 resembles Eq. 12, and the system synthesis can be carried out in the same manner. Application of the calculus of variations to the integral of Eq. 5 with the integrand given in Eq. 33 yields the optimum pulse-transfer function as

$$W(z) = \frac{\left\{\dfrac{K_2(z^{-1})\phi_{r_sr_s}(z) + K_4(z^{-1})\phi_{n_1n}(z)}{K_1^-(z)\phi^-(z)}\right\}_+}{K_1^+(z)\phi^+(z)}. \quad (37)$$

As an illustration, consider the discrete-data feedback control system of Fig. 4. The sampling period is 0.1 second and $G_d(s) = 1$. The transfer functions of the system components are $G_1(s) = \dfrac{(1 - e^{-Ts})}{s}$ and $G_2(s) = \dfrac{10}{(s + 10)}$. The signal and the noise, which are uncorre-

lated, have the spectral densities given by $\phi_{r_s r_s}(\omega) = \dfrac{4}{(0.04 + \omega^2)}$ and $\phi_{nn}(\omega) = 0.1$, respectively. Determine the transfer function of the pulsed-data controller for minimizing the mean-square error.

To follow the above procedure, the design is initiated with the determination of the z-transforms associated with $\phi_{r_s r_s}(s)$, $\phi_{n_1 n_1}(s)$ and $\phi_{n_1 n}(s)$, and the modified transforms associated with $G(s)$, $G_2'(s)$ and $G_d'(s)$. Then $K_1(z)$, $K_2(z^{-1})$ and $K_4(z^{-1})$ are evaluated from Eqs. 13, 14 and 34. It is found that

$$K_1^+(z) = \frac{-0.35(z-0.67)}{(z-0.368)} \qquad K_1^-(z) = \frac{z+8.52}{z(z+2.718)}$$

$$K_2(z^{-1}) = \frac{(z-1)(z+0.75)}{z(z-2.718)} \qquad K_4(z^{-1}) = \frac{-16.32(z-1.66)}{(z-2.718)(z-0.368)}$$

$$\phi_{r_s r_s}(z) = \frac{-0.4z}{(z-1.02)(z-0.98)} \qquad \phi_{n_1 n}(z) = \frac{-z}{z-2.718}$$

$$\phi^+(z) = \frac{-10z(z-0.809)(z+0.049)}{(z-0.987)(z-0.368)} \qquad \phi^-(z) = \frac{z-1.2}{(z-1.02)(z-2.718)}$$

Substituting these functions of z into Eq. 37 and simplifying yields

$$W(z) = \frac{0.02(z + 0.758)(z - 0.368)}{z(z - 0.67)(z - 0.809)(z - 0.049)}.$$

Then, from Eq. 18, the transfer function of the desired pulsed-data controller is determined:

$$D(z) = \frac{0.02(z^2 + 0.39z - 0.279)}{z^4 - 1.53z^3 + 0.615z^2 - 0.039z + 0.01}.$$

Case II

If the input signal $r_s(t)$ and the noise $n(t)$ are correlated, the mean-square value of the error sample is equal to

$$\begin{aligned}\overline{e^2(nT, m)} = {} & \overline{e_d^2(nT, m)} + \overline{c_s^2(nT, m)} + \overline{c_n^2(nT, m)} \\ & - \overline{c_s(nT, m)c_d(nT, m)} - \overline{c_d(nT, m)c_s(nT, m)} \\ & - \overline{c_d(nT, m)c_n(nT, m)} - \overline{c_n(nT, m)c_d(nT, m)} \\ & + \overline{c_s(nT, m)c_n(nT, m)} + \overline{c_n(nT, m)c_s(nT, m)}. \qquad (38)\end{aligned}$$

Following the above argument it can readily be shown that

$$\begin{aligned}\int_0^1 \phi_{ee}(z, m)dm = {} & W(z)W(z^{-1})K_1(z)\phi_{rr}(z) \\ & + K_3(z)\phi_{r_2r_2}(z) + K_5(z)\phi_{nn}(z) \\ & + W(z)\{K_2(z)[\phi_{r_2r_2}(z) + \phi_{r_2n_1}(z)] \\ & + K_4(z)[\phi_{nr_2}(z) + \phi_{nn_1}(z)]\} \\ & + W(z^{-1})\{K_2(z^{-1})[\phi_{r_2r_2}(z) + \phi_{n_1n_2}(z)] \\ & + K_4(z^{-1})[\phi_{r_2n}(z) + \phi_{n_1n}(z)]\} \\ & - K_6(z)\phi_{nr_2}(z) - K_6(z^{-1})\phi_{r_2n}(z), \end{aligned} \quad (39)$$

in which $K_1(z)$, $K_2(z)$, $K_3(z)$, $K_4(z)$ and $K_5(z)$ are defined in Eqs. 13–15 and 34, 35; and

$$K_6(z) = \int_0^1 G_d'(z, m)G_2'(z^{-1}, m)dm \quad (40)$$

$$\phi_{rr}(z) = \phi_{r_2r_2}(z) + \phi_{n_1n_1}(z) - \phi_{r_2n_1}(z) - \phi_{n_1r_2}(z). \quad (41)$$

$\phi_{n_1n_1}(z)$, $\phi_{r_2n_1}(z)$ and $\phi_{n_1n_2}(z)$ are the z-transforms associated with $G(s)G(-s)\phi_{nn}(s)$, $G_2(s)\phi_{r_2n}(s)$ and $G_2(-s)\phi_{nr_2}(s)$, respectively.

The optimum pulse-transfer function can readily be derived by applying the calculus of variations to the integral of Eq. 5 with the integrand given in Eq. 39. Thus,

$$W(z) = \frac{\left\{\dfrac{K_2(z^{-1})[\phi_{r_2r_2}(z) + \phi_{n_1r_2}(z)] + K_4(z^{-1})[\phi_{r_2n}(z) + \phi_{n_1n}(z)]}{K_1^-(z)\phi^-(z)}\right\}_+}{K_1^+(z)\phi^+(z)}. \quad (42)$$

Once the pulse-transfer function $W(z)$ is determined, the transfer function of the required pulsed-data compensator $D(z)$ follows from Eq. 18. Application of the design equations derived above, indeed, makes the optimum synthesis of linear discrete-data feedback control systems with noise in the control loop an easy task, since the synthesis involves only such straightforward operations as z-transformation, simple integration and algebraic manipulation.

SYSTEMS WITH DETERMINISTIC INPUTS

Up to this point discussions are centered upon the optimum synthesis of linear discrete-data control systems which are subjected to stochastic inputs. However, the modified z-transform technique can also be applied to the synthesis of linear discrete-data control systems for optimum transient response. The commonly used performance criterion for the optimum design of control systems with deterministic inputs is the minimization of integral-square error. The design of discrete-data control systems for minimum integral-square error may be

carried out in close parallel with the design of continuous-data control systems to meet the same criterion, if use is made of the modified z-transform technique and the following theorem.

Theorem: If $e(t) = c_d(t) - c(t)$ *represents the error of a discrete-data control system, and* $E(z, m)$ *is the modified z transform of* $e(t)$, *then the integral-square error is given by*

$$\int^{\infty} e^2(t)dt = \frac{1}{2\pi j} \oint_{\Gamma} \left[T \int_0^1 E(z, m)E(z^{-1}, m)dm \right] z^{-1}dz, \quad (43)$$

where the contour Γ *is the unit circle of the z plane, and* T *is the sampling period.*

It is interesting to note that the above expression for the integral-square error resembles the well-known Parseval's Theorem, which is of fundamental importance in control-system design for optimum transient response. The proof of the expression given in Eq. 43 is presented in Appendix II. In view of the resemblance of this theorem to Parseval's Theorem, the procedure for the optimum synthesis of continuous-data control systems for minimum integral-square error may be readily extended to the optimum synthesis of discrete-data control systems via modified z transformation.

CONCLUSION

This paper presents the optimum synthesis of linear discrete-data feedback control systems via the modified z-transform method. The system performance is optimized in the sense of minimum mean-square error. The system inputs are assumed to be functions of stationary random processes. A general synthesis procedure is introduced. Both the design of systems with noise occurring in the input channel and that of systems with noise occurring in the control loop are discussed. This leads to the derivation of the design equation for each case. Application of these design equations reduces the optimum synthesis to an easy task, since the design equations involve only straightforward operations of z-transformation, simple integration and algebraic manipulation. In fact, through modified z-transformation, the statistical design of linear discrete-data systems is made no more difficult than the statistical design of linear continuous-data systems. Although only error-sampled systems are considered here, the techniques presented in this paper can readily be extended to discrete-data control systems of other configurations. Furthermore, the design principles described above together with the Lagrange-multiplier method can be applied to the optimum synthesis of linear discrete-data feedback control systems subjected to such practical constraints as saturation and power limitation. Finally, a theorem is introduced which facilitates the ex-

tension of the procedures for optimum design of continuous-data control systems for mimimum integral-square error to the optimum synthesis of discrete-data control systems.

APPENDIX I

Determination of W(z) *given in Eq. 17*

The minimization problem can readily be solved by applying the calculus of variations to the integral of Eq. 5 with the integrand given in Eq. 12. The condition for minimizing the mean-square error is determined by giving the pulse-transfer function $W(z)$ a small variation $\lambda\eta(z)$ and the pulse-transfer function $W(z^{-1})$ a small variation $\lambda\eta(z^{-1})$, where $\eta(z)$ is an arbitrary function of z, and λ is a parameter. A small variation in $W(z)$ will cause the mean-square error $\overline{e^2(t)}$ to undergo a variation $\delta\overline{e^2(t)}$. Replacing $W(z)$ by its neighboring function $W(z) + \lambda\eta(z)$ and $W(z^{-1})$ by its neighboring function $W(z^{-1}) + \lambda\eta(z^{-1})$, the mean-square error becomes $\overline{e^2(t)} + \delta\overline{e^2(t)}$. Then $\overline{e^2(t)}$ is a minimum, if

$$\left.\frac{d[\overline{e^2(t)} + \delta\overline{e^2(t)}]}{d\lambda}\right|_{\lambda=0} = 0. \tag{44}$$

Carrying out the operations involved in Eq. 44 and simplifying leads to

$$\frac{1}{2\pi j}\oint_\Gamma \eta(z^{-1})\{W(z)K_1(z)\phi_{rr}(z) - K_2(z^{-1})[\phi_{r_2r_2}(z) + \phi_{r_1r_2}(z)]\}z^{-1}dz$$

$$+ \frac{1}{2\pi j}\oint_\Gamma \eta(z)\{W(z^{-1})K_1(z)\phi_{rr}(z) - K_2(z)[\phi_{r_2r_2}(z) + \phi_{r_2r_1}(z)]\}z^{-1}dz = 0. \tag{45}$$

To determine the optimum $W(z)$, the z-transforms $K_1(z)$ and $\phi_{rr}(z)$ are factored into two parts (17, 18)

$$K_1(z) = K_1^+(z)K_1^-(z) \tag{46}$$

and

$$\phi_{rr}(z) = \phi_{rr}^+(z)\phi_{rr}^-(z). \tag{47}$$

The plus part contains zeros and poles inside the unit circle, and the minus part contains zeros and poles outside the unit circle. By doing so, Eq. 45 may be written as

$$\frac{1}{2\pi j}\oint_\Gamma \eta(z)K_1^+(z)\phi_{rr}^+(z)\left\{W(z)K_1^+(z)\phi_{rr}^+(z) - \frac{K_2(z^{-1})[\phi_{r_2r_2}(z)+\phi_{r_1r_2}(z)]}{K_1^-(z)\phi_{rr}^-(z)}\right\}z^{-1}dz$$

$$+\frac{1}{2\pi j}\oint_\Gamma \eta(z)K_1^+(z)\phi_{rr}^+(z)\left\{W(z^{-1})K_1^-(z)\phi_{rr}^-(z) - \frac{K_2(z)[\phi_{r_2r_2}(z)+\phi_{r_2r_1}(z)]}{K_1^+(z)\phi_{rr}^+(z)}\right\}z^{-1}dz = 0. \tag{48}$$

Since for physical realizability and stability $W(z)$ and $\eta(z)$ can have no pole outside the unit circle, and $W(z^{-1})$ and $\eta(z^{-1})$ can have no pole inside the unit circle, the function $\eta(z)K_1^+(z)\phi_{rr}^+(z)$ contains poles inside the unit circle only and the function $\eta(z^{-1})K_1^-(z)\phi_{rr}^-(z)$ contains poles outside the unit circle only. Equation 48 then reduces to

$$\frac{1}{2\pi j}\oint_\Gamma \eta(z^{-1})K_1^-(z)\phi_{rr}^-(z)\left[W(z)K_1^+(z)\phi_{rr}^+(z) - \left\{\frac{K_2(z^{-1})[\phi_{r_2r_2}(z)+\phi_{r_1r_2}(z)]}{K_1^-(z)\phi_{rr}^-(z)}\right\}_+\right]z^{-1}dz$$

$$+\frac{1}{2\pi j}\oint_\Gamma \eta(z)K_1^+(z)\phi_{rr}^+(z)\left[W(z^{-1})K_1^-(z)\phi_{rr}^-(z) - \left\{\frac{K_2(z)[\phi_{r_2r_2}(z)+\phi_{r_2r_1}(z)]}{K_1^+(z)\phi_{rr}^+(z)}\right\}_-\right]z^{-1}dz = 0. \tag{49}$$

In the above equation, the term of $\{\ \}_+$ denotes the part of $\{\ \}$ with poles inside the unit circle, and the term of $\{\ \}_-$ denotes the other part of $\{\ \}$ with poles outside the unit circle. That is,

$$\frac{K_2(z^{-1})[\phi_{r_0r_0}(z) + \phi_{r_0r_0}(z)]}{K_1^-(z)\phi_{rr}^-(z)} = \left\{\frac{K_2(z^{-1})[\phi_{r_0r_0}(z) + \phi_{r_0r_0}(z)]}{K_1^-(z)\phi_{rr}^-(z)}\right\}_+ + \left\{\frac{K_2(z^{-1})[\phi_{r_0r_0}(z) + \phi_{r_0r_0}(z)]}{K_1^-(z)\phi_{rr}^-(z)}\right\}_- \quad (50)$$

If $W(z)$ is the optimum pulse-transfer function in the sense of minimum mean-square error, Eq. 49 must be fulfilled for an arbitrary $\eta(z)$. Consequently, the optimum $W(z)$ is given by Eq. 17.

APPENDIX II

Proof of the Theorem

Since the area under the curve of $e^2(t)$ for $(n-1)T \leq t \leq nT$ can be determined from

$$T\int_0^1 e^2(nT, m)dm, \quad (51)$$

the total area under the curve of $e^2(t)$ for $t \geq 0$ is then equal to

$$T\sum_{n=1}^{\infty}\int_0^1 e^2(nT, m)dm. \quad (52)$$

Thus,

$$\int_0^{\infty} e^2(t)dt = \int_0^1 \sum_{n=1}^{\infty} e^2(nT, m)dm. \quad (53)$$

It is noted that, by definition,

$$e(nT, m) = e(\overline{n-1}\,T + mT). \quad (54)$$

From the inversion integral

$$e(nT, m) = \frac{1}{2\pi j}\oint_\Gamma E(z, m)z^{n-1}dz. \quad (55)$$

Then

$$\sum_{n=1}^{\infty} e^2(nT, m) = \sum_{n=1}^{\infty} e(nT, m)\frac{1}{2\pi j}\oint_\Gamma E(z, m)z^{n-1}dz$$

$$= \frac{1}{2\pi j}\oint_\Gamma E(z, m)[\sum_{n=1}^{\infty} e(nT, m)z^n]z^{-1}dz$$

$$= \frac{1}{2\pi j}\oint_\Gamma E(z, m)E(z^{-1}, m)z^{-1}dz. \quad (56)$$

Hence

$$\int_0^{\infty} e^2(t)dt = \frac{1}{2\pi j}\oint_\Gamma [T\int_0^1 E(z, m)E(z^{-1}, m)dm]z^{-1}dz. \quad (57)$$

REFERENCES

(1) JULIUS T. TOU, "Digital and Sampled-Data Control Systems," New York, McGraw-Hill Book Co., Inc., 1959.
(2) JOHN R. RAGAZZINE AND GENE F. FRANKLIN, "Sampled-Data Control Systems," New York, McGraw-Hill Book Co., Inc., 1958.
(3) ELIAHU I. JURY, "Sampled-Data Control Systems," New York, John Wiley & Sons, Inc., 1958.
(4) J. R. RAGAZZINI AND L. A. ZADEH, "The Analysis of Sampled-Data Systems," *AIEE Trans.*, Vol. 71, pt. II, pp. 225–234 (1952).
(5) R. H. BARKER, "The Pulse Transfer Function and Its Application to Sampling Servo Systems," *IRE Proc.*, Vol. 99, pt. IV, pp. 302–317 (1952).
(6) R. E. KALMAN AND J. E. BERTRAM, "General Synthesis Procedure for Computer Control of Single-loop and Multiloop Linear System," *AIEE Trans.*, Vol. 78, pt. II, pp. 602–609 (1959).
(7) E. O. GILBERT, "A Method for the Symbolic Representation and Analysis of Linear Periodic Feedback Systems," *Ibid.*, Vol. 79, Pt. II, pp. 512–523 (1960).
(8) R. E. KALMAN AND J. E. BERTRAM, "A Unified Approach to the Theory of Sampling Systems," JOUR. FRANKLIN INST., Vol. 267, pp. 405–436 (1959).
(9) J. T. TOU AND B. VADHANAPHUTI, "Optimum Control of Nonlinear Discrete-Data Systems," *AIEE TP* 61–76, *AIEE Trans.*, Vol. 80, pt. II, March, 1961.
(10) G. FRANKLIN, "Linear Filtering of Sampled-Data," *IRE Convention Record*, pt. 4, pp. 119–128 (1955).
(11) R. M. STEWART, "Statistical Design and Evaluation of Filters for the Restoration of Sampled Data," *IRE Proc.*, Vol. 44, pp. 253–257 (1956).
(12) M. MORI, "Statistical Treatment of Sampled-Data Control Systems for Actual Random Inputs," *ASME Trans.*, Vol. 80, pp. 444–456 (1958).
(13) A. S. ROBINSON, "The Synthesis of Computer-limited Sampled-Data Control Systems," *AIEE Special Publication T-101*, May, 1958, pp. 77–87.
(14) S. S. L. Chang, "Statistical Design Theory for Digital-Controlled Continuous Systems," *AIEE Trans.*, Vol. 77, pt. II, pp. 191–201 (1958).
(15) J. T. TOU, "Statistical Design of Digital Control Systems," *IRE Trans. on Automatic Control*, Vol. AC-5, No. 4, pp. 290–297 (1960).
(16) T. F. HIGGINS AND R. W. GREER, "Classified Bibliography on Feedback Control Systems, Pt. I, Sampled-Data Systems," *AIEE paper* 58–1269.
(17) H. S. TSIEN, "Engineering Cybernetics," New York, McGraw-Hill Book Co., Inc., 1954.
(18) N. WIENER, "Extrapolation, Interpolation, and Smoothing of Stationary Time Series," New York, John Wiley & Sons, Inc., 1949.

A FREE BOUNDARY PROBLEM FOR THE WAVE EQUATION

BY

WILLARD L. MIRANKER[1]

SUMMARY

In this paper we discuss the motion of a frictionless piston contained in a tube which is filled with a hydraulic fluid. The fluid is assumed to be inviscid but compressible. The mathematical problem is that of solving the wave equation in a domain with an a priori unknown boundary (the piston trajectory). The methods for solving the problem amount essentially to a wave tracing technique. The report is concluded with some numerical results and a comparison of these results with an entirely linear analysis of the same problem.

1. INTRODUCTION

In this paper we will consider a free boundary problem for the wave equation. This problem arises as a model of the motion of a piston in a compressible fluid. Free boundary problems for the heat equation and Laplace's equation have been extensively studied in the recent literature (1, 2, 3, 4).[2] However, with the exception of (5), a paper by J. Keller and I. Kolodner which deals with explosion bubbles in a compressible fluid, free boundary problems for the wave equation appear not to have received much mathematical attention.

The physical model which we have in mind is a tube containing a free piston and filled with a compressible inviscid fluid at rest. At $t = 0$, pressures are introduced at the ends of the tube which cause the piston to move. This situation is described by the wave equation in the fluid density variation. The piston trajectory is an undetermined interface (the free boundary) interior to the domain of definition of the solution of the wave equation.

The object of this paper is to solve this free boundary problem and determine the piston trajectory. A typical approach to problems of this type is to assume that the motion of the free boundary is small so that it may be set equal to some mean value at the same time neglecting one of the free boundary conditions. This is done in the study of water waves (see (6)). The resulting fixed boundary problem is then solved and a virtual motion for the free boundary is obtained by inserting this fixed boundary solution into the discarded free boundary condition. This analysis was carried through by H. Greenberg (7) for the present problem.

Our analysis on the other hand treats the full free boundary prob-

[1] International Business Machines Research Center, Yorktown Heights, N. Y.

[2] The boldface numbers in parentheses refer to the references appended to this paper.

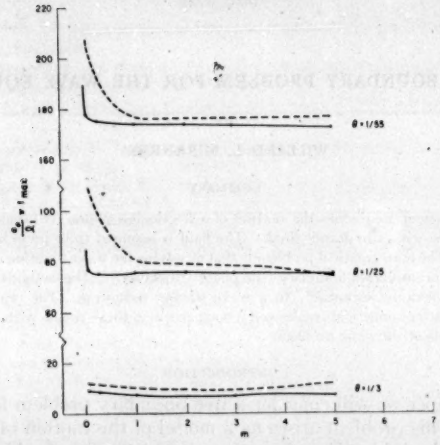

FIG. 1. Profile of $\pi t_{\max}$ *versus* m for three values of θ. Here $t_{\max}$ is the actual time it takes the piston to reach its maximum displacement, $\theta = l_1/(l_1 + l_2)$ and $m = \rho_0 l_1/M$. The remaining independent parameters ρ_1/ρ_2 and ρ_1/ρ_0 and a_0 were chosen to have the respective values of 1, 0.003, and 150,000.

lem. We show that this problem may be reduced to a difference-differential equation of motion for the piston trajectory which is valid piecewise in time. This equation is solved exactly for small time. The method used would enable one to obtain the solution explicitly for all time but is laborious and leads to involved formulae. For purposes of comparison with the results of the linearized analysis of Greenberg, the equations were instead integrated directly by a numerical integration procedure described below. The comparisons are shown in Figs. 1, 2, 3 over a range of the basic parameters of mass and geometry. In these figures the broken curves represent the results of the linear theory while the solid curves represent the results obtained here. We will now give a precise derivation and statement of our problem.

Let

$$x = \xi(t), \tag{1}$$

be the free boundary and let the tube have length $l_1 + l_2$. The time is designated by t and the piston is initially at $x = l_1$ in the tube (see Fig. 4).

Then the free boundary problem is

$$\rho_{xx} = \frac{1}{a_0^2}\rho_{tt}, \qquad t > 0, \qquad 0 < x < l_1 + l_2, \qquad x \neq \xi(t) \tag{2}$$

$$\rho(x, 0) = \rho_t(x, 0) = 0 \tag{3}$$

$$\left.\begin{aligned} &\rho(0, t) = \rho_1, \qquad \rho(l_1 + l_2, t) = \rho_2 && (4)\\ &[\rho] = -\frac{M}{a_0^2}\ddot{\xi}(t) && (5)\\ &\rho_x^+ = \rho_x^- = -\frac{\rho_0}{a_0^2}\ddot{\xi}(t) && (6) \end{aligned}\right\} \quad t > 0$$

$$\xi(0) = l_1, \qquad \dot{\xi}(0) = 0. \tag{7}$$

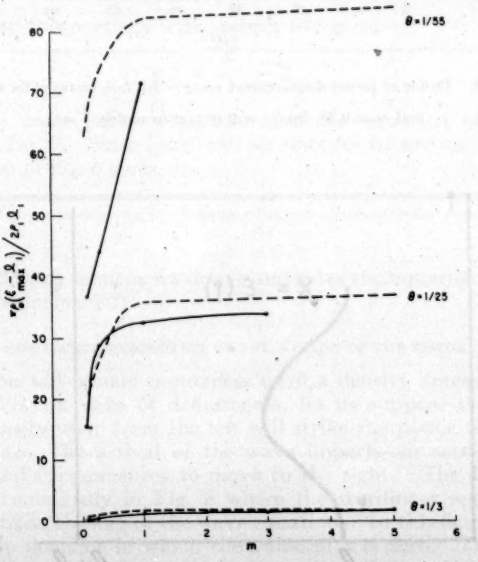

FIG. 2. With the same notation of Fig. 1, Fig. 2 represents a plot of $\pi\rho_0(\xi_{max} - l_1)/2\rho_1 l_1$ *versus* m for three values of θ. $\xi_{max} - l_1$ is the maximum deviation of the piston.

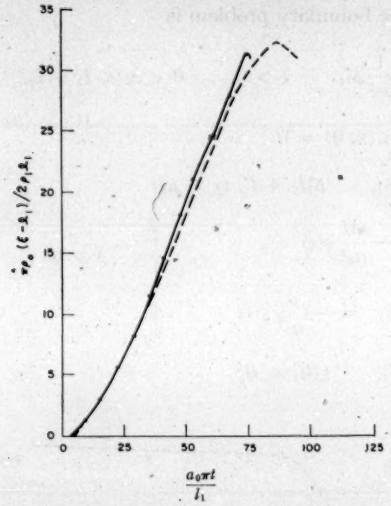

FIG. 3. Profile of piston displacement $\pi\rho_0(\xi - l_1)/2\rho_1 l_1$ *versus* πt for $\theta = 1/25$ and $m \doteq 0.25$, from $t = 0$ to approximately $\frac{a_0}{l_1}\pi t_{\max}$.

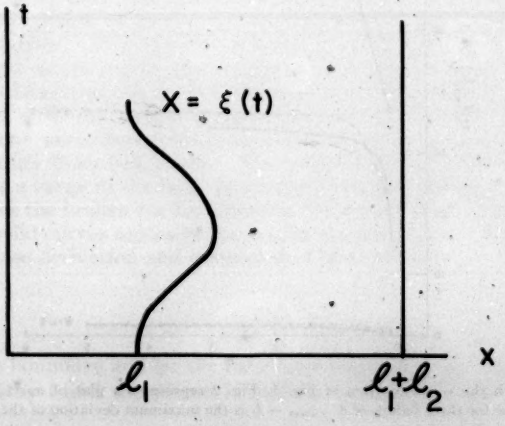

FIG. 4.

Here we have used the notation $[\rho] = \rho^+ - \rho^- = \rho(\xi(t)^+, t) - \rho(\xi(t)^-, t)$. $\rho(x, t)$ is the density of the fluid measured from the rest density ρ_0. $a_0^2 = \left.\frac{\partial P(\rho)}{\partial \rho}\right|_{\rho=0}$, is the sound speed where $p = P(\rho)$ is an equation of state. M is the mass per cross-sectional area of the piston which we have assumed to be a rigid body. $\rho_0 + \rho_1$ and $\rho_0 + \rho_2$ are the values of ρ maintained at the ends of the tube. Equation 2 comes from the equations of conservation of mass and linear momentum, while Eqs. 3 and 7 follow from the fact that initially the fluid is at rest. The free boundary conditions Eqs. 5 and 7 are obtained as follows: From Newton's law

$$M\ddot{\xi}(t) = p^- - p^+. \tag{8}$$

This and the equation of state give Eq. 5. Let $u(x, t)$ be the fluid velocity. Since the fluid in contact with the piston has the velocity of the piston we have

$$u^+ = u^- = \dot{\xi}. \tag{9}$$

Differentiating this partially with respect to t gives

$$u_t^+ = u_t^- = \ddot{\xi}. \tag{10}$$

Applying the conservation equations and the equation of state to Eq. 10 gives Eq. 6. Since $[\rho_x] = 0$, we note for future use that total differentiation of Eq. 6 gives

$$[\rho_t] = -\frac{M}{a_0^2}\dddot{\xi}. \tag{11}$$

In the following sections we derive and solve the equation of motion for the free boundary $\xi(t)$.

2. QUALITATIVE DESCRIPTION OF THE MOTION OF THE PISTON

The piston will remain motionless until a density (pressure) wave strikes it. For the sake of definiteness, let us suppose that $l_1 < l_2$. Then the density wave from the left will strike the piston first and at time $t = l_1/a_0$. The arrival of the wave imparts an acceleration to the piston and it commences to move to the right. The situation is indicated schematically in Fig. 5 where the rectilinear segments are portions of characteristics of the wave equation. In this figure we have indicated two domains in which the value of ρ is zero. The path of the density wave, Λ, is thus a discontinuity line of the solution. Then we can expect that at the point of contact of Λ with $\xi(t)$ there will be a reflected discontinuity propagated back along Λ_1 and possibly a trans-

mitted discontinuity along Λ_2. When the discontinuity along Λ_1 arrives at $x = 0$, we can expect a reflected discontinuity to move out along Λ_3. When Λ_3 touches the piston an abrupt change will occur in ξ since ξ is proportional to a difference in densities. This state of affairs is continued indefinitely with similar effects occurring on the right hand side of the piston.

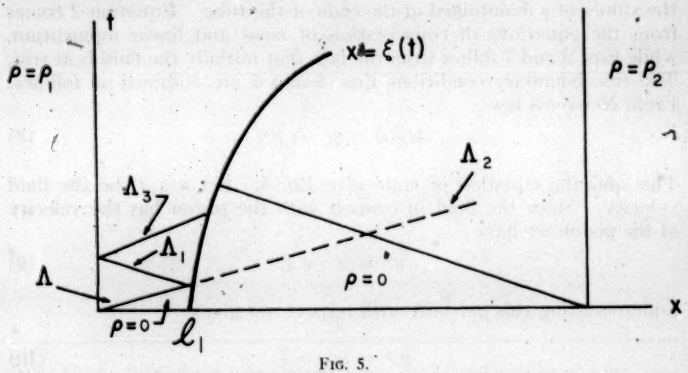

FIG. 5.

To determine these abrupt changes (jumps) in the acceleration, we use the equation of conservation of mass across a discontinuity in a solution of the wave equation. It states

$$\rho'_b v_b = \rho'_a v_a, \tag{12}$$

where

$$v = u - U. \tag{13}$$

Here U is the velocity of the propagation of the discontinuity. (In our case $U = \pm a_0$), ρ' is the fluid density and u is the fluid velocity. The subscripts a and b refer to the opposite sides of the discontinuity. (In our case $\rho' = \rho_0 + \rho$.) Making these substitutions in Eq. 12 and linearizing, we get
we get

$$u_b - u_a = \pm \alpha(\rho_b - \rho_a), \tag{14}$$

with $\alpha = \dfrac{U}{\rho_0} = \dfrac{a_0}{\rho_0}$. We now apply this equation to the situation of the arrival of a density discontinuity at the piston (see Fig. 6). At the point P on the piston trajectory where a discontinuity wave arrives from the left, we distinguish the five indicated regions. Applying Eq. 14 to the characteristics separating regions 1 and 2, 2 and 3, and 4 and 5, respectively, we obtain

$$u_2 - u_1 = \alpha(\rho_2 - \rho_1), \tag{15}$$

$$u_2 - u_3 = -\alpha(\rho_2 - \rho_3), \tag{16}$$

$$u_4 - u_5 = \alpha(\rho_4 - \rho_5). \tag{17}$$

These relations are valid all along the characteristics in question and in particular at the point P. At this point the regions in contact with the piston have their fluid velocities equal to $\dot{\xi}(P)$. These regions are 1, 3, 4 and 5. Thus Eq. 17 reduces to

$$\rho_4 = \rho_5, \tag{18}$$

that is, there is no transmitted discontinuity in ρ. Since $u_1 = u_3 = \dot{\xi}(P)$, subtracting Eq. 16 from Eq. 15 gives

$$\rho_2 - \rho_1 = \rho_3 - \rho_2. \tag{19}$$

Thus the reflected discontinuity is equal to the incident discontinuity. We will show below in Sec. 3 that a discontinuity in ρ across a characteristic is constant along it. Thus if

$$\rho_2 - \rho_1 = J, \tag{20}$$

we have

$$\rho_3 - \rho_4 = 2J + \rho_1 - \rho_5. \tag{21}$$

Since $-\frac{M}{a_0^2}\ddot{\xi} = [\rho]$, according to Eq. 5, the jump in $\ddot{\xi}$ is computable from Eq. 21 and is

$$\Delta\ddot{\xi} = \frac{2a_0^2}{M} J. \tag{22}$$

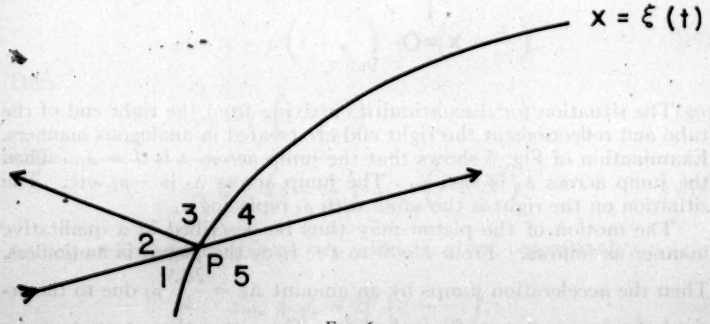

FIG. 6.

To consider a reflection at the end of the tube, we distinguish the three regions in Fig. 7. We have

$$u_1 - u_2 = -(\rho_1 - \rho_2) \tag{23}$$

and

$$u_2 - u_3 = (\rho_2 - \rho_3). \tag{24}$$

Here because of the boundary condition $\rho(0, t) = \rho_1$, we have $\rho_3 = \rho_1$ in Eq. 24. Subtracting Eqs. 23 and 24 gives

$$u_1 - u_2 = u_2 - u_3. \tag{25}$$

Thus if $\rho_2 - \rho_1 = J$,

$$\rho_3 - \rho_2 = -J. \tag{26}$$

Then in this situation the reflected discontinuity is the negative of the incident one.

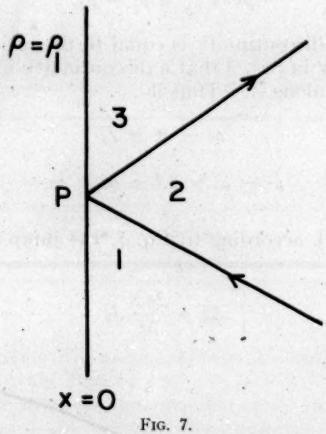

FIG. 7.

The situation for discontinuities arriving from the right end of the tube and reflections at the right end are treated in analogous manners. Examination of Fig. 5 shows that the jump across Λ is $J = \rho_1$. Then the jump across Λ_1 is also ρ_1. The jump across Λ_3 is $-\rho_1$, etc. The situation on the right is the same with ρ_2 replacing ρ_1.

The motion of the piston may thus be described in a qualitative manner as follows. From $t = 0$ to $t = l_1/a_0$ the piston is motionless. Then the acceleration jumps by an amount $\Delta\ddot{\xi} = \dfrac{2a_0^2}{M}\rho_1$ due to the arrival of a pressure wave from the left. The piston then starts to move

to the right. After some time, the reflection of this pressure wave rearrives at the piston. Then the acceleration suffers a jump $\Delta\ddot{\xi} = -\frac{2a_0^2}{M}\cdot\rho_1$. The piston then slows down. After sometime ξ jumps again by $+\frac{2a_0^2}{M}\rho_1$ and it picks up speed to the right. This situation continues indefinitely. Of course, interlaced in this situation are the changes of acceleration due to pressure waves from the right. These cause jumps in the acceleration of $-\frac{2a_0^2}{M}\rho_2, +\frac{2a_0^2}{M}\rho_2, - + \cdots$. The effect of these latter jumps is to slow the piston down and ultimately turn it back. We summarize this discussion by stating

$$\Delta\ddot{\xi} = 2\frac{a_0^2}{M}[\pm\rho_1, \pm\rho_2], \tag{27}$$

as the case may be.

3. THE EQUATION OF MOTION OF THE PISTON

In this section we will derive the equation of motion of the piston. To do this we make use of three well known properties of solutions of the wave equation. These are given in the form of lemmas.

Lemma 1: If $\rho(x, t)$ is a solution of the wave equation, $\rho_{tt} = a_0^2\rho_{xx}$, then $a_0\rho_x \pm \rho_t$ is constant on the family of straight lines (characteristics):

$$t \pm \frac{x}{a_0} = \text{constant}. \tag{28}$$

Proof: Since $\rho(x, t)$ is a solution of the wave equation, there exist two functions $f(x)$ and $g(x)$ such that

$$\rho(x, t) = f\left(t + \frac{x}{a_0}\right) + g\left(t - \frac{x}{a_0}\right). \tag{29}$$

Thus

$$a_0\rho_x = f'\left(t + \frac{x}{a_0}\right) - g'\left(t - \frac{x}{a_0}\right), \tag{30}$$

while

$$\rho_t = f'\left(t + \frac{x}{a_0}\right) + g'\left(t - \frac{x}{a_0}\right). \tag{31}$$

Adding and subtracting these two relations gives, respectively,

$$a_0\rho_x + \rho_t = 2f'\left(t - \frac{x}{a_0}\right), \tag{32}$$

and

$$a_0\rho_x - \rho_t = -2g'\left(t - \frac{x}{a_0}\right), \tag{33}$$

which prove the lemma.

Lemma 2: If $\rho(x, t)$ has a jump discontinuity at a point then this discontinuity persists along the characteristics emanating from that point. Moreover, the magnitude of the discontinuity as the point varies along a characteristic is preserved.

Lemma 3: Along a characteristic which is a jump discontinuity of $\rho(x, t)$, the derivative in the direction tangential to this characteristic is continuous across the characteristic.

Remark: $a_0\rho_x \pm \rho_t$ is the derivative of ρ in the direction tangential to the characteristic $t \pm \dfrac{x}{a_0} = \text{constant}$.

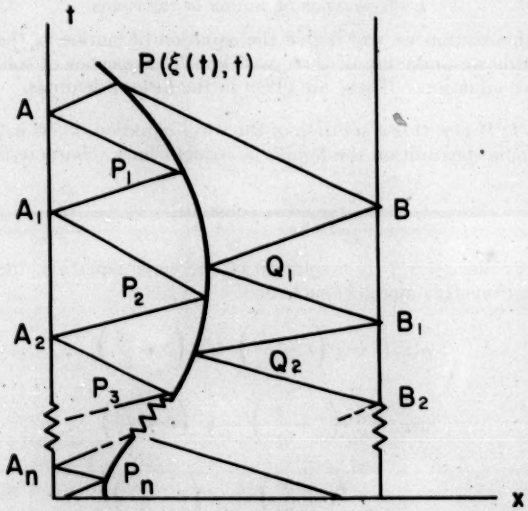

FIG. 8.

The proofs of lemmas 2 and 3 are similar to the proof of lemma 1 and so are omitted.

Now to derive the equation of motion, consider Fig. 8. In this figure the segments $\overline{AP}$ and $\overline{BP}$ are portions of characteristics. P is

supposed to be the point not lying on a discontinuity of ξ. The segments $\overline{AP}$ and $\overline{BP}$ may be crossed by characteristics which bear jump discontinuities of ρ. Now

$$a_0\rho_x(P) - \rho_t(P^-) = a_0\rho_x(A) - \rho_t(A), \tag{34}$$

by lemma 1 and the remark following it (independently of whether or not $\overline{AP}$ is crossed by a characteristic bearing a jump). Similarly

$$a_0\rho_x(P) + \rho_t(P^+) = a_0\rho_x(B) + \rho_t(B). \tag{35}$$

Adding Eqs. 34 and 35 gives

$$2a_0\rho_x(P) + \rho_t(P^+) - \rho_t(P^-) = a_0\rho_x(A) + \rho_x(B), \tag{36}$$

since by Eq. 4, $\rho_t(A) = \rho_t(B) = 0$. Applying the free boundary conditions (Eqs. 6 and 11) to Eq. 36 yields

$$-\frac{2\rho_0}{a_0}\ddot{\xi} - \frac{M}{a_0^2}\dddot{\xi} = a_0[\rho_x(A) + \rho_x(B)]. \tag{37}$$

Applying the same reasoning, the following sequence of equations may be derived.

$$\begin{aligned}
a_0\rho_x(A) &= a_0\rho_x(A) + \rho_t(A)\\
&= a_0\rho_x(P_1) + \rho_t(P_1)\\
&= 2a_0\rho_x(P_1) - a_0\rho_x(P_1) + \rho_t(P_1)\\
&= 2a_0\rho_x(P_1) - a_0\rho_x(A_1) + \rho_t(A_1)\\
&= 2a_0\rho_x(P_1) - a_0\rho_x(A_1) - \rho_t(A_1)\\
&= 2a_0\rho_x(P_1) - a_0\rho_x(P_2) - \rho_t(P_2)\\
&= 2a_0\rho_x(P_1) - 2a_0\rho_x(P_2) + a_0\rho_x(P_2) - \rho_t(P_2)\\
&\cdots\\
&= -\frac{2\rho_0}{a_0}[\ddot{\xi}(P_1) - \ddot{\xi}(P_2) + - \cdots],
\end{aligned} \tag{38}$$

by Eq. 6. Similarly

$$a_0\rho_x(B) = -\frac{2\rho_0}{a_0}\cdot[\ddot{\xi}(Q_1) - \ddot{\xi}(Q_2) + - \cdots] \tag{39}$$

Inserting Eqs. 38 and 39 into Eq. 37 gives the equation of motion valid between jumps in $\ddot{\xi}$, *viz*:

$$\begin{aligned}
\frac{M}{2a_0\rho_0}\dddot{\xi}(P) + \ddot{\xi}(P) &= \ddot{\xi}(P_1) - \ddot{\xi}(P_2) + - \cdots\\
&\quad + \ddot{\xi}(Q_1) - \ddot{\xi}(Q_2) + - \cdots.
\end{aligned} \tag{40}$$

4. SOLVING THE EQUATION OF MOTION

From $t = 0$ to $t = l_1/a_0$, the piston is motionless, since the right member of Eq. 40 is zero and $\xi(0) = l_1$, $\dot{\xi}(0) = 0$, and $\ddot{\xi}(0) = 0$. From $t = l_1/a_0$ up to $\min\left\{3\frac{l_1}{a_0}, \frac{l_2}{a_0}\right\}$ the right member of Eq. 40 is still zero. But since $\ddot{\xi}\left(\frac{l_1}{a_0}\right) = \frac{2a_0^2}{M}\rho_1$, we have for the motion between the first and second jumps in ξ:

$$\xi(t) = l_1 - \frac{1}{2}\frac{\rho_1 M}{\rho_0^2} + \frac{a_0\rho_1}{\rho_0}\left(t - \frac{l_1}{a_0}\right) + \frac{1}{2}\frac{\rho_1 M}{\rho_0^2}\exp\left\{-\frac{2a_0\rho_0}{M}\left(t - \frac{l_1}{a_0}\right)\right\}. \quad (41)$$

After the second jump in ξ the equation of motion becomes overly complicated so that little reason exists for exhibiting an analytic expression for the solution. To obtain the solution in this case, we resort to finite differences and numerical computations. The procedure which we used is a straightforward numerical integration of Eq. 40. Of course care needs to be taken to readjust ξ each time a pressure wave strikes the piston. We indicated the results in Figs. 1, 2 and 3, where the solid curves represent the computations based on the free boundary analysis discussed here while the broken curves represent those of the virtual motion-linear theory of (7). The parameters used are described in the captions.

Acknowledgment

The author is grateful to Dr. H. J. Greenberg for his valuable advice and suggestions concerning the matters discussed in these pages. In addition he is grateful to Miss L. Adams and Mr. P. Markstein for performing the numerical and graphical work associated with this investigation.

REFERENCES

(1) I. I. KOLODNER, "Free Boundary Problem for the Heat Equation with Applications to Problems of Change of Phase," *Commun. on Pure and Appl. Math.*, Vol. IX, pp. 1–31 (1956).

(2) W. L. MIRANKER AND J. B. KELLER, "The Stefan Problem for a Non-linear Equation," *J. Math. Mech.*, Vol. IX, pp. 67–70 (1960).

(3) G. BIRKHOFF AND E. H. ZARANTONELLO, "Jets, Wakes, and Cavities," New York, Academic Press, 1957.

(4) A. WEINSTEIN, "Non-linear Problems in the Theory of Fluid Motion with Free Boundaries," *Proc.* First Symposium of Applied Mathematics, A.M.S., 1949.

(5) J. B. KELLER AND I. I. KOLODNER, "Oscillations of Underwater Explosion Bubbles," *J. Appl. Phys.*, Vol. 27, pp. 1152–1161 (1956).

(6) J. J. STOKER, "Water Waves," New York, Interscience, 1957.

(7) H. J. GREENBERG, "Fourier Analysis of the Motion of a Hydraulically Controlled Piston," *IBM J. Res. & Devel.*, Vol. 4, pp. 378–390 (1960).

SATELLITE-BORNE INSTRUMENTATION FOR OBSERVING FLUX OF HEAVY PRIMARY COSMIC RADIATION*

BY

P. SCHWED,[1] M. A. POMERANTZ,[2] H. HANSON[1] AND H. BENJAMIN[3]

ABSTRACT

A lightweight (1150-gram) instrument for measuring the flux of relativistic heavy primary cosmic ray nuclei of $Z \geq 6$ and separating these into three categories according to charge is described. The detector is an ionization chamber 11 cm. in diameter and 11 cm. long filled with 9 atmospheres of argon. The associated electronics which consists of a 400-volt supply for the ionization chamber, a high input impedance amplifier, and a three-channel pulse height analyzer is completely transistorized and consumes 54 mw.

I. INTRODUCTION

One of the notable characteristics of the primary cosmic radiation is its content of so-called heavy nuclei, that is, those with atomic number greater than 2. Because of the significance of this component with regard to the construction of theories of the origin and history of cosmic radiation, it is obviously of value to determine the flux of these nuclei as a function of the relevant parameters. It is further quite apparent that in performing this measurement it is very useful to be able to place the detector in an Earth satellite, an arrangement which makes it possible to determine, over a long period, the flux as a function of magnetic rigidity by making use of the Earth's field. To achieve this purpose, the equipment to be described in the sequel was designed for incorporation in the Explorer VII satellite.

Without laboring the obvious, it seems in place first to outline briefly certain of the auxiliary constraints which had to be satisfied in the design and construction of the equipment. The over-riding requirement, of course, was that it be able to survive unharmed the rigors of launching. Similarly, the apparatus once in operation had to be capable of functioning properly at any temperature in the range between 0° C. and 60° C. and with a projected variation in supply voltages of ca ± 10 per cent. In addition, it was necessary that pick-up from other equipment operating in close proximity be sufficiently small that no spurious signals eventuate. As a final requirement, it was imperative that weight and power consumption be minimal.

* Supported by the U. S. National Science Foundation under US/IGY Project 32.12.

[1] Deceased; formerly, RIAS, Baltimore, Md.

[2] Bartol Research Foundation of The Franklin Institute, Swarthmore, Pa.

[3] University of Colorado, Boulder, Colo.; formerly, RIAS.

II. PRINCIPLES OF OPERATION

The over-all functioning of the system is indicated by the schematic diagram of Fig. 1. The detector is an argon-filled ionization chamber, and the associated circuitry is designed to respond to the short pulse produced by the collection of the electrons released when a charged particle traverses the chamber. The number of such electrons liberated per unit path length by a relativistic stripped nucleus of atomic number Z is substantially energy independent and is proportional to Z^2. In the arrangement used here, all the electrons which are produced consequent to the penetration of the chamber by a particle are collected at the center wire. The resulting current pulse is converted to a voltage pulse, the maximum amplitude of which is proportional to the total

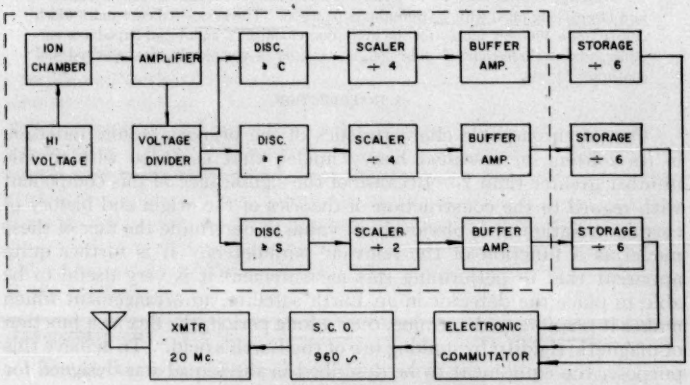

FIG. 1. Block diagram of system.

electronic charge collected and hence to the square of the atomic number of the relativistic nucleus detected (1).[4] The voltage pulse is amplified by means of a feedback stabilized, high gain, high input impedance, transistorized pulse amplifier with a rise time of 3 μsec. and a clipping time of 10 μsec. This latter feature diminishes its sensitivity to random noise and also to the longer pulses associated with the collection of the positive ions. The output of this amplifier is introduced into a three-channel integral pulse height discriminator which is set to pass pulses corresponding to incident nuclei with $Z \geq 6$, $Z \geq 9$, and $Z \geq 16$, respectively. Each of these channels operates independently so that, for instance, any event triggering the last discriminator also triggers the other two. The output of each discriminator in turn is introduced into an associated scaler, the scale factor being 4 for each of the two lower levels and 2 for the highest.

[4] The boldface numbers in parentheses refer to the references appended to this paper.

Because the outputs of these three channels share a single telemetry subcarrier with several other measurements, it was necessary to employ a separate buffer storage unit for each channel. The output of each storage unit is a d-c. voltage which is equal to the total number of pulses received from its associated scaler mod 6. Thus, starting at 0, the voltage in question increases by unity each time the appropriate scaler completes a cycle, attaining a maximum level of 5 volts after which the next impulse resets it to zero. The three storage units employed in this fashion were provided by the Army Ballistic Missiles Agency. During the experiment the output of each storage unit is sampled for one and a half seconds every fifteen seconds. The scaling factors and storage system were chosen with reference to previously measured values (2) of the fluxes of heavy primaries so as to make reasonably small the probability the scaler output would exceed five impulses during the period between consecutive samplings of a single storage unit and thus to eliminate for all practical purposes the ambiguity associated with the limited capacity of the storage units. It may be remarked parenthetically that with this system a rather good determination can also be made of actual counting rates considerably higher than those expected. This is done by observing the output of a storage unit during the 1.5-sec. intervals it is sampled. The lower limit of the counting rates susceptible to this type of determination is given by the requirement that there be a high probability that one or more changes occur in the storage unit during a 1.5-sec. interval—a condition which is satisfied for a rate such that the storage unit changes perhaps once a second on the average. The upper limit to the observable counting rate is given by the frequency response of the telemetry unit and corresponds to 50 changes per second in the storage unit.

As was implied above, a fundamental assumption of this experiment is that the amplitude of the voltage pulse produced when a charged particle penetrates the ionization chamber is proportional to the energy the particle loses to the argon filling the chamber, independent of the energy or nature of the particle. This assumption appears well justified in view of the results of studies of the energy loss of charged particles in argon (3). The empirical evaluation of the constant of proportionality for our ionization chamber was accomplished by measuring the amplitude of the pulse produced when a 5.3-Mev α-particle originating in the decay of Po^{210} dissipated the whole of its energy in the argon. From the results obtained, it is possible to compute the amplitude of the voltage pulse to be expected when a particle of given charge and energy has a known path length within the chamber, employing the standard expression for the energy loss of energetic charged particles (4) within a gas. To obtain the appropriate path length, an auxiliary calculation (5) was carried out which gave the distribution of path lengths within the chamber to be expected for an isotropic flux of particles incident

upon a cylindrical chamber. If the ionization chamber used in the present experiment is taken as equivalent to a cylinder 11 cm. in diameter and 11 cm. long, it follows from this calculation that the average path length within the chamber for particles of an isotropic flux is 7 cm. It is then possible to determine the signal to be expected on the average when a given type of charged particle enters the ionization chamber. Table I gives these values for several cases of interest. It should be

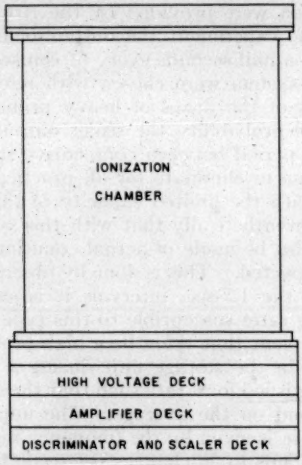

FIG. 2. Configuration of component units.

TABLE I.

Particle Producing Pulse	Amplifier Output, volts
5.3-Mev α-particle	0.35
9-Mev proton ($Z = 1$)	0.42*
40-Mev proton ($Z = 1$)	0.063
relativistic proton ($Z = 1$)	0.014
relativistic C-nucleus ($Z = 6$)	0.42
relativistic F-nucleus ($Z = 9$)	0.95
relativistic S-nucleus ($Z = 16$)	3.0

* This is the largest average signal a proton can produce and corresponds to a proton whose range just equals 7 cm.

noted that the values stated are normalized so that a 0.35-volt amplitude corresponds to a 5.3-Mev α-particle. In practice, our amplifier gain was adjusted to achieve this correspondence.

III. INSTRUMENTATION

A. Physical Arrangement

Figure 2 shows the configuration of the apparatus, which is an assembly of four constituent units, that is, the ionization chamber and the three decks comprising the electronics. To provide protection against damage from shock or vibration, each of the electronics decks is completely encapsulated in Eccofoam[5] to form a disk 14 cm. in diameter. Eccofoam end pieces also are attached to the ends of the ionization chamber to provide flat bearing surfaces. The whole assembly forms a cylinder 14 cm. in diameter and 23 cm. long and in turn represents a subassembly of the satellite instrument column which is in the form of a cylinder of the same diameter. It should be mentioned that the high voltage (400 volts) leads between the ionization chamber and the high voltage deck are completely encapsulated in Armstrong[6] C-1 to prevent a high voltage breakdown between the supply to the center wire of the chamber and ground when the vehicle traverses the upper atmosphere. When such a breakdown occurs, a decoupling condenser, which normally carries 400 volts, discharges through the first transistor of the main amplifier, thus damaging it.

The total weight of the system is 1150 grams. The total power consumption amounts to 54 mw. d.c. variously supplied at 2.65 volts, 6.23 volts, and 10.4 volts.

B. Ionization Chamber

Figure 3 shows the structural details of the ionization chamber. As is evident from the figure, the emphasis in design was on simplicity of construction with the object of achieving a low weight and a high degree of ruggedness. The vessel consists of an extruded cylinder 11 cm. in diameter and 11 cm. long fabricated from magnesium alloy[7] 2.5 mm. thick to which are welded 3-mm. thick end disks of the same material. The center wire is a length of 0.25 mm. Kovar wire held in place by a Kovar seal in each end piece. The choice of magnesium as the structural material may also be advantageous in reducing the background of pulses due to the disruption of nuclei in the chamber wall. Such pulses, which would be spurious from the point of view of the present experiment, can be produced if the interaction between an energetic primary or secondary particle of the cosmic ray flux and a nucleus within the chamber leads to star production. The prongs (6) of such a star typically include low energy (10–50 Mev) protons and α-particles and also some heavier nuclear fragments. Since particles of this type are highly ionizing, the voltage pulse resulting when they

[5] Eccofoam EP, manufactured by Emerson & Cuming, Inc., Canton, Mass.
[6] Adhesive C-1, manufactured by Armstrong Products Co., Warsaw, Ind.
[7] Principal components: 95% Mg, 3% Al, 1% Zn by weight.

slow down within the ionization chamber can be as large as that due to a relativistic heavy nucleus. The probability of this occurrence is diminished by constructing the ionization chamber of a relatively low Z material which necessarily cannot fragment into a large number of multiply charged secondaries when disrupted by an energetic particle.

There are two other features of the ionization chamber which deserve mention. First, as noted earlier, it is supplied with an α-particle source in the form of a short wire plated with Po^{210}. The α-particles leaving this source can be "turned on or off" by varying its potential

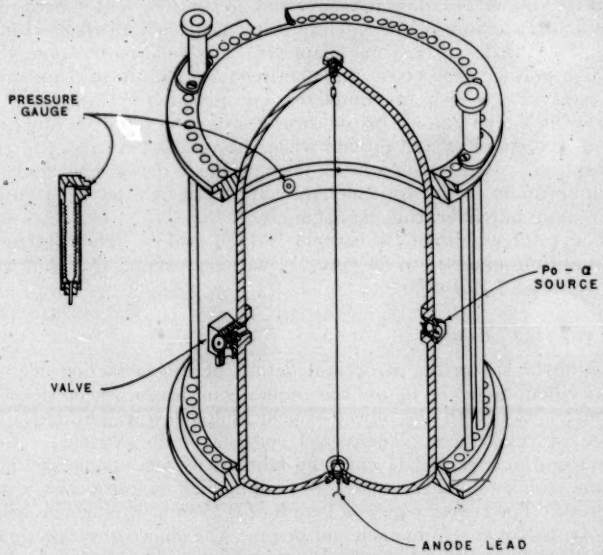

FIG. 3. Ionization chamber construction.

relative to the center wire (1) as can be seen from the following argument. The path length of the 5.3-Mev α-particle within the argon filling the chamber is quite short so that all the electrons liberated when it stops therein are generated in the immediate vicinity of the source wire. If the source wire and center wire are at the same potential (positive relative to the chamber wall), these electrons all are attracted to the source wire whereas, if the source wire is at the potential of the chamber wall, the electrons are free to move to the center wire producing the normal pulse. The source wire, via its capacitive coupling to the center wire, also serves as a convenient means of introducing electrical

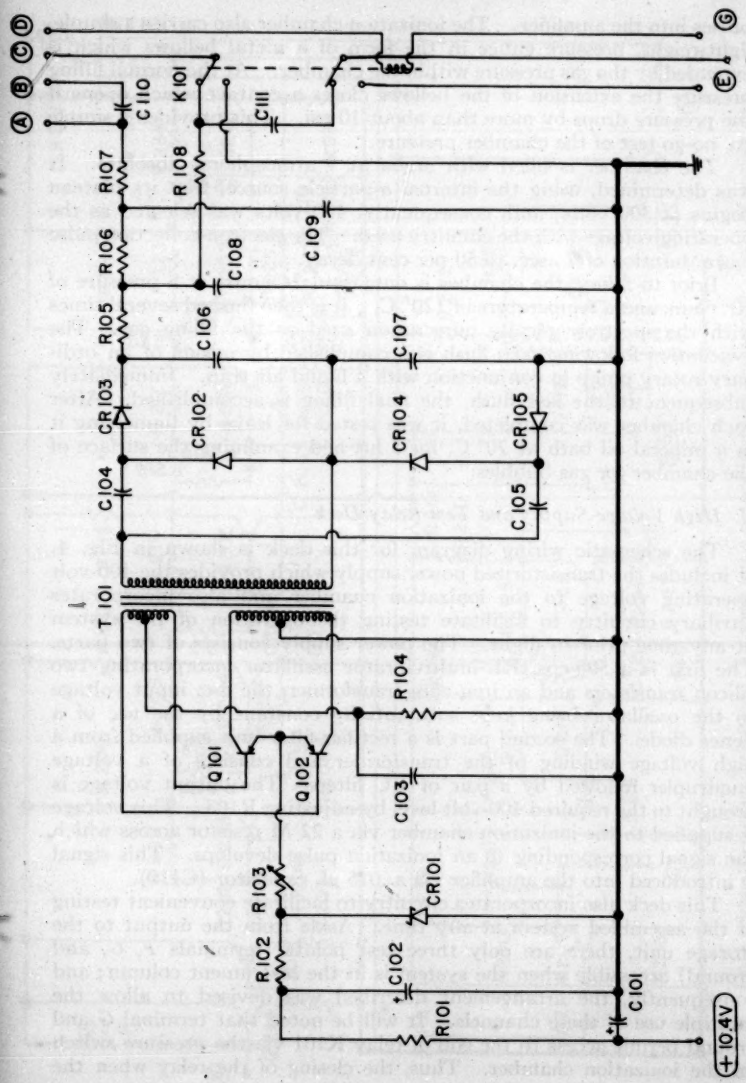

FIG. 4. Schematic diagram of electronics. Terminals with a common label are interconnected. Circuit of high voltage deck.

pulses into the amplifier. The ionization chamber also carries a simple, lightweight, pressure gauge in the form of a metal bellows which is extended by the gas pressure within the chamber. At the normal filling pressure the extension of the bellows closes a contact which opens if the pressure drops by more than about 10 psi. This provides a simple go, no-go test of the chamber pressure.

The chamber is filled with argon at 9 atmospheres absolute. It was determined, using the internal α-particle source, that its plateau begins at 300 volts; and, consequently, 400 volts was selected as the operating voltage with the circuitry used. The electron-collection pulse has a duration of 7 μsec. to 50 per cent decay.

Prior to filling, the chamber is outgassed 24 hours at a pressure of 10^{-4} mm. and a temperature of 120° C. It is then flushed several times with the spectroscopically pure argon used as the filling gas. The evacuation following each flush is accomplished by means of an ordinary rotary pump in conjunction with a liquid air trap. Immediately subsequent to the last flush, the final filling is accomplished. After each chamber was completed, it was tested for leaks by immersing it in a mineral oil bath at 70° C. for 5 hr. and examining the surface of the chamber for gas bubbles.

C. High Voltage Supply and Test Relay Deck

The schematic wiring diagram for this deck is shown in Fig. 4. It includes the transistorized power supply which provides the 400-volt operating voltage to the ionization chamber and also incorporates auxiliary circuitry to facilitate testing the operation of the system at any time prior to flight. The power supply consists of two parts. The first is a 500-cps. RL multivibrator oscillator incorporating two silicon transistors and an iron core transformer, the d-c. input voltage to the oscillator being kept substantially constant by the use of a Zener diode. The second part is a rectifier-filter unit supplied from a high voltage winding of the transformer and consists of a voltage quadrupler followed by a pair of RC filters. The output voltage is brought to the required 400-volt level by adjusting R103. This voltage is supplied to the ionization chamber via a 22 M resistor across which the signal corresponding to an ionization pulse develops. This signal is introduced into the amplifier via a .015 μf. capacitor (C110).

This deck also incorporates circuitry to facilitate convenient testing of the assembled system at any time. Aside from the output to the storage unit, there are only three test points (terminals *F*, *G*, and ground) accessible when the system is in the instrument column; and consequently, the arrangement described was devised to allow the multiple use of these channels. It will be noted that terminal *G* and ground permit access to the coil of relay K101 via the pressure switch on the ionization chamber. Thus, the closing of the relay when the

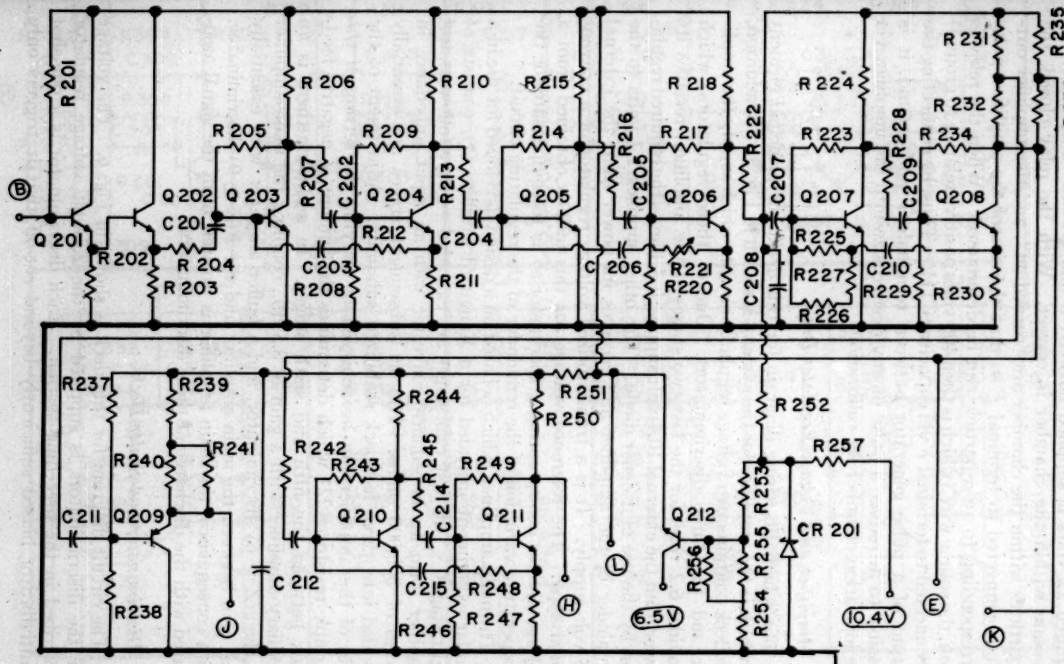

FIG. 5. Schematic diagram of electronics. Terminals with a common label are interconnected. Circuit of amplifier deck.

required 22 volts is supplied between G and ground verifies that the pressure within the chamber is correct. With the relay closed, the α-particles within the chamber are "turned on", and the amplifier output is connected to terminal F so that the size of the amplified pulse corresponding to an α-particle can be determined. When the relay is open, the source wire (which is then 400 volts positive relative to ground) is connected to terminal F via capacitor C111. Thus, by connecting the output of a pulse generator between terminals F and ground, it is possible to introduce a pulse of any desired size into the amplifier via the ionization chamber for calibration.

D. Amplifier and Voltage Regulator Deck

The schematic wiring diagram for this deck, the principal element of which is the amplifier for the system, is shown in Fig. 5. In addition, the deck contains two voltage regulator circuits which supply the amplifier and the three discriminators. One of these regulators, which provides 6.2 volts for the last two stages of the amplifier, receives its power from the external 10.4-volt supply; it achieves the required regulation by the use of a Zener diode. The other supplies 2.7 volts to the remainder of the amplifier and receives its power from the external 6.5-volt supply. It is a transistorized voltage regulator of a conventional type. The reference voltage for this unit is obtained from a voltage divider incorporating a thermistor so as to compensate for the temperature variation of the remainder of the regulating circuit.

The main amplifier, which is based on a design developed for use in a similar experiment intended for a Vanguard satellite (**7**), consists of eight stages. The first two stages are cascaded emitter followers and together form an impedance converter with an input impedance in excess of 500,000 ohms. The six subsequent stages are essentially divided into three feedback stabilized sub-units. Adjustment of the gain of the amplifier can be achieved by varying the setting of the variable resistor R221 which determines the amount of negative feedback between the fifth and sixth stages. In addition, there is an auxiliary amplifier with a gain of 3.5 db., coupling the main amplifier to the $c(Z \geq 6)$ discriminator, and a buffer amplifier with essentially unit gain between the main amplifier and the $F(Z \geq 9)$ discriminator. As a consequence, the main amplifier is isolated from the signal associated with the discharge of these discriminators.

E. Discriminator and Scaler Deck

The circuit diagram for this deck is shown in Fig. 6. The voltage for the discriminators is supplied by the 2.7-volt voltage regulator described in the preceding section. Each discriminator is a one-shot multivibrator biased sufficiently beyond cut-off that it triggers only

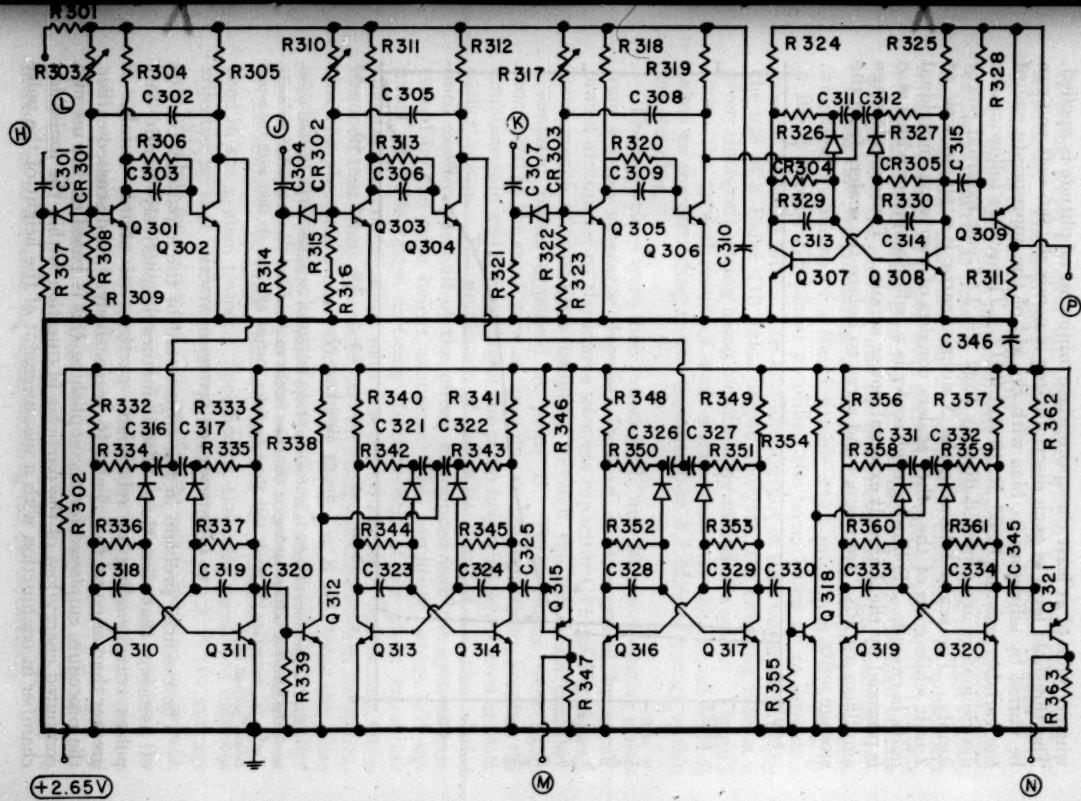

FIG. 6. Schematic diagram of electronics. Terminals with a common label are interconnected. Circuit of scaler-discriminator deck.

when a pulse of at least the appropriate minimum amplitude is applied. The threshold level of each discriminator is nominally 0.6 volt and can be varied by adjusting its bias with the aid of the appropriate one of the variable resistors R303, R310 and R317. The scalers following the discriminators are powered directly from the 2.65-volt external power supply. The scaler following the S discriminator is a single scale of 2 unit while each of the other scalers consists of two such individual units in cascade. Following each scaler is a buffer amplifier which also is powered by the 2.65-volt external power supply. These single stage amplifiers use PNP transistors and serve to isolate the scalers from the storage units.

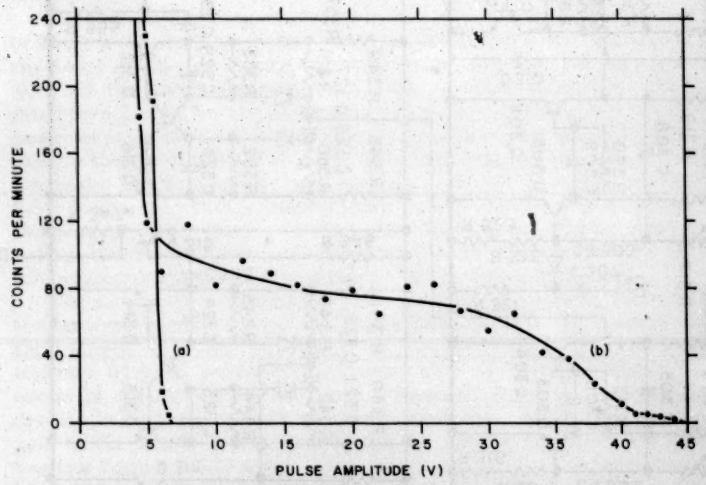

FIG. 7. Spectrum of pulse height output from ionization chamber. The abscissa represents the base-line voltage settings of the pulse height analyzer and thus is in arbitrary units. Curve (*a*) represents the result with the α-particles "turned off" and (*b*) that with the α-particles "turned on."

IV. ADJUSTMENT AND TESTING OF SYSTEM

The essential problem in the adjustment of the apparatus consists of assuring that the three discriminators respectively admit only pulses corresponding to relativistic particles of atomic number Z greater than or equal to 6, 9 and 16, respectively. As discussed earlier, the procedure employed for accomplishing this is based on the use of a computed energy loss of the particles in question within the ionization chamber in conjunction with a measurement of the height of the pulse

resulting when 5.3 Mev are deposited within the chamber (by a Po α-particle). The first part of the procedure is directed toward a determination of this latter quantity.

In order that this measurement be made under conditions duplicating as exactly as possible the operating conditions, the high voltage deck was first assembled on the ionization chamber. In subsequent measurements, all pulses were seen at the output side of the coupling capacitor C110 (point B of Fig. 4). As the first step, the high voltage was supplied the chamber and the α-particles within the chamber were "turned on" by grounding the source wire. The output pulses were amplified by means of a Baird Atomic 219A preamplifier followed by a Baird Atomic 218 Linear amplifier, the latter being set to provide a 10-μsec. clipping time. The amplifier output in turn was monitored by the use of a Baird 210 pulse height analyzer, the counting rate at a given (integral) setting being measured by means of a scaler. Figure 7 shows the typical result of such a measurement; the cut-off level is taken as corresponding to the deposition of 5.3 Mev of energy within the chamber.

The α-particles were then "turned off" and 10-μsec. negative pulses from a pulse generator (Hewlett Packard 212A) supplied by a calibrated attenuator to the source wire via capacitor C111 of Fig. 4; as a consequence of capacitive coupling through the ionization chamber, attenuated pulses appeared at point B. These pulses were again monitored in the same way as those due to the α-particles, keeping the amplifier gain and the setting of the pulse height analyzer fixed at their earlier values. The amplitude of the pulse supplied was then varied until exactly one half of the pulses introduced into the system were passed by the pulse height analyzer. This amplitude, which is designated as P, is taken as being characteristic of the given ionization chamber in combination with its power supply. Specifically, it is assumed that when a particle loses an energy of 5.3λ Mev in the ionization chamber, the pulse produced at the point B will have the same amplitude as that resulting when a pulse of amplitude λP is supplied to the terminal F. This permits a calibration procedure independent of the linearity or noise characteristics of the transistorized amplifier used in the system proper. Specifically, the fully assembled unit was adjusted so that with an input pulse amplitude of 1.2 P, the average rate of pulses passed by the C discriminator was $\frac{1}{2}$ the input pulse rate. Similarly, pulse amplitudes of 2.7 P and 8.6 P were used in adjusting the F and S discriminators, respectively. In each case the adjustment was made so that half the pulses introduced into the system were passed by the discriminator. This serves to average out the effect of noise generated within the system since it should presumably be as likely to increase as to decrease the signal reaching the discriminator.

V. FUNCTIONING OF UNIT

The background curve of the ionization chamber and the pulse distribution corresponding to the stopping of Po α-particles within its volume have already been indicated in Fig. 7. From the viewpoint of the present experiment these are the most important characteristics of the chamber. In the remaining investigation of the behavior of the system, the chamber figured as part of the assembled unit, and its sensitivity was taken as represented by the quantity P, the size of the 10-μsec. pulse which has to be introduced into the source wire in order that the voltage pulse appearing at the amplifier input be the same size as that corresponding to the maximum Po-α-pulse. As far as the amplifier itself is concerned, the most important parameters are noise level and linearity, given a fixed temperature and design supply voltages. The noise is significant for two reasons. First, if the noise level is sufficiently high, it may suffice to trigger one or more discriminators in the absence of any signal from the chamber. Secondly, by mixing with the input signal of the amplifier, the noise present in the system may cause a fluctuation of the apparent amplifier gain so that the size of input required to trigger a given discriminator may fluctuate over a considerable range.

To investigate both of these possibilities an experiment was undertaken in which a pulse train of 10-μsec. pulses of amplitude P with a repetition rate of approximately 200 per second was introduced into the source wire of the ionization chamber. The amplifier output was further amplified by a Tektronix 112 broadband amplifier, the output of which was monitored with a Baird Atomic 210 pulse height analyzer operating in the differential mode with a 2-volt window, employing 1-minute counting periods. The results are displayed in Fig. 8 in which the counting rate is shown on both a linear and a logarithmic scale. Since all the discriminator settings employed were at least 20 per cent greater than P, the sharpness of discrimination will exceed that indicated in the figure. It may also be seen that the maximum amplitude of the noise pulses *per se* was well below the 1.2 P setting of the lowest discriminator. In view of the importance of this result, however, a separate experiment was undertaken in which an assembled unit was operated in vacuum for a period of 12 hours with the Po α-particles "turned off." During this period the C scaler produced only a single pulse, implying that the spurious counting rate was well under one per hour.

In view of the procedure employed for adjusting the system, the amplifier linearity is not especially significant in itself. This follows because the adjustments made automatically compensate for such nonlinearities. In any event, a measurement of amplifier response, in which signals were introduced directly into the point B of Fig. 5, showed the amplifier to be linear to within ± 10 per cent (the accuracy of the

measurement) up to a 4-volt output. Since reference to Table I indicates that the amplifier characteristics are significant to the functioning of the experiment only up to outputs 3 volts in amplitude, this may be considered quite satisfactory. Perhaps more relevant was another measurement of amplifier characteristics in which pulses were introduced directly into the source wire. Measuring the size of the pulses in units of P, the range of pulse heights employed spanned the range from P to $8P$. Over this range the amplifier was found again to

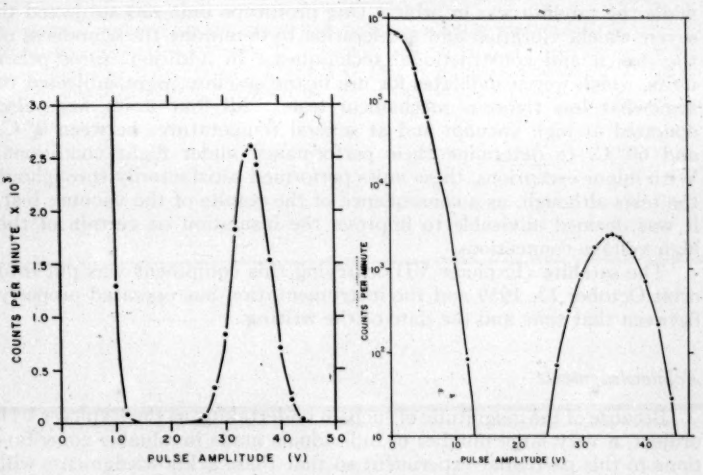

FIG. 8. Pulse height spectrum of amplifier output when pulses of amplitude P (see text) are introduced into the ionization chamber source wire. The abscissa represents the base-line voltage setting of the pulse height analyzer and thus is in arbitrary units. In Fig. 8*a* the ordinate scale is linear and in 8*b* it is logarithmic. The early part of the curve represents the noise output of the system.

be linear within ± 10 per cent. This not only verifies the constancy of the amplifier gain but also verifies so far as possible the correctness of the procedure for setting the discriminator levels. This follows because—assuming the amplifier itself to be linear—it can be inferred from the results that the size of the pulses appearing at the center wire of the ionization chamber is indeed directly proportional to the size of the pulses applied to the source wire. This is the principal assumption of the calibration procedure.

It was found by analyzing the operation of the equipment that a

change in the supply voltages of ±10 per cent caused the level of input signal necessary to trigger each of the discrimators to change by no more than 1 per cent. Over a range of temperature from 0° C. to 60° C., the input level necessary to trigger each of the discriminators varied by no more than 10 per cent.

In order to determine whether the instrumentation for this experiment would operate successfully under actual flight conditions, the ABMA conducted a series of preliminary tests in which the mechanical conditions at launch were simulated as were the operating conditions while the satellite was in orbit. One prototype unit was subjected to severe shock, vibration and acceleration to determine the soundness of the design and constructional techniques. In addition, three other units, which were candidates for use in the satellite, were subjected to somewhat less rigorous mechanical tests. All four units were also operated at high vacuum and at several temperatures between 0° C. and 60° C. to determine their performance under flight conditions. With minor exceptions, these units performed satisfactorily throughout the tests although, as a consequence of the results of the vacuum test, it was deemed advisable to improve the insulation on certain of the high voltage connections.

The satellite (Explorer VII) carrying this equipment was put into orbit October 13, 1959 and the instrumentation has operated properly between that time and the date of the writing.

Acknowledgments

Because of the magnitude of such an undertaking as the Explorer VII project, a very large number of individuals made invaluable contributions to this particular experiment so that these acknowledgments will necessarily be quite incomplete. Above all, there should be mentioned the late Dr. Gerhart K. Groetzinger who was responsible for a very great proportion of the conception, design, and realization of this experiment. R. C. Pfeiffer and S. P. Agarwall of the Bartol Research Foundation played a very vital role in the mechanical design, construction, and testing of the ionization chamber. Harlan Burke of ABMA and Herman LaGow of NASA were of inestimable help in assisting us in orienting the design of our equipment so as to be compatible with the requirements of the satellite environment. Finally, we should like to acknowledge the part played by Olin B. King, of the ABMA, who was responsible for the design of the storage unit described in the introduction.

REFERENCES

(1) This technique for determining the atomic number of cosmic ray primaries was previously employed by M. A. POMERANTZ and G. W. MCCLURE in balloon-borne experiments, *Phys. Rev.*, Vol. 86, p. 536 (1952).

(2) For a review of earlier measurements see, for instance, S. F. SINGER in "Progress in Cosmic Ray Physics," Vol. IV, New York, Interscience Publishers, Inc., 1958, Chapter IV.

(3) W. P. JESSE, H. FORSTAT AND J. SADAUSKIS, *Phys. Rev.*, Vol. 77, p. 782 (1950).

(4) H. A. BETHE AND JULIUS ASHKIN in "Experimental Nuclear Physics," Vol. I, New York, John Wiley & Sons, Inc., 1952, Part II.

(5) G. GROETZINGER, P. SCHWED AND W. RAY, *Bull. Am. Phys. Soc. II*, Vol. 4, p. 270 (1959.) A detailed presentation of these calculations will be presented in a RIAS report currently being prepared.

(6) B. ROSSI, "High Energy Particles," New York, Prentice-Hall, 1952, Chapter 8.

(7) H. PINCKERNELL, L. WILKES, E. RUHSTRAD AND H. HANSON, "Instrumentation for Measuring Heavy Primary Cosmic Ray Flux in an Earth Satellite," *Proc. I.R.E. National Telemetering Conference*, Baltimore, Maryland, June 1958, p. 154.

JUMP RESONANCE IN A THIRD ORDER NONLINEAR CONTROL SYSTEM

BY

WELLINGTON W. KOEPSEL[1]

SUMMARY

An analysis is presented in which a graphical method is used to gain a better understanding of jump resonance. In the frequency range of interest the orthogonal components, u and v, of the steady state first harmonic approximation are plotted in a u–v plane. Constant angular frequency loci are drawn on the plane and intersected by a circle of radius F, the magnitude of the sinusoidal forcing function. These intersections determine the amplitude of the first harmonic solution. The locus of vertical tangents, normally associated with the amplitude-frequency curve, plotted on the u–v plane is used to determine the lower jump resonant frequency. The approximation reveals that jump resonance can be precluded if the forcing function does not exceed a calculable value referred to as the threshold value. The threshold value is determined from the system parameters.

For a forcing function sufficiently large it is shown that real solutions in the immediate neighborhood of angles of lag of $\pi/2$ do not exist. A critical forcing function such that a maximum lag angle of $\pi/2$ is possible may be determined from system parameters. An electronic analog computer was used to verify the results of the study.

A nonlinear system is characterized by three entities: jump resonance, subharmonic and superharmonic generation and frequency entrainment. The first of these is the subject of this paper. Jump resonance or ferroresonance as some writers have called it has been studied extensively in second order systems (**1**, **2**, **3**, **4**, **5**).[2] It has been studied in power systems in problems associated with the use of series capacitors to compensate for line drop and in feedback control systems it has been studied in systems which possess nonlinear gain (**6**). The purpose of this paper is to present an analysis that was recently made by the author of a third order control system (**7**). The analysis is one in which only the first harmonic is considered and uses the Ritz-Galerkin Method to obtain a solution (**8**).

SYSTEM EQUATION

If one considers the elementary control system shown in Fig. 1, the equations

$$r - f(c) = e \tag{1}$$

and

$$E(s)G(s) = C(s) \tag{2}$$

[1] Department of Electrical Engineering, University of New Mexico, Albuquerque, N. Mex.

[2] The boldface numbers in parentheses refer to the references appended to this paper.

may be written. $E(s)$ and $C(s)$ are the Laplace transforms of the respective time functions e and c. It is necessary here to use a mixture of complex and real time functions for the nonlinear aspect of the problem has no complex domain representation. For the third order system studied the transfer function $G(s)$ was defined as

$$G(s) = \frac{K}{s(T_1 s + 1)(T_2 s + 1)} \tag{3}$$

where K, T_1, and T_2 have the usual meanings. If Eq. 3 is substituted into Eq. 2 and transformed into the time domain there results the equation

$$T_1 T_2 \frac{d^3c}{dt^3} + (T_1 + T_2)\frac{d^2c}{dt^2} + \frac{dc}{dt} = Ke. \tag{4}$$

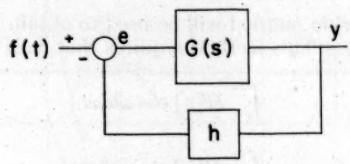

FIG. 1. Elementary nonlinear control system.

Equation 1 substituted into Eq. 4 yields

$$T_1 T_2 \frac{d^3c}{dt^3} + (T_1 + T_2)\frac{d^2c}{dt^2} + \frac{dc}{dt} + Kf(c) = Kr. \tag{5}$$

This equation is nonlinear if the function $f(c)$ is nonlinear. In this paper $f(c)$ is assumed to take the form

$$f(c) = c + mc^3 \tag{6}$$

where m is a positive real number much less than 1. If r is now written as a sinusoidal function of time, Eq. 5 becomes

$$\mu \frac{d^3c}{dt^3} + \gamma \frac{d^2c}{dt^2} + \delta \frac{dc}{dt} + \alpha c + \beta c^3 = F \cos(\omega t - \varphi) \tag{7}$$

In this expression

$$\mu = 1 \tag{8}$$

$$\gamma = (T_1 + T_2)/(T_1T_2) \tag{9}$$

$$\delta = 1/T_1T_2 \tag{10}$$

$$\alpha = K/T_1T_2 \tag{11}$$

$$\beta = Km/T_1T_2 \tag{12}$$

$$F = Kr_{max}. \tag{13}$$

This is the system equation and it is the equation for which a steady state solution is desired. φ is the angle of lag between the applied forcing function and approximated first harmonic solution.

FIRST HARMONIC STEADY STATE SOLUTION

The Ritz-Galerkin method will be used to obtain the first harmonic approximation (9). This method requires that each of the integrals

$$\int_0^{2\pi} H[c] \cos \omega t d\omega t \tag{14}$$

$$\int_0^{2\pi} H[c] \sin \omega t d\omega t \tag{15}$$

be zero.

$H[c]$ is obtained by transposing the quantity to the right of the equality in Eq. 7 and substituting the assumed solution

$$c = A_1 \cos \omega t. \tag{16}$$

In this equation $A_1 > 0$. Upon performing the integrations required by (14) and (15) there is obtained:

$$(\alpha - \gamma\omega^2 + \tfrac{3}{4}\beta A_1^2)A_1 = v \tag{17}$$

$$(\mu\omega^2 - \delta)\omega A_1 = u \tag{18}$$

$$u^2 + v^2 = F^2 \tag{19}$$

$$\varphi = \tan^{-1} u/v. \tag{20}$$

The solution now lies in the evaluation of A_1 and φ for fixed values of F. The fundamental amplitude A_1 may be found by substituting Eqs. 17 and 18 into Eq. 19; however, it is immediately apparent that

difficulty would be experienced in attempting a solution for A_1 in the resulting sixth degree equation. A more reasonable approach to a solution may be made by plotting the parametric equations (Eqs. 17 and 18) in a u–v plane. If ω is fixed and A_1 is allowed to take on various real values constant ω loci in the u–v plane result. These loci are shown in Fig. 2. A circle of radius F drawn on this plane intersecting

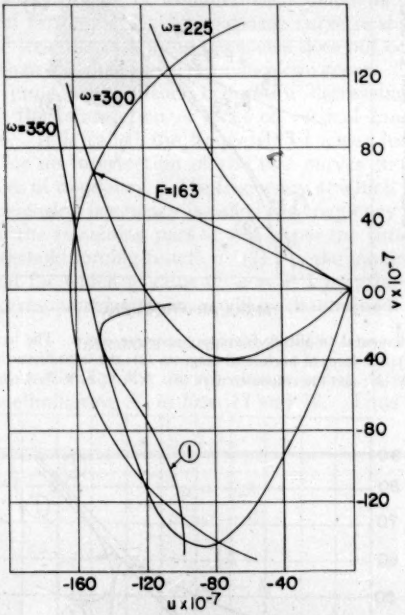

FIG. 2. Constant ω loci in the u–v plane.
((1) u–v plane locus of vertical tangents)

the constant ω loci will determine the u and v components of F. Since u and v are known, A_1 and φ may be determined.

$$A_1 = \frac{u}{\omega(\mu\omega^2 - \delta)} \tag{21}$$

$$\varphi = \tan^{-1} u/v. \tag{20}$$

In this way a fundamental amplitude frequency response curve is obtained. A typical curve is shown in Fig. 3. On Fig. 3 are shown the

usual curves associated with the response curve of a nonlinear system. These are the locus of vertical tangents, the backbone curve and the locus of horizontal tangents. On the figure are also shown loci of constant F for the condition that $v = 0$. This is the condition for

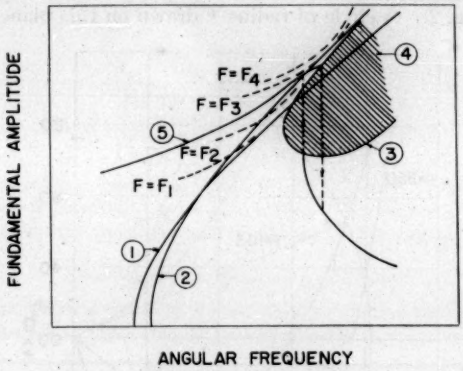

FIG. 3. Fundamental amplitude frequency response curve. The figure illustrates: the backbone curve (1); the locus of horizontal tangents (2); the locus of vertical tangents (3); a region of instability (4); and the response curve (5). ($F_1 < F_2 < F_3 < F_4$.)

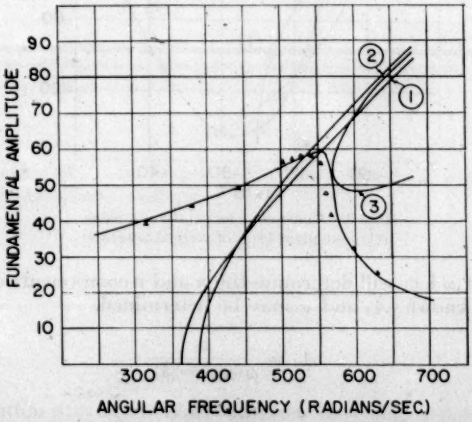

FIG. 4. Fundamental amplitude frequency response curve for a system for which $F = F_T$. ((1) locus of horizontal tangents, (2) backbone curve, (3) locus of vertical tangents, Δ experimental values, ——— analytical.)

which the backbone is defined and $\varphi = \pi/2$. Intersections of the backbone and locus of constant F will thus define a solution for A_1. The important thing to be noted from the figure is that for F sufficiently large intersections cannot occur. This is interpreted to mean that real solutions are nonexistent in a region in the neighborhood of $\varphi = \pi/2$.

It should be pointed out that if $F = F_T$, the threshold forcing function, a response curve may be obtained such that it is tangent to the locus of vertical tangents. Such a response curve is shown in Fig. 4. For values of F less than F_T, jump resonance does not occur; however, if F is greater than F_T, then jump resonance can occur. The frequency at which this jump in amplitude occurs for decreasing frequency is determined by the intersection of locus of vertical tangents and the response curve. It is called the frequency of lower jump resonance. It is possible for an intersection of the two curves to occur also for increasing values of frequency. The frequency at which the two curves intersect for increasing frequency is called the frequency of upper jump resonance. In the remaining part of this paper the three quantities—(1) F_T, the threshold forcing function; (2) F_φ, the maximum allowable forcing function for which a value of $\varphi = \pi/2$ may be obtained; and (3) lower jump resonant frequency—will be determined.

THRESHOLD FORCING FUNCTION F_T

The representation for the curves shown in Fig. 2 may be written as $v = f(u)$ by eliminating A_1 in Eqs. 17 and 18. Thus

$$v = au + bu^3 \tag{22}$$

where

$$a = \frac{\alpha - \gamma\omega^2}{\omega(\mu\omega^2 - \delta)} \tag{23}$$

$$b = \frac{\frac{3}{4}\beta}{\omega^3(\mu\omega^2 - \delta)^3}. \tag{24}$$

A careful examination of Fig. 2 will reveal that for decreasing values of u for ω sufficiently large, F will pass through a maximum value, decrease in magnitude, pass through a minimum and then increase without limit. These extremum values may be found by taking the derivative of F with respect to u and setting this derivative equal to zero. The expression for F^2 from Eq. 19 becomes

$$b^2u^6 + 2abu^4 + (1 + a^2)u^2 = F^2 \tag{25}$$

when the value of v from Eq. 22 is substituted. The derivative of F^2 equated to zero is thus

$$3b^2u^4 + 4abu^2 + a^2 + 1 = 0. \tag{26}$$

The solution for u^2 in this expression is

$$u^2 = \frac{1}{3b}\left[-2a \pm \sqrt{a^2 - 3}\right]. \tag{27}$$

This value of u^2 yields the u at which a maximum or minimum of F occurs for a given angular frequency ω. The u for which neither a maximum nor minimum of F occurs is $a^2 = 3$ or

$$u^2 = -\frac{2}{3}\frac{\sqrt{3}}{b} \tag{28}$$

and

$$F_T = \sqrt{-\frac{8}{9}\frac{\sqrt{3}}{b}}. \tag{29}$$

This will be called the threshold value of forcing function. For values of $F \leq F_T$ jump resonance does not occur. If $F > F_T$ jump resonance can occur. The value of F_T is important for it establishes the maximum allowable value of forcing function for which no jump can occur. The value of b as required by Eq. 28 is calculated using Eq. 24 in which ω is the positive real root of

$$\sqrt{3}\mu\omega^3 + \gamma\omega^2 - \sqrt{3}\delta\omega - \alpha = 0. \tag{30}$$

FORCING FUNCTION F_φ

The forcing function F_φ is the value of forcing function for which $|u|$ is a maximum and $v = 0$. The value of F_φ is thus

$$F_\varphi = |u|_{\max}. \tag{31}$$

The value of F_φ so defined is the limiting value of F for which solutions of $\varphi = \pi/2$ exist. For F greater than F_φ, positive real solutions for A_1 do not exist in the immediate neighborhood of $\varphi = \pi/2$. The $|u|_{\max}$ may be determined by taking the derivative of u with respect to ω and equating the result to zero. This yields the frequency for which a maximum $|u|$ occurs. This frequency is

$$\omega^2 = \frac{1}{8\mu\gamma}\left[2\gamma\delta + 3\alpha\mu \pm \sqrt{(2\gamma\delta + 3\alpha\mu)^2 - 16\alpha\delta\mu\gamma}\right]. \tag{32}$$

The value of $|u|_{\max}$ is

$$|u|_{\max} = 2\omega^2(\mu\omega^2 - \delta)\sqrt{\frac{\gamma(\delta - \mu\omega^2)}{3\beta(3\mu\omega^2 - \delta)}}. \tag{33}$$

LOWER JUMP RESONANT FREQUENCY

The lower jump resonant frequency, in Fig. 3 the point at which a sudden increase in amplitude occurs for decreasing frequency, may readily be found with the aid of the u–v plane. The lower jump frequency occurs for decreasing frequency at the intersection of the response curve and the locus of vertical tangents. The locus of vertical tangents is found by taking the implicit derivative of the response curve with respect to A_1 and equating the derivative of ω with respect to A_1 to zero. When these operations are carried out the result is

$$(\alpha - \gamma\omega^2 + \tfrac{3}{4}\beta A_1^2)(\alpha - \gamma\omega^2 + \tfrac{9}{4}\beta A_1^2) + \omega^2(\mu\omega^2 - \delta)^2 = 0. \quad (34)$$

This equation represents the locus of vertical tangents in the $A_1 - \omega$ plane (response curve). If Eq. 34 is divided by $\omega^2(\mu\omega^2 - \delta)^2$ and the values of u, a and b from Eqs. 18, 23 and 24, respectively, substituted, there results

$$(a + bu^2)(a + 3bu^2) + 1 = 0 \quad (35)$$

or

$$3b^2u^4 + 4abu^2 + a^2 + 1 = 0. \quad (36)$$

This is the same result obtained by taking the derivative with respect to u of Eq. 25, the u–v plane representation for the response curve. Solutions for u out of Eq. 36 for different values of a and b will locate the intersection of the locus of vertical tangents with the constant ω loci drawn for the same values of a and b. The u–v plane locus of vertical tangents is shown on Fig. 2. The lower jump resonant frequency for driving force F may now be determined by drawing a circle of radius F on the u–v plane. The intersection of the circle with the u–v plane locus of vertical tangents determines the lower jump resonant frequency. If this point of intersection is (u_2, v_2) then the point u_2^2 is given by

$$u_2^2 = \frac{1}{3b}[-2a + \sqrt{a^2 - 3}]. \quad (37)$$

In this expression a and b determine a particular locus on which the point (u_2, v_2) lies. The point v_2 must satisfy the expression

$$v_2 = au_2 + bu_2^3. \quad (38)$$

If Eq. 37 is solved for b the result is

$$b = \frac{1}{3u_2^2}[-2a + \sqrt{a^2 - 3}]. \quad (39)$$

From Eq. 38 the solution for a is

$$a = \frac{v_2 - bu_2^3}{u_2} \tag{40}$$

or

$$a = \frac{v_2}{u_2} - bu_2^2. \tag{41}$$

Upon substituting b from Eq. 39 into Eq. 41 and solving for a, there results

$$a = \frac{3}{2}\frac{v_2}{u_2} + \frac{1}{2}\frac{u_2}{v_2}. \tag{42}$$

The positive real root of the cubic

$$a\mu\omega^3 + \gamma\omega^2 - a\delta\omega - \alpha = 0 \tag{43}$$

is the lower jump resonant frequency.

ELECTRONIC COMPUTER SIMULATION

A Donner electronic analog computer was used to simulate Eq. 7 using values for the constants given in Eqs. 8 through 13 as follows:

$$\mu = 1$$
$$\gamma = 1.6 \times 10^3$$
$$\delta = 6 \times 10^5$$
$$\alpha = 24 \times 10^7$$
$$\beta = 8.4 \times 10^4$$
$$F_T = 984 \times 10^7$$
$$F_\varphi = 1058 \times 10^7$$
$$T_1 = 1 \times 10^{-3}$$
$$T_2 = 16.7 \times 10^{-3}$$
$$K = 400$$
$$m = 0.35 \times 10^{-3}.$$

For forcing functions $F = F_T$, $F = F_\varphi$ and $F > F_T$ the response of the system was determined. The experimental data points are indicated on Figs. 4, 5 and 6. The solid lines represent the response as determined by the method described in this paper. Figure 4 is drawn for $F = F_T$ and indicates the tangency of the response curve to the locus

of vertical tangents. Figure 5 is drawn for $F = F_\varphi$ and it shows the jumps in amplitude for increasing and decreasing frequency. The

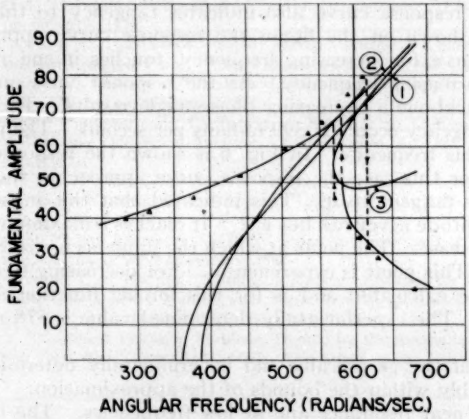

FIG. 5. Fundamental amplitude frequency response curve for a system for which $F = F_\varphi$. ((1) locus of horizontal tangents, (2) backbone curve, (3) locus of vertical tangents, Δ experimental values, ——— analytical.)

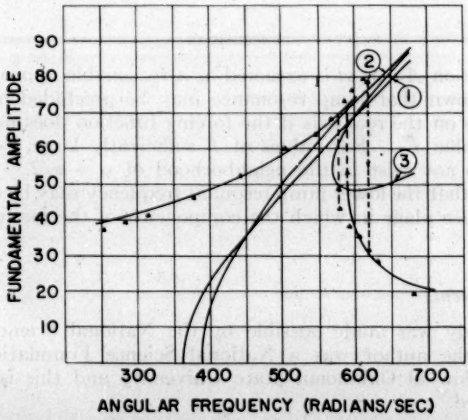

FIG. 6. Fundamental amplitude frequency response curve for a system for which $F > F_\varphi$. ((1) locus of horizontal tangents, (2) backbone curve, (3) locus of vertical tangents, Δ experimental values, ——— analytical.)

calculated lower jump resonant frequency is 582 radians per second. The experimentally determined value was 571 radians per second. The upper jump resonant frequency could not be determined analytically. The response curve also indicates tangency to the backbone curve. As shown on the figure the response curve approaches the backbone curve for increasing frequency, touches it and then moves away for increasing frequency. As the response curve moves away from the backbone a decreasing phase angle results. The frequency at which tangency occurs is 590 radians per second. The phase angle is $\pi/2$ for this frequency. In Fig. 6 is shown the response curve for $F > F_\varphi$. For this case the response curve approaches the backbone but is never tangent to it. This indicated that the angle of fundamental amplitude never reaches $\pi/2$. It reaches a maximum value and starts to decrease. The point at which the jump occurs is indicated on the curve. This point is experimental. For decreasing frequency the jump can be calculated and is for this forcing function 590 radians per second. The experimentally determined value is 578 radians per second.

In general the graphically and experimentally determined points agree favorably within the bounds of the approximation. The largest errors occur near resonance and at low frequencies. The large errors near resonance are a consequence of the graphical analysis which is susceptible to large errors in this region. Errors at low frequency are of course due to the approximation which is invalid at low frequencies.

CONCLUSIONS

If a solution $A_1 \cos \omega t$ is assumed as a reasonable approximation it has been shown that jump resonance may be precluded in a system having poles on the real axis if the forcing function does not exceed a threshold value F_T. For values of F sufficiently large, positive real solutions do not exist in the neighborhood of $\varphi = \pi/2$. It has also been shown that the lower jump resonant frequency may be determined by using a u–v plane in which the components of the forcing function are plotted.

Acknowledgments

This study was made possible by the National Science Foundation while the author was a National Science Foundation Science Faculty Fellow at Oklahoma State University and this is gratefully acknowledged.

REFERENCES

(1) G. D. DUFFING, "Erzwungene Schwingungen bei veranderlicher Eigenfrequenz," Braunschweig, F. Vieweg u. Sohn, 1918.

(2) E. V. APPLETON, "Anomalous Behavior of a Vibration Galvanometer," *Phil. Mag.* Ser. 6. Vol. 47, pp. 609–619 (1924).

(3) L. S. JACOBSEN AND H. J. JESPERSON, "Steady Forced Vibration of a Single Mass System with a Nonlinear Restoring Force," JOUR. FRANKLIN INST., 220, 467–496 (1935).

(4) J. W. BUTLER AND C. CONCORDIA, "Analysis of Series Capacitor Application Problems," *AIEE-Trans.*, Vol. 56, pp. 975–988 (1937).

(5) C. P. ATKINSON, "Superharmonic Oscillations as Solutions to Duffing's Equation as Solved by Electronic Differential Analyzer," *ASME-Trans., J. Appl. Mech.*, Vol. 24, pp. 520–525 (1957).

(6) A. M. HOPKIN AND K. OGATA, "An Analytic Frequency-Response Solution for a Higher Order Servo with a Nonlinear Control Element," *ASME-Trans., J. Basic Eng.*, Vol. 81, n. 1, Ser. D, pp. 41–45 (1959).

(7) W. W. KOEPSEL, "Jump Resonance in a Third Order Nonlinear Control System," Ph.D. Dissertation, Oklahoma State University, 1960.

(8) C. P. ATKINSON AND C. P. BOURNE, "Solution of Duffing's Equation for Softening Spring System Using Ritz-Galerkin Method with Three Term Approximation," *Proc. Third U. S. Natl. Congr. Appl. Mech.* ASME, New York, 1958, pp. 71–77.

(9) K. KLOTTER, "Nonlinear Vibration Problems Treated by the Averaging Method of W. Ritz," *Proc. First Natl. Congr. Appl. Mech.*, Ann Arbor, Mich., Edwards Bros., Inc., 1952.

BOOK REVIEWS

ADVANCES IN COMPUTERS, VOL. 1, edited by Franz L. Alt. 316 pages, diagrams, 6 × 9 in. New York and London, Academic Press, 1960. Price, $10.00.

The title "Advances in Computers—Vol. I" inadequately connotes the areas of major concern of the editor, Franz L. Alt, in the edition of articles appearing within. In Mr. Alt's words from the preface, "The *Advances* will bring together articles about diverse aspects of the design of electronic computing systems and their components, about methods of machine programming and numerical analysis, and about computer applications to scientific and engineering problems, to business management and data processing, to statistics, control of operations, and 'pseudo-logical' problems." Thus, although the title suggests an occupation with computer design, it is apparent that a much broader range is intended and that a rather misleading title was perhaps a necessary compromise with brevity.

Mr. Alt has chosen for Volume I six articles, each of them excellent and impressive in its own right and each of them providing an additional comprehensive bibliography. Most of these articles are primarily in the nature of a survey of the results and directions being taken in the field to which they pertain, but in each case the author has made valuable technical contributions of his own to the same field. The individual authors are thus able to speak with a high degree of authority and their opinions are incisive.

The Table of Contents of Vol. I is as follows:

1. "General-Purpose Programming for Business Applications," by Calvin C. Gotlieb.
2. "Numerical Weather Prediction," by Norman A. Phillips.
3. "The Present Status of Automatic Translation of Languages," by Yehoshua Bar-Hillel.
4. "Programming Computers to Play Games," by Arthur L. Samuel.
5. "Machine Recognition of Spoken Words," by Richard Fatehchand.
6. "Binary Arithmetic," by George W. Reitwiesner.

In the preface Mr. Alt makes reference to the desirability of making ". . . mathematicians, computer engineers, and computer users aware of each other's problems." These areas of specialty suggest the somewhat broader classifications denoted by "techniques," "design," and "applications" that are increasingly being used in computer literature to designate the specialization of knowledge that exists. Accordingly, the "techniques" area is meant to encompass knowledge represented by mathematics and numerical analysis, statistics, logic, computer programming, and programming languages, the use of computing and off-line equipment, and data-processing techniques such as sorting, collating, editing, etc. The "application" area refers to the special field of knowledge from which the problem usually comes, as for example meteorology, heat transfer, accounting, linguistics, etc. The "design" area, of course, refers to development of the electrical, mechanical and electronic equipment involved. Viewed in this light, considerable variation in emphasis is apparent in the six articles.

The first article stresses data-processing techniques. Little attention is given to any particular application area of equipment design. Assembler, interpreter, complier, and generator programs are discussed with particular reference to *FORTRAN*, *A-2*, and *Flowmatic* as examples of compilers. Sorting and merging of records are discussed, as are utilization of storage, program maintenance, and data-handling techniques.

The article on weather prediction is concerned with the application area of meteorology and the mathematical techniques appropriate to the solving of partial differential equations numerically. Computer techniques are not discussed nor is equipment design. A good understanding of mathematics and meteorology is necessary on the part of the reader.

The articles on language translation, the playing of games, and voice recognition are all highly readable and require little technical knowledge on the part of the reader to follow. They are mainly oriented toward their re-

spective application areas though the first two of these do compare various specific computing, logical, and statistical techniques necessary to the analysis of their subjects. The last educates the reader to the problems of articulation, sound, phonetics, "fricatives," "plosives" and the like prior to a discussion of the design of various specific speech recognition machines. In the second to last paragraph of this 34-page article the author observes that, "Computers are now also in use for speech recognition studies, as we shall see." Thus, the use of computers to this application is given negligible treatment. Mr. Alt has indeed interpreted *Advances in Computers* broadly.

The final article is concerned with binary arithmetic and its potential application to computer design. It is highly mathematical and occupied with minimality properties, uniqueness proofs, existence proofs, and other properties equally abstruse. Its mathematical content will slow even the more sophisticated reader to a pace midway between reading and studying.

The editor, in his choice of articles for Volume I, seems to require that these articles have recent importance and a reference, even if remote, to digital computers. Needless to say, this opens a very broad door. The subsequent admission of only six such articles, while necessary to an economical volume size, creates the impression of a technical potpourri much too small, varied, and atypical to sample the vast field implied. Many a prospective buyer of this volume will be disturbed to find that only two or three of the varied articles are of sufficient interest to him to consider a purchase. The Volume I edition of *Advances in Computers* contributes purposely and, in the opinion of this reviewer, unwisely to the informational entropy already too abundant to this field.

JOHN T. GODFREY
General Electric Co.

SCIENCE AND GOVERNMENT, by C. P. Snow. 88 pages, 5¼ × 7¾ in. Cambridge, Harvard University Press, 1961. Price, $2.50.

The Godkin Lectures on the Essentials of Free Government and the Duties of the Citizen were established at Harvard University in memory of Edwin Lawrence Godkin. The Godkin Lectures of 1960, included in this small but meaty volume, forcibly but subtly demonstrate the impact of the subject of this endowment when handled by an expert. A series of notes elucidates the text.

Sir Charles Snow, who started his professional life as a physicist, was a Fellow of Christ's College, Cambridge, from 1930 to 1950. While continuing his professional activities, he has written novels which search the lives and motives of scientists, politicians and bureaucrats; his most recent novel is "The Affair."

The problem of the present work, urgent with democratic societies, is simply stated: How can we make use of scientists in government with the greatest effect and the least risk?

This problem is treated, appropriately, by means of a case history, made more dramatic by the impact of strong emotions and aggressive personalities. The principal actors were Sir Henry Tizard and F. A. Lindemann, later Lord Cherwell and for years right-hand man of Winston Churchill.

The conflict between Tizard's campaign for the development of radar and Lindemann's opposition and championship of strategic bombing, and the use of parachute bombs and infrared detection, provide the body of the story, interlarded with politics and jealousies. The reconstitution of the Committee for the Scientific Study of Air Defence, called the Tizard Committee, to include E. V. Appleton, radio expert, as well as other distinguished scientists, presaged the eventual triumph and success of radar and the defense of Britian.

"One of the most bizarre features of any advanced industrial society in our time is that the cardinal choices have to be made by a handful of men: in secret: and, at least in legal form, by men who cannot have a first-hand knowledge of what those choices depend upon or what their results may be."

"We are immensely competent; we know our own pattern of operations . . . . It is not enough. That is why I want some scientists mixed up in our affairs. It would be bitter if, when this storm of history is over, the best epitaph that anyone could write of us was only that: 'The wisest men who had not the gift of foresight.' "

CARL T. CHASE
The Franklin Institute

ORGANOMETALLIC CHEMISTRY, edited by H. Zeiss. ACS Monograph No. 147. 549 pages, diagrams, 6 × 9 in. New York, Reinhold Publishing Corp., 1960. Price, $17.50.

This is one of the best monographs to come out of this series by the American Chemical Society. The field of organometallic chemistry is an interdisciplinary area, fortified recently by novel approaches on different fronts. It is very satisfying to see so many of these recent advances reviewed in one book by the scientists most responsible for the advances. Editor Zeiss, after selecting his very outstanding authors, has wisely made no attempt to equate the styles of presentation, so that each chapter truly reflects the views of the scientists at the center of the field and allows the readers to follow the rational development of the subject.

The arrangement of chapters is logical. The first chapter on "Carbon-Metal Bonding," by Dr. James W. Richardson of Purdue University, considers the present state of theory regarding organometallic bond and is a useful basic introduction to sigma- and pi-bonded compounds and complexes in subsequent chapters. Using MO method qualitatively, charge distribution and orbitals are described and energy effects are summarized in correlation diagrams for a variety of organometallics. Discussion of the conditions for stability of alkyl and aryl transition metal compounds is designed to be of help in further preparation and isolation.

The second chapter is a timely review of infant benzyne chemistry by Dr. Rolf Huisgen of University of Munich, Germany. It is apparently a translation of a review that appeared earlier in the year in *Angewendete Chemie* (R. Huisgen and T. Sauer, *Angew. Chemie*, Vol. 72, p. 91 (1960). Evidence for the existence of benzyne intermediate in nucleophilic aromatic sustitution is presented in comprehensive detail. The discussion of the mechanism of aryne formation, reactions of arynes and the nature and the structure of arynes represent a considerable original contribution to this fascinating development in organic chemistry.

Next comes the description of vinylmetallics by Drs. H. D. Kaesz and F. G. A. Stone of Harvard University. Dr. Herbert C. Brown of Purdue presents the chemistry of organoboranes, which developed mostly in his laboratories. And this is also true of Dr. Karl Ziegler's presentation of organo-aluminum compounds that follows. This is Ziegler's fourteenth review article in the last eight years on this subject. Most important facts in the field have been described and the information regarding recent work has been brought up-to-date. Aluminum alkyls represent a third important tool for organometallic synthesis, besides the magnesium and lithium alkyls and it appears that it is going to rapidly surpass the two others for large scale technical uses.

Drs. H. Gilman and H. J. S. Winkler of the Iowa State University describe the organosilylmetallic chemistry. One of the outstanding merits of this chapter is the systematic consideration of the chemical bonds between silicon and various elements. Reactions of organosilyl compounds are presented in detail and comparison between organosilylmetallic and organogermylmetallic chemistry has been presented.

Many review articles on ferrocenes have appeared. One in the present book is by Dr. P. L. Pauson of Royal College of Science and Technology, Glasgow, Scotland. This is certainly not the most comprehensive one; however, considerable new material has been included. The chapter on the arene complexes of the transition metals by the editor, Dr. H. Zeiss of the Monsanto Chemical Company, is on the other hand a completely new review. It considers the polyphenylchromium chemistry, *bis*-arene metal complexes, acetylenic metal complexes and the Job-Cassal reaction to prepare hexacarbonyl chromium. The complementary chapter on the transition metal alkyls and aryls (including the acetylenic derivatives of transition metals) is by Drs. G. E. Coates and F. Glockling of The University, Durham, England. The last chapter is on metal carbonyls and related compounds by Drs. J. Chatt (ICI, England) P. L. Pauson and L. M. Venanzi (Oxford University, England).

Reading through this book, one is impressed by the extraordinary convergence of organic and inorganic chemistry in this area of organometallic chemistry. The present effort to inform the chemical literate of new significant advances has a major scientific merit of in-

creasing the communication between organic and inorganic chemists.

S. B. MAINTHIA
The Franklin Institute Laboratories

THE QUANTUM THEORY OF ATOMIC STRUCTURE, VOL. I, by John C. Slater. 502 pages, diagrams, 6 × 9 in. New York, McGraw-Hill Book Co. Inc., 1960. Price, $11.00.

Despite rather abundant literature in this field, the clarity and the method of presentation of material make Slater's book a welcome addition.

From the point of view of usefulness and value the book can be clearly divided in two parts. The first part from Chapters 1 to 8 contains the foundations of the quantum theory. The second part starts with the presentation of the Hartree method and proceeds with application of this method to calculations of atomic structures. The selection of topics in the first part was made carefully in order to serve as an introduction and base to the second part of the book. Hence, only certain aspects of the quantum theory are fully emphasized, and some are omitted or only sketched briefly. The physical ideas are fully explained step by step in every chapter and are accompanied always with the historical evolution of the problem. If the student is previously acquainted with some book on quantum theory giving a fuller and more rigorous mathematical treatment, the first part of this book will give him a thorough understanding of the physical ideas underlying the quantum theory. Unfortunately a few subjects, such as the harmonic oscillator and especially the W.K.B. method are explained very briefly. Even the Appendices on these subjects do not help overmuch in their clarification.

The second part of the book, pivoted on two chapters—the self-consistent field method (Ch. 9) and Antisymmetry of Wave Function and the Determinantal Method (Ch. 12)—is written with great clarity and pedagogical mastery. The ideas of the Hartree method are introduced and explained in Ch. 8 and the procedure outlined in simple but very instructive problems at the end of this chapter. Then, the mathematical formalism of the Hartree method is built up step by step (used throughout all of the book) in Ch. 9. This formalism is then applied, in the chapter on Elementary Theory of Multiplets to calculations of the energy values, that is, the diagonal matrix component of the Hamiltonian for simple multiplets. Examples are calculated for non-equivalent as well as for equivalent electrons. The next logical step is to express multiplet energies in terms of average energies and this is done in the chapter on closed shells. This logical build-up of the theory and its application then proceeds to the Hartree-Fock method, introduced in the chapter dealing with multiplet calculations for light atoms. The theory is then tried and checked on the elements with partially filled d-shells, that is, on the iron group. This part of the book is written in a coherent and logical method, every step being fully and clearly explained.

One should also emphasize the careful selection of very instructive problems, well worth while being worked out in details by students.

B. LALEVIC
The Franklin Institute Laboratories

PUBLICATIONS RECEIVED

SMALL PARTICLE STATISTICS, by G. Herdan. Revised and enlarged second edition, 418 pages, diagrams, 6 × 9¼ in. New York, Academic Press Inc., 1960. Price, $14.50.

MULTIVIBRATOR CIRCUITS, by A. H. Bruinsma. Second revised edition, 66 pages, diagrams 5¼ × 8 in. New York, The Macmillan Company, 1961. Price, $2.00.

PRACTICAL ROBOT CIRCUITS, by A. H. Bruinsma. Second revised edition, 125 pages, diagrams, plates, 5¼ × 8 in. New York, The Macmillan Company, 1961. Price, $3.95.

HEAT TREATMENT AND PROPERTIES OF IRON AND STEEL. NBS Monograph 18. 40 pages, illustrations, 8 × 10½ in. Washington, U. S. Government Printing Office, 1960. Price: $0.35 (domestic); $0.45 (foreign).

SCIENCE IN SPACE. CHAPTER VIII. GALACTIC AND EXTRAGALACTIC ASTRONOMY. 49 pages, diagrams, 8½ × 11 in. Washington, National Research Council, 1960. No price.

BOOK NOTES

AN INTRODUCTION TO CELESTIAL MECHANICS, by Theodore E. Sterne. 206 pages, diagrams, 5½ × 8 in. New York, Interscience Publishers, Inc., 1960. Price: $4.50 (cloth); $2.50 (paper).

This is No. 9 of the Interscience Tracts on Physics and Astronomy. It has been prepared because there are currently so few specialists in celestial mechanics—the subject which must be understood to solve many of the current and future problems in space technology. This book is designed for physicists, engineers and astronomy students interested in orbital problems of artificial satellites. Readers should be familiar with fundamental physical principles, higher mathematics and classical mechanics.

BLOCK AND GRAFT POLYMERS, by William J. Burlant and Allan S. Hoffman. 166 pages, diagrams, 6 × 9 in. New York, Reinhold Publishing Corp., 1961.

The authors cover the reactions and experimental techniques used to initiate block and graft polymerization, as well as physical properties and structures of the products. It demonstrates that molecular engineering of polymers is possible. Sample chapter headings are: Separation and Isolation of Block and Graft Polymers; Chain Transfer Reactions; Photolytic Reactions; and Stereoblock Polymers. The index is handily arranged, with the polymers under discussion listed alphabetically in boldface type under the backbone or starting polymer.

MODERN CHEMICAL PROCESSES, VOL. 6. 126 pages, illustrations, 8½ × 11 in. New York, Reinhold Publishing Corp., 1961. Price, $6.00.

Volume 6 in this series of compilations of articles from *Industrial & Engineering Chemistry* contains seventeen articles on recently developed chemical processes. Included are processes for manufacturing silicone products, for deriving chemicals from wood, for obtaining detergents continuously, for manufacturing catalysts, etc. The articles all appeared originally in 1958 and 1959.

THE TECHNIQUE OF PHOTOMICROGRAPHY, by Douglas Lawson. 256 pages, plates, diagrams, 5½ × 8¼ in. New York, The Macmillan Co., 1961. Price, $12.75.

Modern techniques of photomicrography are discussed in this book by an expert in the field. It is suitable both for the laboratory research worker and for the amateur who wants a permanent record of the field viewed in his microscope. Sixteen chapters cover equipment, processing, mounting, staining and specialized types of photomicrography such as infra-red, ultra-violet, X-ray, fluorescence, and interference. The unusually excellent reproductions of photomicrographs (some in color) add immeasurably to the value of the work.

ADAPTIVE CONTROL PROCESSES, by Richard Bellman. 225 pages, diagrams, 6 × 9¼ in. Princeton, Princeton University Press, 1961. Price, $6.50.

Based on a series of lectures delivered at Hughes Aircraft Company, this book covers control theory, particularly as applicable to machine solution of problems involving linear and nonlinear processes. Eighteen chapters cover such topics as feedback control, multistage decision processes, dynamic programming, sequential machines, random processes, stochastic processes, theory of games, adaptive control processes and successive approximation. Scientists interested in automation, psychologists, communications engineers, mathematicians, statisticians and control engineers will find this book profitable reading.

INTRODUCTION TO CERAMICS, by W. D. Kingery. 781 pages, illustrations, 6 × 9 in. New York, John Wiley & Sons, Inc., 1960. Price, $15.00.

Ceramics are treated as a class of materials rather than the product of a special industry, in this new text. Treatment of subject matter is general, and is based on a rational approach to ceramic phenomena and properties. After a short introductory section, four major sections deal with: ceramic processes (raw mate-

rials and forming processes); characteristics of ceramic solids (crystal structure, noncrystalline solids, structural defects, surfaces and interfaces, and atomic mobility); development of microstructure in ceramics (equilibrium diagrams, crystal growth, nonequilibrium phases, grain growth, and microstructure characteristics in various materials); and properties of ceramics (thermal, optical, deformation, strength, conductivity and dielectric). Dr. Kingery's book is a welcome new approach to the subject of ceramics.

WAVES IN LAYERED MEDIA, by Leonid M. Brekhovskikh, translated by David Lieberman and edited by Robert T. Beyer. 561 pages, diagrams, 6 × 9 in. New York, Academic Press Inc., 1960. Price, $16.00.

English-speaking readers will welcome this translation of the 1956 Russian work of Prof. Brekhovskikh, giving a systematic exposition of the theory of the propagation of elastic and electromagnetic waves in layered media. The six chapters cover: Plane Waves in Layers; Some Applications of the Theory of Plane Wave Propagation in Layered Media; Plane Waves in Layered-inhomogeneous Media; Reflection and Refraction of Spherical Waves; Wave Propagation in Layers; and The Field of a Concentrated Source in a Layered-inhomogeneous Medium. The book is valuable because it presents a complete picture of Soviet researches in this field. The author presents the theory of propagation of elastic and electromagnetic waves simultaneously, which is advantageous, since the same mathematical methods apply in both cases.

HANDBUCH DER PHYSIK (ENCYCLOPEDIA OF PHYSICS), BAND IX (VOLUME IX), edited by S. Flügge and C. Truesdell. 815 pages, illustrations, 6½ × 9¼ in. Berlin, Springer-Verlag, 1960. Price, DM 198.

Issued as Part III of Vol. IX on Fluid Dynamics, this new addition to the monumental *Handbuch der Physik* covers the following six phases of this subject: Analytical Theory of Subsonic and Supersonic Flows (Menahem Schiffer); Théorie des ondes de choc (Henri Cabannes); Theory of Characteristics of Inviscid Gas Dynamics (Richard Meyer); Linearized Theory of Unsteady Flow of a Compressible Fluid (R. Timman); Jets and Cavities (David Gilbarg); and Surface Waves (Wehausen & Laitone). Five of the monographs are in English, the sixth is in French. The index is published both in German-English and English-German.

Each treatise is a thorough, scholarly discussion, well illustrated and well organized; the bibliographies accompanying each article are selective, voluminous, and should be invaluable to those wishing to pursue the subject further.

It is impossible, in a review of such a work, to cover all the papers in detail. Instead, the reviewer will attempt to deal with one paper —that on surface waves—as an example of the others. Here the authors deal with fluids subject to a gravitational force, and, in most cases, there exist surfaces between two fluids of different densities. After an introductory section, the problem of mathematical formulation is discussed, for coordinate systems, equations of motion, boundary conditions at an interface, boundary conditions on rigid surfaces, and other types of boundary surfaces. From here, the authors move on to progressive waves and wave velocity, energy, momentum, etc. Nearly 200 pages are then devoted to the theory of infinitesimal waves; in this section the authors cover group velocity, special boundary problems, gravity waves in the presence of surface tension, waves in a viscous fluid, etc. Shallow-water waves are treated in the next section, both linear and nonlinear theories, and the final chapter sets forth exact solutions for some kinematical theorems, for waves in heterogeneous fluids, for transformations of the boundary-value problem, etc. The bibliography for this monograph covers 20 pages, and there are 56 illustrations, including an excellent reproduction of seven particle trajectories in progressive and standing waves.

No research library of any standing can afford to be without this up-to-date, authoritative *Handbuch*.

FINITE-DIFFERENCE METHODS FOR PARTIAL DIFFERENTIAL EQUATIONS, by George E. Forsythe and Wolfgang R. Wasow. 444 pages, diagrams, 6 × 9 in. New York, John Wiley & Sons, Inc., 1960. Price, $11.50.

An account of the more important aspects of finite difference methods for partial differential equations is given in this volume.

The authors have touched on most of the really important achievements in the field, but do not claim that this is a complete or comprehensive treatment. Both initial-value and boundary-value problems are covered, and the topics of greatest importance in the solution of these problems with highspeed automatic computers are emphasized. A graduate course in partial differential equations has not been presupposed. However, a mathematically sound treatment of these questions cannot be undertaken without assuming some familiarity with advanced calculus and matrix theory. Most topics have been omitted that have no bearing on the understanding of numerical analysis; only a few computational details or programming tricks will be found. Therefore, this book is directed primarily to those who wish to understand the numerical analysis underlying the use of difference methods.

PHYSICAL CHEMISTRY OF SURFACES, by Arthur W. Adamson. 629 pages, diagrams, 6 × 9 in. New York, Interscience Publishers, Inc., 1960. Price, $12.75.

This text has been prepared to serve as a senior or first year graduate level course in surface chemistry. It requires only undergraduate physical chemistry as a specific prerequisite, so that the use of advanced thermodynamics and of statistical mechanics is somewhat restrained. In the first half, problems have been inserted as the author deems it helpful in gaining an understanding of the material. Emphasis, however, is on exercises requiring some analysis as opposed to a simple substitution into equations already provided. In the second half of the course as given here a report involving critical appraisal of some appropriate aspect of the literature takes the place of problem assignments. It is hoped also that professional chemists will find the book a useful bridge between their basic physical chemistry and the proliferating general literature and specialized monographs.

NUMERICAL METHODS FOR SCIENCE AND ENGINEERING, by Ralph G. Stanton. 266 pages, 6 × 9 in. Englewood Cliffs, N. J., Prentice-Hall, Inc., 1961. Price, $6.75.

This book represents a modern, practical introduction to numerical analysis dealing fully with the essentials needed for translating analytical processes into numerical results. A firm foundation is provided in the actual methods of problem solving. Over a hundred completely solved numerical examples are included to illustrate the principles and theory of numerical analysis in practice. Many of the illustrations and problems have been taken from actual physical situations. Throughout the text emphasis is on the most up-to-date computer applications. The author has designed the book to point out the transition from hand calculation to desk calculation and on to electronic computers. A general exposition on computers, in the concluding chapter, leads logically to the actual programming of problems for a digital computer. Clearly organized, the book provides the beginner in the field with an introduction to the most frequently encountered branches of numerical analysis. With only a knowledge of basic calculus presupposed, all other background material, such as determinants and matrices, is included.

E. I. T. REVIEW, by Virgil M. Faires and Joy O. Richardson. 256 pages, diagrams, 6 × 9 in. Englewood Cliffs (N. J.), Prentice-Hall, Inc., 1961. Price, $6.75.

This manual is designed for those wishing to take state registrations examinations for engineer-in-training, but it may also be used as a study manual for the professional engineering license exams. Basic principles and fundamentals of all phases of engineering are set forth briefly; the reader is expected to use this manual only as a guide for review. There are numerous problems and a selected list of references for each of the fourteen "subject" chapters; the last chapter gives lists of sample examination questions in several fields, exclusively for the professional examination.

THE ENCYCLOPEDIA OF SPECTROSCOPY, edited by George L. Clark. 787 pages, illustrations, 7 × 10 in. New York, Reinhold Publishing Corp., 1961. Price, $25.00.

Over 160 internationally known contributors are represented in this new encyclopedia covering all branches of spectroscopy. The main topics (for example, Band Spectroscopy, Flame Photometry, Mass Spectroscopy) are subdivided into more specialized topics. For instance, there are 54 articles under the head-

ing of "Emission Spectroscopy—Light" but only one under "X-Ray Diffraction or Crystal Spectra." Each article covers the major phases of one topic, in readily understandable language. The encyclopedia was designed for scientists, engineers, teachers, students and manufacturers. It is well printed and well bound to stand up under heavy use.

SOLID PROPELLANT ROCKET RESEARCH, edited by Martin Summerfield. 692 pages, illustrations, 6 × 9¼ in. New York, Academic Press Inc., 1960. Price, $6.50.

Sponsored by the American Rocket Society, this new series entitled "Progress in Astronautics and Rocketry" has been established in order to make available the technical contributions which cannot be accommodated in the Society's two regular publications. This first volume is an outgrowth of a symposium held in January, 1960, at Princeton. The 27 papers are grouped under six headings: Mechanical Properties of Grains; Steady-State Burning Mechanisms; Combustion of Metals; Theories of Unstable Combustion; Experiments on Unstable Burning; and Solid Propellant Ignition. Printed by the offset method, the type faces and sizes vary from chapter to chapter. This is somewhat disconcerting to the reader, but the comparatively low price compensates, in part, for these variations.

COMPLEX VARIABLES AND THE LAPLACE TRANSFORM FOR ENGINEERS, by Wilbur R. LePage. 475 pages, diagrams, 6 × 9 in. New York, McGraw-Hill Book Co., Inc., 1961. Price, $12.50.

A graduate-level text, this new work presents the theory of Fourier and Laplace transforms, and the basic theory of functions of a complex variable. Its approach is midway between strictly engineering and abstract mathematics, with emphasis on interpretation. The text is divided into two parts: Part I covers functions of a complex variable, beginning at a relatively low level; Part II deals with transform theory. The author's preface contains valuable suggestions to those who may wish to use the text in a shortened form.

MODERN PHYSICS FOR THE ENGINEER, Second Series, edited by Louis N. Ridenour and William A. Nierenberg. 383 pages, illustrations, 6 × 9 in. New York, McGraw-Hill Book Co., Inc., 1961. Price, $9.50.

This new volume comprises a second series of lectures coordinated by Dr. William Nierenberg and given during the academic year 1957–1958 at various institutions throughout California. Following the technical organization of the earlier volume, it is divided into three main parts treating, respectively: The Laws of Nature; Man's Physical Environment; and Technology. In the first part the topics covered are: New Particles and Old Principles; Status Report on New Particles; Nuclear Shell Structure; Electron Scattering and Nuclear Structure; Electrons and Nuclei in Ideal Crystals; The Properties of Liquid Helium; Superconductivity; Magnetohydrodynamic Waves. The second part covers: The Origin of Nuclear Species by Means of Nuclear Reactions in Stars; Radio Astronomy; Origin of the Earth's Magnetic Field. The third part: Controlled Thermonuclear Fusion; Nuclear Reactors—A Novel Technology; Particle Accelerators; Frontiers of Aerodynamic Research. Sixteen authors have presented papers on these various subjects.

ANNUAL REVIEW OF NUCLEAR SCIENCE, edited by Emilio Segrè. Vol. 10, 1960. 617 pages, diagrams, 6 × 8¼ in. Palo Alto (Calif.), Annual Reviews, Inc., 1960. Price: $7.00 (U.S.A.); $7.50 (elsewhere).

Eighteen papers are included in this tenth volume of the *Review*. The first paper, "Neutrino Interaction" (by Reines) discusses the role of the neutrino as a direct experimental tool in low-energy and high-energy research programs, and touches on cosmic ray neutrinos and their relation to cosmology. The final paper treats late effects of vertebrate radiobiology (both on man and on animals) such as life shortening, leukemogenesis, and genetic damage. The other sixteen papers discuss a variety of subjects, such as bubble chambers, optics of high-energy beams, subsurface prospecting, cellular radiobiology, and nucleon-nucleon scattering (three papers).

THE FRANKLIN INSTITUTE

MINUTES OF THE STATED MEETING

March 15, 1961

The Stated Meeting of The Franklin Institute was held at 8:15 P.M. in the Lecture Hall, with J. G. Richard Heckscher, Executive Vice President, presiding. Mr. Heckscher called the meeting to order with approximately 400 members and guests present.

Mr. Heckscher stated that the minutes of the Annual Meeting of January 18, 1961 were published in the February issue of the JOURNAL. There being no corrections or additions, the minutes were approved as published. The minutes of the Stated Meeting of February 15, 1961, will be published in the March issue of the JOURNAL and will be presented for approval at the next Stated Meeting of The Institute.

Mr. Heckscher announced that tonight's lecture is the Twelfth Charles Day Lecture. This endowed lectureship was established in June 1941, for the purpose of providing lectures on engineering and science. Mr. Day was a member of The Institute from 1900 and became a life member in 1910. He was a member of the Board of Managers from 1908 to his death in 1931, and Vice President of The Institute from 1920 to 1923.

Mr. Heckscher then introduced the speaker of the evening, Athelstan F. Spilhaus, Dean of the Institute of Technology, University of Minnesota, and an international authority on meteorology and oceanography.

Dean Spilhaus' talk on "Look to the Sea—New Frontiers in Oceanography" included the interesting background of the exploration of the seas and modern methods of exploration. It was illustrated with many explanatory slides.

Dean Spilhaus' talk was enthusiastically received with many questions following the talk.

After thanking Dean Spilhaus for his outstanding talk, Mr. Heckscher adjourned the meeting at 9:20 P.M.

WILLIAM F. JACKSON, JR.
Secretary

MEMBERSHIP ROLL OF HONOR

The following are Gold Card Members, having belonged continuously for fifty years or more. The dates are years of election to membership.

Fred H. Colvin '88
G. H. Clamer '91
J. H. Granberry '95
E. A. Muller '99
James M. Caird '01
Charles H. Howson '03
Frank S. Busser '04
C. Mahlon Kline '04
George R. Hall '05
Darthela Clark '07
W. M. C. Kimber '08
Theobald F. Clark '09
Walton Clark, Jr. '09
James McGowan, Jr. '09
T. Edward Ross '09
Richard P. Brown '10
Joseph S. Hepburn '10
Joseph W. Lippincott '10
J. D. Shattuck '10
J. M. Weiss '10

The following are Silver Members, having belonged continuously for twenty-five years or more. The dates are years of election to membership.

1912
James Barnes
Edwin Elliot
Walter Palmer
Julian S. Simsohn
Howard S. Worrell

1913
Irenee duPont
S. B. Eckert
Ralph E. Flanders
N. E. Funk
Lionel F. Levy
E. Mallinckrodt, Jr.
Frank M. Masters
Franklin P. McConnell
William Maul Measey
W. Chattin Wetherill
D. Robert Yarnall

1914
George S. Crampton
Ernest L. Huff
K. G. Mackenzie
George Wharton Pepper

1915
Thomas D. Cope
H. Jermain Creighton
Thomas W. Elkinton
W. Wallace McKaig

1916
Henry B. Allen
James G. Detwiler
Zay Jeffries
Frank H. Sauer
B. E. Shackelford
Arthur Synnestvedt
Charles N. Weyl

1917
A. D. Chambers
Francis J. Chesterman
Walter S. Crowell
William J. Fitzmaurice, Jr.
Rolfe E. Glover, Jr.
Arthur W. Lowe
Frank S. MacGregor
C. H. Quinn
Sylvan D. Rolle
Robert L. Wood
Henry Woodhouse

1918
Charles H. Colvin
Walter O. Snelling

1919
Charles E. Brinley
Henry Colvin, 2nd
E. A. Eckhardt
George W. Furness
Frank H. Griffin
J. Howard Pew
Edmund G. Robinson
L. K. Sillcox

1920
Chester Lichtenberg
P. S. Lyon
Haviland H. Platt
Carl D. Pratt

1921
Roland L. Andreau
Leonard T. Beale
J. Ed. Brewer
Frederic Palmer, Jr.
Howard Stoertz
James Stokley

1921 (Cont.)
Edward R. Weidlein
S. Weinberg

1922
Joseph F. Greene

1923
Henry Clay Gibson
Howard S. Levy
William C. Melcher, Jr.
John F. Metten
Richard G. Sagebeer
Joseph J. Vogdes

1924
Peter Abrams
T. R. Harrison
Valentine Hiergesell
Karl F. Oerlein
Edward B. Patterson
Nicholas G. Roosevelt
Alfred O. Tate
James Lloyd Weatherwax
Alexander Wilson
William Zimmermann

1925
Jack G. Binswanger
John Graham Foley
J. V. Giesler
C. R. Kraus
H. F. Porter
W. F. G. Swann

1926
Charles B. Bazzoni
Niels Bohr
William Findlay Downs
Henry C. Evans

1926 (Cont.)
Edward L. Forstall
Lewis H. Hendrixson
Alfred L. Loomis
J. H. Manning
Clement B. Newbold
O. M. Patton
Dexter N. Shaw
Sydney L. Wright
Charles S. Wurtz, Jr.

1927
T. K. Cleveland
William DeKrafft
Alfred Iddles
Philip Sporn
Charles A. Stanwick

1928
William R. Dohan
Walton Forstall, Jr.
C. W. Hansell
Walter A. MacNair
Fred P. Nabenhauer
Joseph N. Pew, Jr.
William Rogers, Jr.
Frank N. Speller

1929
N. E. Bonn
Bernard Davis
Rupen Eksergian
Edward C. Haines
Malcolm Lloyd Hayward
Linn Helander
Randal Morgan
Lawrence Saunders
A. Kelvin Smith
I. Melville Stein
William Stericker
Harden Franklin Taylor
Jacques L. Vauclain
Albert J. Williams, Jr.
Arthur M. Wilson, Jr.
Enos E. Witmer

1930
Mildred Allen
William M. Barret
Aldus Fogelsanger
John Gardiner, Jr.
Morton Gibbons-Neff
Norman R. Gibson
Carroll Hodge
Walter J. Lehman
R. P. Long

1930 (Cont.)
S. B. Morehouse
William C. Peterman
G. E. Wiltbank

1931
Charles E. Berger
Carl Breer
Abraham D. Caesar
Daniel B. Curll, Jr.
Edward Dawson
J. Bennett Hill
Frederick C. Holtz
Penrose R. Hoopes
William Melas
Julius Neumueller
Laurence P. Sharples

1932
Arthur Fleischer
William A. Heine
Wynn Laurence LePage
Robert McLean
E. Burke Wilford

1933
George E. Crofoot
George S. Gardner
Walter H. Hartung
Karl S. Howard
Edward R. Hughes
Annetta R. Masland
Ellen-Jarden Nolde
George A. Smith
Floyd T. Tyson
Wilfred H. Wickersham

1934
Add B. Anderson
Leighton F. Appleman
Eleanor Bartol
Thomas Campbell Bagg
Charles G. Berwind
Henry W. Breyer
Reynolds D. Brown, Jr.
Edward Browning
Orville H. Bullitt
Herbert Church
Norbert A. Considine
Jay Cooke
Joseph Curry
Charles D. Dickey
Harold Evans
Philo Taylor Farnsworth
Mrs. Charles Fearon
Kermit Fischer

1934 (Cont.)
Mrs. S. K. Fuller
Mrs. William H. Greene
Mrs. Charles F. Griffith
J. G. Richard Heckscher
Russell P. Heuer
Walter M. Jeffords
William J. Kassimir
M. Albert Linton
H. Gates Lloyd
C. Townsend Ludington
C. H. MacDonald
Orus J. Matthews
Arthur H. Nellen
Arthur Neumann, Jr.
Horace Pettit
Mrs. Edgar Allan Poe
B. Brannan Reath, 2nd
Stanley C. Snow
Julian F. Spiegel
Charles Gormley Stehle
Harry C. Tily, 2nd
Clarence A. Warden, Jr.
Paul T. Warner
Mrs. William White
Miss Marion B. Wood
Mrs. Efrem Zimbalist

1935
Mrs. Daniel Moore Bates
Henry B. Bryans
E. Lewis Burnham
Mrs. Thomas Harvey Dougherty, Jr.
E. D. Doyle
Mrs. Thomas S. Gates
George R. Harrington
Harry C. Hart
R. Sturgis Ingersoll
Leon Levy
John Frederick Lewis, III
Richard W. Lloyd
H. W. Lockwood
W. S. Pardoe
Mrs. E. Florens Rivinus
Walter Roth
Phillip G. Rust
Mrs. Philip T. Sharples
Edward Starr, Jr.
Linwood F. Tice
David Travis
Mrs. J. Rogers Ullrich
S. Dana Weeder
M. Russell Wehr
L. Caspar Wister

NEW BOOKS IN THE FRANKLIN INSTITUTE LIBRARY

MATHEMATICS

Frontiers of Numerical Mathematics, by R. E. Langer. University of Wisconsin Press, 1960.

An Introduction to Homological Algebra, by D. G. Northcott. Cambridge University Press, 1960.

Statistical Theory and Methodology in Science and Engineering, by K. A. Brownlee. Wiley, 1960.

Finite-Difference Methods for Partial Differential Equations, by G. E. Forsythe. Wiley, 1960.

Analog Computation in Engineering Design, by A. E. Rogers. McGraw-Hill, 1960.

PHYSICS

Elementare Schalenstatik, von A. Pflüger. 3. aufl. Springer, 1960.

The Hall Effect and Related Phenomena, by E. Putley. Butterworths, 1960.

Mechanik der Festen Körper, von H. Parkus. Springer, 1960.

Introduction a l'Étude de la Rhéologie, par B. Persoz. Dunod, 1960.

Flammenphotometrie, von R. Hermann. 2. aufl. Springer, 1960.

Strömungslehre, von O. Tietjens. Springer, 1960.

International Conference on Nuclear Structure. Proceedings. University of Toronto Press, 1960.

Electrons and Phonons, by J. M. Ziman. Clarendon Press, 1960.

Mécanique Quantique, par A. Messiah. Dunod, 1959–60.

Radiation Pyrometry and its Underlying Principles of Radiant Heat Transfer. Wiley, 1960.

From Dualism to Unity in Quantum Physics, by A. Landé. Cambridge University Press, 1960.

Introduction to Mechanics, Matter, and Waves. by U. Ingard. Addison-Wesley, 1960.

Classical Electricity and Magnetism, by E. S. Shire. Cambridge University Press, 1960.

On Motion, and on Mechanics, by G. Galilei. University of Wisconsin Press, 1960.

The Theory of Linear Viscoelasticity, by D. R. Bland. Pergamon, 1960.

CHEMISTRY AND CHEMICAL ENGINEERING

International Symposium on Macromolecular Chemistry. Proceedings. Academy of Sciences, 1960.

Kolloidchemie, von J. Stauff. Springer, 1960.

Atomic Radiation and Polymers, by A. Charlesby. Pergamon, 1960.

Classifications of High Polymers, by R. Houwink. Butterworths, 1960.

Symposium on the Mechanical Properties of Intermetallic Compounds, Philadelphia, 1959, edited by J. H. Westbrook. Wiley, 1960.

Symposium on Nonmilitary Defense. American Chemical Society, 1960.

ELECTRICAL ENGINEERING

International Conference on Medical Electronics. Proceedings. Thomas, 1960.

Logique Generale des Systems et des Effects, par A. Ducrocq. Dunod, 1960.

National Symposium on Space Electronics and Telemetry. Proceedings. IRE, 1960.

National Telemetering Conference. Proceedings. IRE, 1960.

National Convention on Military Electronics. Proceedings. IRE, 1960.

Werkstoffe für Elektrische Kontakte, von Albert Keil. Springer, 1960.

Die Wissenschaftlichen Grundlagen der Elektrotechnik, von A. Schönfeld. Springer, 1960.

Electromagnetic Wave Propagation, edited by M. Desirant. Academic, 1960.

Méthodes Modernes d'Étude de Systèmes Asservis, par J. C. Gille. Dunod, 1960.

STATISTICAL THEORY OF SIGNAL DETECTION, by C. W. HELSTROM. Pergamon, 1960.
NATIONAL ELECTRICAL CODE HANDBOOK, revised by Frank Stetka. 10th ed. McGraw-Hill, 1960.
PRINCIPLES OF CONTROL SYSTEMS ENGINEERING, by V. Del Toro. McGraw-Hill, 1960.
THERMOELECTRIC MATERIALS AND DEVICES, edited by Irving B. Cadoff. Reinhold, 1960.
THE CONTROL OF MULTIVARIABLE SYSTEMS, by M. D. Mesarović. Wiley, 1960.
TECHNIK DER MAGNETSPEICHER, von F. Winckel. Springer, 1960.

SPACE SCIENCE

AN INTRODUCTION TO ASTRODYNAMICS, by R. M. Baker. Academic, 1960.
PROPERTIES OF DOUBLE STARS, by L. Binnendijk. University of Pennsylvania Press, 1960.
SPACE TRAJECTORIES, edited by the technical staff, Research Division, Radiation Incorporated. Academic, 1960.
NATIONAL SPECIALISTS MEETING ON GUIDANCE OF AEROSPACE VEHICLES. PROCEEDINGS. IAS, 1960.
DIE ENTSTEHUNG VON STERNEN DURCH KONDENSATION DIFFUSER MATERIE, von G. R. Burbridge. 1960.

MATERIALS SCIENCE

THEORY AND APPLICATION OF FERRITES, by R. F. Soohoo. Prentice-Hall, 1960.
SYMPOSIUM ON NONDESTRUCTIVE TESTING IN THE MISSILE INDUSTRY. American Society for Testing Materials, 1960.
REPORT ON THE ELEVATED-TEMPERATURE PROPERTIES OF ALUMINUM AND MAGNESIUM ALLOYS. American Society for Testing Materials, 1960.

YOU CAN ADVANCE SCIENCE EDUCATION

Today, more than ever before in its 137-year history, there is vital need for The Franklin Institute to effectively promote education in science and technology. It is imperative that we meet this challenge by providing adequate educational opportunities in these fields. This requires vision, objective planning, and money. We have more than enough of the first two requisites, but far too little of the third.

Our programs are aimed at professional scientists and industry, as well as the lay public and young people seeking inspiration and guidance in choosing a career. The Institute's educational programs are impressive. They begin with students in the early grades of our elementary schools and continue throughout an individual's professional or industrial life. With more funds at our disposal, the scope and vigor of these activities could be greatly increased and increasingly effective.

The Franklin Institute is not richly endowed. It is a non-profit organization, depending for encouragement and support on an understanding public. Capable and conservative management assures wise administration of all funds.

Your gift or bequest, large or small, will be deeply appreciated and will be used effectively to broaden the Institute's educational usefulness. There is a warm satisfaction in giving financial support to an organization that has pioneered in, and is dedicated to, the advancement of science and technology.

When property is transferred, title should be in the name of The Franklin Institute of the State of Pennsylvania for the Promotion of the Mechanic Arts.

The Secretary of The Franklin Institute will gladly furnish you with additional information. Write to him at The Franklin Institute, Benjamin Franklin Parkway at Twentieth Street, Philadelphia 3, Pennsylvania.

BARTOL RESEARCH FOUNDATION
M. A. POMERANTZ, DIRECTOR

OBSERVATIONS NEAR THE NORTH AND SOUTH POLES OF BURSTS OF COSMIC RAYS FROM THE SUN*

BY

M. A. POMERANTZ, S. P. DUGGAL[1] AND K. NAGASHIMA[2]

Sudden increases in cosmic-ray intensity, observed rarely since the inception of systematic continuous recording about 25 years ago, provide a powerful basis for investigating fundamental physical and astrophysical problems, especially those relating to the electromagnetic state of interplanetary space. Simultaneously with the associated Hα flare on the sun, major radio outbursts, aurora, and other geomagnetic disturbances also occur. Theories accounting for the various phenomena in terms of direct arrival of particles from the sun, coupled with modulations introduced by the presence of clouds carrying frozen-in magnetic fields, have been proposed (**1**).[3]

Prior to 1951, only four cosmic-ray intensity enhancements had been recorded simultaneously by ground-based equipment at widely separated points on the Earth's surface (**2**). Since then, a network of neutron monitors has evolved following the pioneering development by Simpson of the so-called "pile geometry," comprising a detector of locally-produced nucleons (**3**). In contrast with ionization chambers and meson telescopes, the neutron monitor responds mainly to the progeny of the low energy portion of the primary spectrum. Previously, these instruments have recorded three cosmic-ray intensity increases associated with solar flares. The greatest event of this type occurred on February 23, 1956, when the intensity of the nucleonic component increased by a factor as high as 46 at some locations. The integral magnetic rigidity spectrum of the flare-produced cosmic radiation was very steep, varying approximately according to the relationship $N(>R) = AR^{-7}$ on this occasion (**4**). In this case only, the increase was observed even at equatorial latitudes (**5**), indicating that protons having energies of 15 Bev or higher were produced at or near the surface of the sun.

The Bartol Research Foundation maintains two neutron monitor stations which are currently closest to the north and south geomagnetic poles. The Arctic station at Thule, Greenland (geomagnetic latitude 88° N) has been in operation since August 13, 1957. The two subsequent increases on July 17, 1959, (**6**) and May 4, 1960, (**7**), respectively, were observed there. The Antarctic neutron monitor station at McMurdo Sound (geomagnetic latitude 79° S) was activated on

* This work was supported in part by grants from the National Science Foundation, and was also assisted by the Office of Naval Research.

[1] On leave of absence from Physical Research Laboratory, Ahmedabad, India.

[2] On leave of absence from the Department of Physics, Nagoya University, Japan.

[3] The boldface numbers in parentheses refer to the references appended to this paper.

May 11, 1960. This note constitutes a preliminary report of the first simultaneous observation by these two stations of the sudden arrival of solar-produced cosmic radiation of sufficient energy to be detectable at ground stations.

Two distinct events occurred on November 12 and November 15, 1960, respectively. The relevant data are given in Table I. A number

TABLE I.—*Pressure Corrected Neutron Intensity. Thule and McMurdo.*

Period: Nov. 12–15, 1960
Scaling Factor: 64
Pressure Coefficient: −.98% per mm. Hg

Date	Time U.T.	Hourly Rate Thule	Hourly Rate McMurdo
Nov. 12	0000–0100	329.6	329.7
	0100–0200	335.6	331.4
	0200–0300	331.3	337.6
	0300–0400	330.6	331.0
	0400–0500	328.0	332.7
	0500–0600	332.4	335.6
	0600–0700	331.0	329.2
	0700–0800	332.0	328.9
	0800–0900	328.0	328.9
	0900–1000	337.0	333.4
	1000–1100	325.1	331.7
	1100–1200	333.0	337.9
	1200–1215	338.8	355.6
	1215–1230	334.8	323.1
	1230–1245	326.8	336.2
	1245–1300	326.8	329.3
	1300–1315	316.4	335.6
	1315–1330	324.4	335.6
	1330–1345	340.8	341.8
	1345–1400	356.8	380.6
	1400–1415	398.8	451.2
	1415–1430	398.8	528.7
	1430–1445	438.8	573.7
	1445–1500	515.6	573.7
	1500–1515	563.6	592.4
	1515–1530	547.6	573.1
	1530–1545	559.6	605.5
	1545–1600	567.6	566.8
	1600–1615	598.0	631.2
	1615–1630	581.6	650.5
	1630–1645	528.8	656.8
	1645–1700	508.4	644.3
	1700–1715	473.6	611.8
	1715–1730	494.0	611.8

TABLE I.—*Continued.*

Date	Time U.T.	Hourly Rate Thule	McMurdo
Nov. 12	1730–1745	477.6	573.0
	1745–1800	473.6	560.0
	1800–1815	476.4	553.7
	1815–1830	496.8	553.7
	1830–1845	472.4	553.7
	1845–1900	472.4	496.2
	1900–1915	565.2	560.5
	1915–1930	631.2	573.1
	1930–1945	664.4	605.5
	1945–2000	689.2	650.6
	2000–2015	690.0	657.5
	2015–2030	648.4	
	2030–2045	636.0	
	2045–2100	594.8	
	2100–2115	574.8	534.9
	2115–2130	558.4	547.4
	2130–2145	562.4	534.9
	2145–2200	537.2	521.8
	2200–2215	542.4	529.9
	2215–2230	513.2	516.8
	2230–2245	521.6	536.2
	2245–2300	500.8	478.1
	2300–2315	488.0	491.2
	2315–2330	475.2	471.8
	2330–2345	467.2	459.3
	2345–2400	446.4	446.2
Nov. 13	0000–0015	441.6	446.8
	0015–0030	420.8	414.3
	0030–0045	416.8	427.4
	0045–0100	416.8	414.3
	0100–0115	411.6	401.8
	0115–0130	436.4	395.6
	0130–0145	411.6	395.6
	0145–0200	395.6	388.7
	0200–0215	411.2	395.0
	0215–0230	403.2	375.6
	0230–0245	395.2	375.6
	0245–0300	390.8	388.7
Nov. 15	0000–0015	297.6	293.1
	0015–0030	290.0	286.2
	0030–0045	290.0	286.2
	0045–0100	286.0	279.3
	0100–0115	294.4	293.1
	0115–0130	294.4	299.9

TABLE I.—*Continued.*

Date	Time U.T.	Hourly Rate Thule	Hourly Rate McMurdo
Nov. 15	0130–0145	302.0	293.1
	0145–0200	294.4	279.3
	0200–0215	302.4	286.2
	0215–0230	302.4	286.2
	0230–0245	313.6	306.2
	0245–0300	363.6	374.3
	0300–0315	379.2	435.6
	0315–0330	490.4	462.4
	0330–0345	513.2	483.1
	0345–0400	517.2	503.7
	0400–0415	513.2	523.1
	0415–0430	524.8	509.9
	0430–0445	528.4	523.7
	0445–0500	498.0	496.2
	0500–0515	498.4	509.9
	0515–0530	502.0	482.4
	0530–0545	490.8	476.2
	0545–0600	475.6	455.6
	0600–0615	464.8	442.4
	0615–0630	445.6	449.3
	0630–0645	449.6	421.8
	0645–0700	445.6	421.8
	0700–0715	422.8	422.4
	0715–0730	438.4	395.0
	0730–0745	411.6	415.6
	0745–0800	403.6	381.2
	0800–0815	399.6	388.1
	0815–0830	403.6	354.3
	0830–0845	403.6	395.0
	0845–0900	380.8	374.3
	0900–0915	385.2	381.2
	0915–0930	385.2	381.2
	0930–0945	366.0	374.9
	0945–1000	381.6	340.6
	1000–1015	369.6	361.2
	1015–1030	369.6	354.9
	1030–1045	365.6	341.2
	1045–1100	358.0	354.9
	1100–1115	376.8	348.1
	1115–1130	357.6	354.9
	1130–1145	349.6	334.3
	1145–1200	349.6	341.2
	1200–1215	346.4	327.4
	1215–1230	342.8	334.3
	1230–1245	334.8	340.6

TABLE I.—*Continued.*

Date	Time U.T.	Hourly Rate Thule	McMurdo
Nov. 15	1245–1300	342.8	320.6
	1300–1315	345.6	340.6
	1315–1330	342.0	340.6
	1330–1345	353.2	313.1
	1345–1400	345.6	326.8
	1400–1415	337.6	326.8
	1415–1430	337.6	333.7
	1430–1445	330.0	326.8
	1445–1500	330.0	306.2
	1500–1600	323.4	314.8
	1600–1700	319.2	308.9
	1700–1800	315.1	319.3
	1800–1900	319.3	307.3
	1900–2000	314.8	297.6
	2000–2100	309.7	302.9
	2100–2200	311.0	299.7
	2200–2300	305.3	301.8
	2300–2400	303.0	293.7

of related observations have been reported by various observatories. Region HH25 on the sun produced a flare of Importance 3 on November 10, 1960 (**8, 9**). No cosmic-ray intensity increase was observed at the ground stations in association with this flare. However, 52 hours later, on November 12, a magnetic storm commenced. On the same date, a 3+ flare occurred in the same region of the sun, followed by an increase in the cosmic-ray intensity. Major radio outbursts on frequencies from 55 to 600 MHz, as well as aurora at low latitudes, were also observed on November 12. A Forbush-type decrease in the cosmic-ray intensity, which was detected by meson telescopes and ionization chambers which had revealed no appreciable increase earlier, also commenced on the same day. A sudden commencement geomagnetic storm associated with this flare began about 72 hours later. A second 3+ flare occurred in region HH25 in association with major geomagnetic activity on November 15, 1960, and this also was accompanied by an increase in the intensity of the nucleonic component.

As is seen in Fig. 1, which is a plot of mean bi-hourly counting rates at McMurdo and Thule from November 9 to November 16, 1960, the intensity increased by about 80 per cent on November 12, and by about 70 per cent on November 15. Furthermore, the general intensity level before the onset on November 15 was below that on November 11, characterizing a Forbush-type decrease.

In Figs. 2 and 3, the hourly pressure-corrected counting rate has

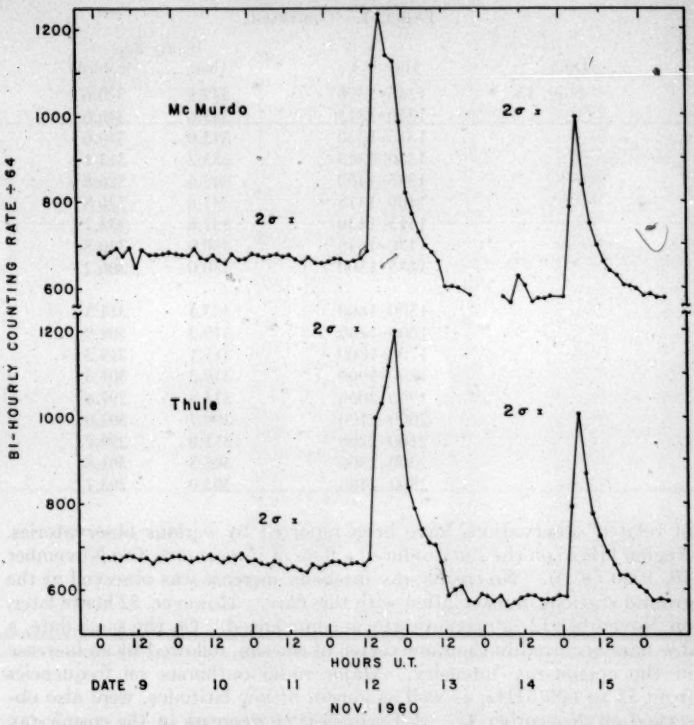

FIG. 1. Mean bi-hourly pressure-corrected counting rates at Thule and McMurdo during the period Nov. 9–15, 1960. The statistical uncertainties at various times are indicated by the 2σ symbols.

been plotted in 15-minute intervals. Figure 2 shows that, before these events, the nucleonic intensity was approximately the same at the two stations. The data have not been normalized, and the agreement between the absolute counting rates at Thule and McMurdo is significant since control has been exercised to insure that the sensitivity of both of the neutron monitors is the same.

On November 12, the intensity increase displayed a two-hump structure. This unprecedented shape was observed at most of the stations from which data have been received thus far. A similar double hump characteristic is not present in either the Hα photometric

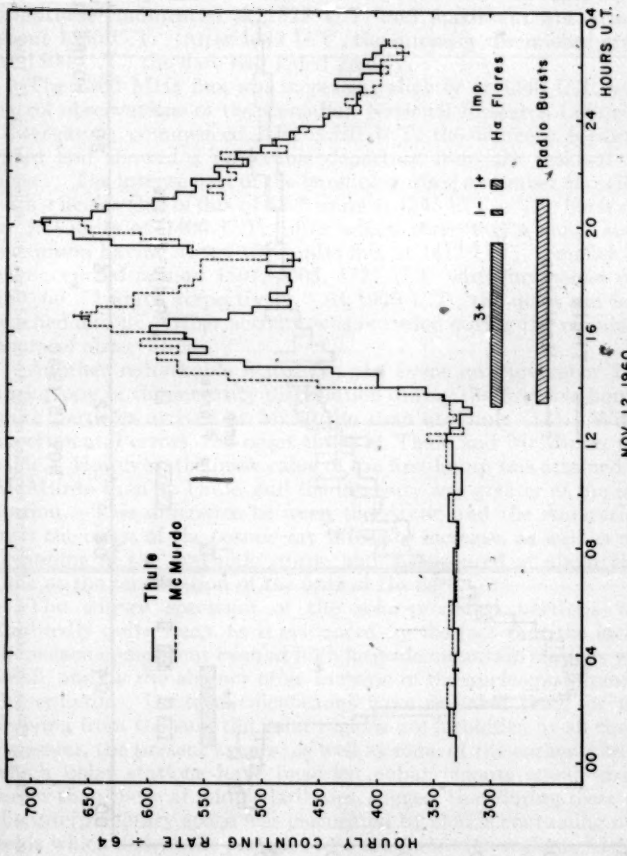

FIG. 2. Histograms representing the counting rates at Thule and McMurdo on Nov. 12, 1960, plotted in 15-minute intervals. The data have been pressure-corrected, but not normalized.

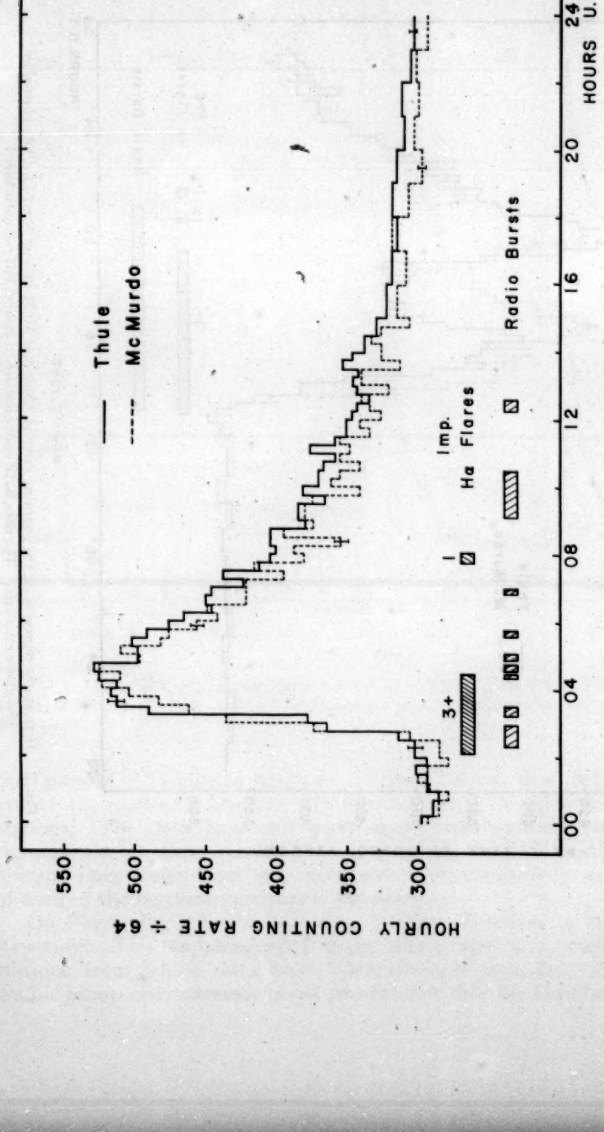

FIG. 3. Plot, in 15-minute intervals, of the data recorded at the Arctic and Antarctic stations on Nov. 15, 1960.

measurements (10) or in the 2800 MHz flux records (11). Observations at the McMath-Hulbert Observatory show that the flare began to brighten quite gradually around 1317 to 1322 U.T. A rapid increase in brightness commenced at 1325 U.T. and maximum was attained at about 1330 U.T. After 1342 U.T., the intensity diminished gradually. At 1500 U.T., the flare had faded greatly.

The 2800 MHz flux was increasing slightly at 1240 U.T. when the patrol observations of the Canadian National Research Council Radio Observatory commenced. By 1320 U.T. the increase became more rapid and showed a noticeable departure from the residual receiver noise. The intense part of the burst comprised a number of oscillations, with a peak value of flux of 5500 units at 1345 U.T. The burst declined to 300 units at 1406 U.T., after which there was a small secondary maximum having about 1500 units flux at 1412 U.T. Smaller maxima also occurred around 1507, 1603, 1727 U.T. with flux values of about 180, 66, 72 units, respectively. At 1900 U.T., the quiet sun level was reached and no further activity was recorded during the remaining two hours of observations.

Another remarkable feature of the event on November 12 is the anisotropy in the intensity distribution during the first five hours when more particles arrived at McMurdo than at Thule (12). Within the experimental errors, the onset times at Thule and McMurdo were the same. However, the peak value of the first hump was attained later at McMurdo than at Thule, and the intensity was greater at the southern station. This difference between the Arctic and the Antarctic set in near the onset of the cosmic ray intensity increase, as well as near the beginning of the magnetic storm, and disappeared at about the same time as the termination of the optical Hα flare.

The energy spectrum of the solar-produced particles was undoubtedly quite steep, as is evidenced by the fact that the increase in the meson component even at high latitude mountain stations was very small, and by the absence of an increase in the nucleonic intensity near the equator. Detailed calculations have revealed that, for particles arriving from the sun, the polar regions are forbidden at all times (13). However, the present events, as well as some of the earlier increases, in which polar stations have recorded enhancements equal to or even larger than those at middle latitudes, suggest that during these periods, the interplanetary space was permeated by clouds containing magnetic fields which deflect the particles into the forbidden regions. It appears that during the event of November 12, the Earth was located near the boundary of a modulating region which later completely surrounded the Earth.

A detailed analysis of these events involving a comparison among the data recorded at many stations is now in progress.

Acknowledgments

We are grateful to the following colleagues for promptly transmitting their cosmic-ray data: D. C. Rose (Canada), Resolute, Ottawa, Sulphur Mountain, Churchill; J. A. Simpson (U. S. A.), Chicago; K. G. McCracken (U. S. A.), M.I.T.; T. Thambyahpillai (England), London; A. E. Sandström (Sweden), Uppsala; H. Carmichael and J. F. Steljes (Canada), Deep River; V. I. Escobar (Bolivia), LaPaz; G. Schwachheim and R. Palmeira (Brazil), Rio de Janiero; J. R. Manzano (Argentina), Ellsworth; and J. Hladky and P. Mokry (Czechoslovakia), Praha.

We also wish to thank Robert Clements of New Zealand for providing tracings of the magnetograms recorded at neighboring Scott Base, Antarctica, and Dr. H. D. Prince and Dr. A. E. Covington for their data and comments.

It is a pleasure to acknowledge the important contributions to the program by Hugo A. C. Neuburg and Jamie Chapman who were in charge of the stations at McMurdo and Thule, respectively. Appreciation is expressed to the Geophysics Research Directorate for maintaining the Arctic station at its Polar Research Facility, operated by the American Geographical Society under contract with the U. S. Air Force. The Antarctic station is part of the U. S. Antarctic Research Program.

REFERENCES

(1) See, for example, W. R. WEBBER, "Time Variations of Low Rigidity Cosmic Rays during the Recent Sunspot Cycle," *Prog. Cosmic Ray Physics*, Vol. 6, in press.

(2) See, for example, H. ELLIOT, "Time Variations of Cosmic Ray Intensity," *Prog. Cosmic Ray Physics*, Vol. I, Chapter VIII, 1952.

(3) J. A. SIMPSON, W. FONGER AND S. B. TREIMAN, "1. Neutron Intensity Variation Method and Meteorological Factors," *Phys. Rev.*, Vol. 90, p. 934 (1953).

(4) P. MEYER, E. N. PARKER AND J. A. SIMPSON, "Solar Cosmic Rays of February, 1956 and their Propagation through Interplanetary Space," *Phys. Rev.*, Vol. 104 (3), p. 768 (1956).

(5) V. SARABHAI, S. P. DUGGAL, H. RAZDAN AND T. S. G. SASTRY, "A Solar Flare Type Increase in Cosmic Rays at Low Latitudes," *Proc. Ind. Acad. of Sci.*, Vol. 43A, No. 5, p. 309 (1956).

(6) D. K. BAILEY AND M. A. POMERANTZ, "The Cosmic Ray Increase of 17 July 1959," *Can. J. Phys.*, Vol. 38, p. 332 (1960).

(7) M. A. POMERANTZ AND V. R. POTNIS, "Solar-Produced Cosmic Radiation near the Geomagnetic Pole on May 4, 1960," JOUR. FRANKLIN INST., Vol. 270, p. 227 (1960).

(8) "Flares and Flare-associated Events 11–17 Nov. 1960," preliminary report of solar activity, High Altitude Observatory, Boulder, Colorado, TR 481, Nov. 18, 1960.

(9) R. HANSEN AND D. E. TROTTER, "Solar Activity Associated with the Great Flare of 12 November 1960," private communication.

(10) H. D. PRINCE, private communication.

(11) A. E. COVINGTON, G. A. HARVEY AND L. R. MCNARRY, "The Solar Noise Burst of November 12, 1960," *Can. J. Physics*, to be published.

(12) M. A. POMERANTZ, S. P. DUGGAL AND K. NAGASHIMA, "Solar Produced Cosmic Rays near the North and South Poles," *Phys. Rev. Letters*, Vol. 6, p. 123 (1961).

(13) A. SCHLÜTER, *Z. Naturforsch*, Vol. 6a, p. 613 (1951).

BARTOL RESEARCH FOUNDATION
M. A. POMERANTZ, DIRECTOR

UNUSUAL INCREASE IN THE COSMIC RAY INTENSITY ON NOVEMBER 20, 1960*

BY

M. A. POMERANTZ AND S. P. DUGGAL

The history of observations of sudden increases in cosmic ray intensity, and the particular significance of data from the polar regions, have been outlined in an accompanying note (1).[1] A small but interesting event was detected by both the Arctic and Antarctic stations at about 2100 U.T. on November 20, 1960, and the relevant data are presented herewith.

The bi-hourly pressure-corrected counting rates at McMurdo and Thule from November 16 to November 30, 1960 have been plotted in Fig. 1. The slope of the curve on November 16–18 characterizes the recovery following a Forbush type decrease. The maximum intensity during the last 2-hour interval on November 20 is greater than that before or after this period at both stations. The data are listed in Table I. Figure 2 displays deviations from the pre-event level at the

TABLE I.—*Neutron Intensity—Thule and McMurdo.*

Period: Nov. 16–30, 1960
Scaling factor: 64
Pressure coefficient: −.98% per mm. Hg

Date	Time U.T.	Bi-hourly Counting Rate Thule	McMurdo
Nov. 16	0000–0200	595.1	580.0
	0200–0400	575.9	579.9
	0400–0600	577.5	577.2
	0600–0800	576.0	576.1
	0800–1000	600.3	577.8
	1000–1200	585.0	585.3
	1200–1400	599.4	596.9
	1400–1600	600.4	595.2
	1600–1800	597.6	585.7
	1800–2000	594.3	597.2
	2000–2200	589.4	599.2
	2200–2400	583.7	591.6
Nov. 17	0000–0200	601.0	595.7
	0200–0400	596.2	604.6
	0400–0600	597.0	605.6
	0600–0800	607.5	608.5

* This work was supported in part by grants from the National Science Foundation, and was also assisted by the Office of Naval Research.

[1] The boldface numbers in parentheses refer to the references appended to this note.

TABLE I.—*Continued.*

Date	Time U.T.	Bi-hourly Counting Rate Thule	McMurdo
Nov. 17	0800–1000	597.4	604.7
	1000–1200	610.7	611.0
	1200–1400	606.0	621.7
	1400–1600	609.7	611.8
	1600–1800	609.0	624.8
	1800–2000	604.8	605.9
	2000–2200	600.8	603.5
	2200–2400	613.2	614.5
Nov. 18	0000–0200	610.4	619.9
	0200–0400	618.6	615.9
	0400–0600	613.8	606.7
	0600–0800	617.7	631.5
	0800–1000	624.7	624.1
	1000–1200	630.5	632.9
	1200–1400	628.3	633.9
	1400–1600	626.2	644.4
	1600–1800	626.7	641.4
	1800–2000	627.1	651.3
	2000–2200	627.7	653.3
	2200–2400	636.5	634.6
Nov. 19	0000–0200	632.5	638.2
	0200–0400	637.4	635.9
	0400–0600	630.3	648.0
	0600–0800	625.8	641.5
	0800–1000	621.9	632.3
	1000–1200	630.8	629.9
	1200–1400	618.6	634.2
	1400–1600	632.9	626.3
	1600–1800	620.7	633.2
	1800–2000	614.3	634.2
	2000–2200	626.4	633.2
	2200–2400	636.5	639.0
Nov. 20	0000–0200	635.2	634.6
	0200–0400	620.4	633.6
	0400–0600	626.4	650.3
	0600–0800	632.6	645.1
	0800–1000	628.9	651.7
	1000–1200	636.3	637.8
	1200–1400	622.9	642.8
	1400–1600	627.8	640.5
	1600–1800	630.4	655.3
	1800–2000	624.5	658.2
	2000–2200	638.2	658.8
	2200–2400	664.2	705.5

TABLE I.—*Continued.*

Date	Time U.T.	Bi-hourly Counting Rate Thule	McMurdo
Nov. 21	0000–0200	653.0	658.5
	0200–0400	653.6	660.0
	0400–0600	652.6	668.4
	0600–0800	632.1	657.2
	0800–1000	639.8	657.6
	1000–1200	643.1	649.7
	1200–1400	639.4	660.9
	1400–1600	636.1	664.1
	1600–1800	629.9	624.0
	1800–2000	647.4	666.5
	2000–2200	634.1	650.1
	2200–2400	626.7	646.7
Nov. 22	0000–0200	634.3	638.3
	0200–0400	641.8	639.2
	0400–0600	637.9	649.9
	0600–0800	634.1	640.4
	0800–1000	640.5	623.7
	1000–1200	643.2	630.6
	1200–1400	635.4	627.6
	1400–1600	638.2	628.7
	1600–1800	638.0	632.3
	1800–2000	644.9	622.6
	2000–2200	637.0	636.0
	2200–2400	632.1	
Nov. 23	0000–0200	635.5	
	0200–0400	626.5	
	0400–0600	638.0	
	0600–0800	640.0	624.3
	0800–1000	626.7	629.7
	1000–1200	642.5	629.9
	1200–1400	633.0	631.1
	1400–1600	638.1	635.5
	1600–1800	637.1	642.7
	1800–2000	641.6	635.4
	2000–2200	641.0	
	2200–2400	634.1	
Nov. 24	0000–0200	642.6	644.7
	0200–0400	635.9	624.0
	0400–0600	657.4	644.0
	0600–0800	637.4	630.8
	0800–1000	631.4	638.1
	1000–1200	634.5	637.0
	1200–1400	629.9	638.2

TABLE 1.—*Continued.*

Date	Time U.T.	Bi-hourly Counting Rate Thule	McMurdo
Nov. 24	1400–1600	629.8	632.4
	1600–1800	641.6	637.4
	1800–2000	635.2	640.1
	2000–2200	627.8	620.3
	2200–2400	634.7	659.6
Nov. 25	0000–0200	623.7	653.6
	0200–0400	627.2	632.5
	0400–0600	624.8	636.7
	0600–0800	629.0	630.9
	0800–1000	625.9	638.8
	1000–1200	637.2	634.7
	1200–1400	638.4	632.6
	1400–1600	638.0	631.6
	1600–1800	649.4	635.7
	1800–2000	639.2	637.0
	2000–2200	649.2	645.7
	2200–2400	642.9	655.3
Nov. 26	0000–0200	655.7	650.6
	0200–0400	645.6	661.1
	0400–0600	653.8	647.6
	0600–0800	645.0	645.4
	0800–1000	641.3	638.6
	1000–1200	649.5	643.4
	1200–1400	657.7	642.2
	1400–1600	651.4	652.9
	1600–1800	653.4	645.7
	1800–2000	645.6	657.5
	2000–2200	650.1	647.9
	2200–2400	653.8	650.4
Nov. 27	0000–0200	665.1	650.6
	0200–0400	652.2	647.6
	0400–0600	663.7	645.0
	0600–0800	651.9	653.7
	0800–1000	664.0	658.0
	1000–1200	655.8	648.8
	1200–1400	655.1	652.6
	1400–1600	658.6	655.0
	1600–1800	659.7	647.2
	1800–2000	663.8	644.7
	2000–2200	659.1	654.1
	2200–2400	660.1	649.9

TABLE I.—*Continued.*

Date	Time U.T.	Bi-hourly Counting Rate Thule	McMurdo
Nov. 28	0000–0200	669.9	665.4
	0200–0400	656.3	665.7
	0400–0600	665.7	661.5
	0600–0800	648.6	668.8
	0800–1000	654.7	666.1
	1000–1200	657.6	659.0
	1200–1400	657.2	651.7
	1400–1600	669.1	659.7
	1600–1800	658.3	647.1
	1800–2000	656.7	654.0
	2000–2200	654.8	656.0
	2200–2400	644.1	642.6
Nov. 29	0000–0200		648.6
	0200–0400		654.1
	0400–0600		639.7
	0600–0800		639.2
	0800–1000		648.4
	1000–1200		645.3
	1200–1400		647.4
	1400–1600	661.8	640.7
	1600–1800	665.1	637.6
	1800–2000	658.0	643.2
	2000–2200	660.9	639.0
	2200–2400	655.0	642.5
Nov. 30	0000–0200	656.7	643.9
	0200–0400	653.2	651.3
	0400–0600	661.7	650.6
	0600–0800	659.1	650.0
	0800–1000	655.8	661.9
	1000–1200	662.6	645.8
	1200–1400	657.2	655.1
	1400–1600	661.6	647.1
	1600–1800	662.3	647.1
	1800–2000	661.0	651.9
	2000–2200	655.0	638.6
	2200–2400	648.4	644.6

two stations. The percentage differences from the initial counting rates during hourly intervals are summarized in Table II. The pre-event level has been defined as the mean hourly counting rate, corrected for pressure, during the period 0000 to 1000 U.T. on November 20, 1960.

Figure 2 reveals that the maximum amplitude was attained at both stations between 2200 and 2300 U.T. Although the increase is rela-

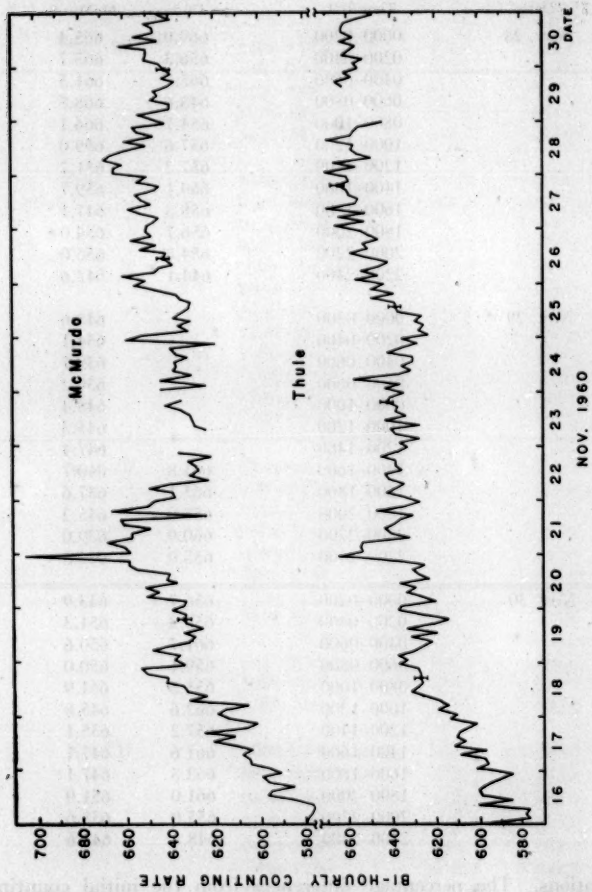

FIG. 1. Pressure-corrected bi-hourly counting rates at McMurdo and Thule.

TABLE II.—*Deviations at Thule and McMurdo, in Percentage of Pre-increase Level.*

Period: Nov. 20–21, 1960

Date	Time U.T.	Percentage Deviation Thule	McMurdo
Nov. 20	0900–1000	+2.3	+0.7
	1000–1100	+1.8	+1.3
	1100–1200	0	−3.0
	1200–1300	−0.5	−0.5
	1300–1400	−2.0	+0.1
	1400–1500	−0.6	−1.1
	1500–1600	−0.1	+0.5
	1600–1700	+0.1	+1.1
	1700–1800	+0.1	+2.7
	1800–1900	−1.6	+3.0
	1900–2000	−0.4	+2.9
	2000–2100	−1.1	+4.0
	2100–2200	+3.5	+6.6
	2200–2300	+6.3	+10.4
	2300–2400	+4.2	+6.2
Nov. 21	0000–0100	+5.2	+1.9
	0100–0200	+1.6	−0.2
	0200–0300	+3.5	+2.6
	0300–0400	+5.6	+2.7
	0400–0500	+3.7	+2.6
	0500–0600	+3.0	+5.3
	0600–0700	−0.1	+2.1
	0700–0800	+0.3	+2.4
	0800–0900	+2.7	+2.1
	0900–1000	−0.1	+2.5
	1000–1100	+2.7	+0.2
	1100–1200	+1.0	+2.0
	1200–1300	+1.2	+1.2
	1300–1400	+1.2	+4.4
	1400–1500	+0.8	+4.3
	1500–1600	+0.8	+2.3
	1600–1700	−1.0	+1.1
	1700–1800	+0.5	+2.5

tively small, the difference between the maximum deviation at McMurdo (10.4 per cent) and that at Thule (6.3 per cent) is statistically significant, and indicates an anisotropy in the flux reaching the north and south polar regions.

No major flare activity has been reported on November 20 (2). Lockheed Observatory reported a flare of Importance I from 2017 to 2024 U.T. Sacramento Peak Observatory reported a flare of Impor-

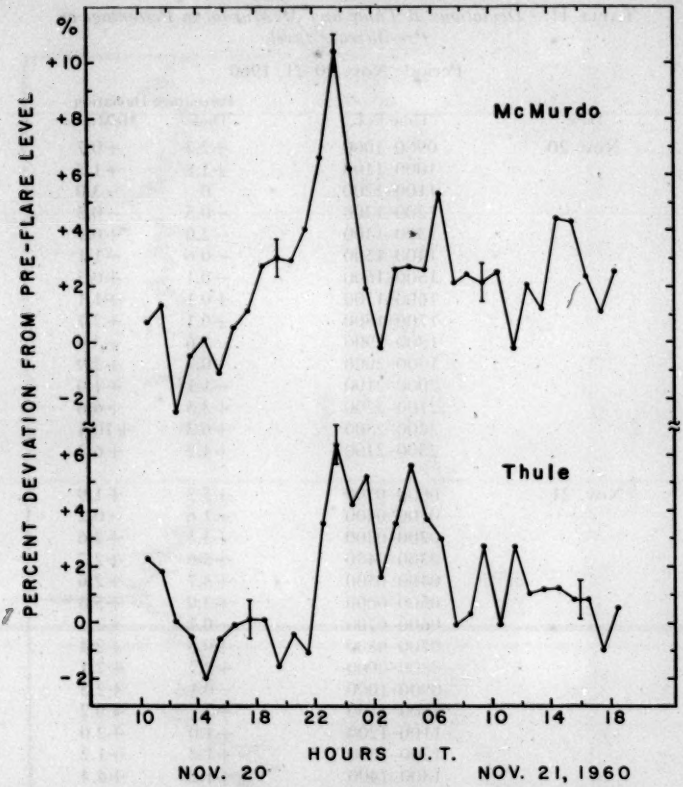

FIG. 2. Percentage deviations from the pre-event level during hourly intervals at McMurdo and Thule.

tance I from 2106 to 2143 U.T. An extremely interesting explosive limb flare was observed from 2126 to 2258 U.T. (3). The ejected cloud in this case had apparent radial velocities of about 1000 km/sec. However, Covington and Harvey (4) have attributed the solar radio burst at 10.7 cm. which commenced at 2023 U.T. and attained a peak of 400 units, to a solar flare on the far side of the sun. Carmichael *et al.* (5) have also interpreted the cosmic ray records as evidence for the occurrence of a cosmic ray increase in association with a flare on the unseen side of the sun. They have postulated that the region HH25, which

produced solar flares on November 10, 12, and 15, was also the site of a flare on November 21 when this region was at 120° W of the central meridian, that is, 30° behind the limb.

REFERENCES

(1) M. A. POMERANTZ, S. P. DUGGAL AND K. NAGASHIMA, "Observations Near the North and South Poles of Bursts of Cosmic Rays from the Sun," see this issue of the JOURNAL, p. 317.

(2) Solar-Geophysical Data—December 1960, U. S. Dept. of Commerce CRPL-F 196 Part B, Boulder, Colo.

(3) R. HANSEN AND D. E. TROTTER, "Solar Activity Associated with the Great Flare of 12 Nov., 1960," private communication.

(4) A. E. COVINGTON AND G. A. HARVEY, "10.7-cm. Solar Noise Burst of November 20, 1960," *Phys. Rev. Letters*, Vol. 6, No. 2, p. 51 (1961).

(5) H. CARMICHAEL, J. F. STELJES, D. C. ROSE AND B. G. WILSON, "Cosmic-ray Neutron Increase from a Flare on the Far Side of the Sun," *Phys. Rev. Letters*, Vol. 6, No. 2, p. 49 (1961).

THE FRANKLIN INSTITUTE LABORATORIES
J. G. RICHARD HECKSCHER, ACTING DIRECTOR

NOTE ON A VARIATIONAL APPROACH TO THE THEORY OF COMPOSITE ELASTIC MATERIALS*

BY

Z. HASHIN[1] AND S. SHTRIKMAN[2]

The problem of the determination of the effective moduli of two-phase composite materials has received considerable attention (1).[3] Here a method for obtaining bounds on the effective moduli is outlined and results of its application to the case of two phase linear elastic and isotropic materials are given.

The question that immediately arises is: Are the effective moduli determined by the moduli of the phases and their fractional volumes? It has been shown by Brown (2) that the effective magnetic permittivity of isotropic two-phase materials is not completely defined by such information and that the statistical details of phase configurations influence the results. A similar result can be expected in the present case. Accordingly the present work is concerned with the construction of bounds on the moduli that are independent of the statistics, assuming that the composite material is isotropic.

These bounds are obtained by using some variational principles in the theory of elasticity for linear and isotropic materials which will now be formulated (3):

Assume that in a deformed elastic body of volume V and boundary surface S, the stress and strain tensor components are related by Hooke's law

$$\sigma_{ij}^{(0)} = \lambda_0 \epsilon_{kk}^{(0)} \delta_{ij} + 2G_0 \epsilon_{ij}^{(0)} = L_0(\epsilon_{ij}^{(0)}). \tag{1}$$

Here λ_0 and G_0 are the Lamé constant and the shear modulus which for simplicity are taken to be constant throughout the body. The index range is 1, 2, 3, a repeated index denotes summation, and δ_{ij} are the Kronecker delta. The strains are given in terms of the elastic displacement components u_i, by

$$\epsilon_{ij}^{(0)} = \tfrac{1}{2}(u_{i,j}^{(0)} + u_{j,i}^{(0)}) \tag{2}$$

where a comma denotes differentiation.

* The authors gratefully acknowledge the support by the Air Force Office of Scientific Research of the Air Research and Development Command and by the office of Naval Research.

[1] The University of Pennsylvania, Philadelphia, Pa., on leave of absence from the Technion-Israel Institute of Technology, Haifa, Israel.

[2] The Franklin Institute Laboratories for Research and Development, Philadelphia, Pa., on leave of absence from the Weizmann Institute of Science, Rehovot, Israel.

[3] The boldface numbers in parentheses refer to the references appended to this paper.

Let the surface displacements $u_i^{(0)} = u_i^{(0)}(S)$ be prescribed on the surface of the body and let part or whole of the body now be changed to material of different constants λ and G which may vary in space, the surface displacements being held fixed.

Define the stress polarization tensor[4] p_{ij} by

$$\sigma_{ij} = L_0(\epsilon_{ij}) + p_{ij}. \tag{3}$$

Here σ_{ij} and ϵ_{ij} are the stress and strain tensor components in the changed body.

Define

$$\epsilon'_{ij} = \epsilon_{ij} - \epsilon_{ij}^{(0)} \tag{4}$$

and

$$u'_i = u_i - u_i^{(0)}. \tag{5}$$

Then the volume integral

$$U_p = \tfrac{1}{2}\int_{(V)} [\sigma_{ij}^{(0)}\epsilon_{ij}^{(0)} - p_{ij}H(p_{ij}) + p_{ij}\epsilon'_{ij} + 2p_{ij}\epsilon_{ij}^{(0)}]dV \tag{6}$$

is stationary for

$$p_{ij} = L(\epsilon_{ij}) - L_0(\epsilon_{ij}) \tag{7}$$

subject to the subsidiary condition

$$[L_0(\epsilon'_{ij})]_{,j} + p_{ij,j} = 0 \tag{8}$$

and the boundary condition

$$u'_i(S) = 0. \tag{9}$$

The operator L in Eq. 7 is equivalent to Hooke's law in terms of λ and G. The operator H in Eq. 6 is given by

$$H = (L - L_0)^{-1}. \tag{10}$$

Accordingly in Eq. 6

$$p_{ij}H(p_{ij}) = -\frac{\lambda - \lambda_0}{2(G - G_0)[3(\lambda - \lambda_0) + 2(G - G_0)]}p_{kk}^2 + \frac{1}{2(G - G_0)}p_{ij}p_{ij}. \tag{11}$$

[4] The polarization tensor has been introduced into the theory of elasticity by Eshelby (4). The name has been coined by Kroener (5) in analogy to the polarization vector in electrostatics.

Equation 8 expressed in terms of the u'_i, defined in Eq. 5, assumes the form

$$(\lambda_0 + G_0)u'_{j,ji} + G_0 u'_{i,jj} + p_{ij,j} = 0. \tag{12}$$

The stationary value of the expression U_p is an absolute maximum when $\lambda > \lambda_0$, $G > G_0$ and an absolute minimum when $\lambda < \lambda_0$, $G < G_0$. Furthermore, it is equal to the strain energy stored in the changed body.

Analogous variational theorems have been established when instead of surface displacements, surface tractions are prescribed. In this case a strain polarization tensor is defined and the subsidiary condition involves the differential operators of the compatibility equations of the theory of elasticity.

For application of these theorems consider a two phase isotropic and quasi-homogeneous material of volume V which consists of two phases of volumes V_1 and V_2. The fractional volumes of these are denoted by v_1 and v_2 where

$$v_1 + v_2 = 1. \tag{13}$$

Let λ_1, G_1 and λ_2, G_2 be the elastic moduli of the phases, where $\lambda_2 > \lambda_1$ and $G_2 > G_1$, and $p_{ij}^{(1)}$ and $p_{ij}^{(2)}$ the stress polarization components in them. For convenience the bulk modulus defined by

$$K = \lambda + \tfrac{2}{3}G \tag{14}$$

is now introduced.

The effective bulk modulus K^* is defined as follows: Let a displacement

$$u_i^{(0)} = \epsilon^{(0)} x_i \tag{15}$$

be applied to the boundary of the composite body, where the x_i are cartesian coordinates and $\epsilon^{(0)}$ is a constant. The strain energy U^* of the body is then taken to be given by

$$U^* = \tfrac{9}{2}K^* \epsilon^{(0)2} V. \tag{16}$$

With reference to the variational formulation it is now assumed that

$$\begin{aligned} K_0 &= K_1 \\ K &= K_2 \end{aligned} \tag{17}$$

$$\begin{aligned} p_{ij}^{(1)} &= 0 \\ p_{ij}^{(2)} &= p\delta_{ij} \end{aligned} \tag{18}$$

where p is a constant.

Introducing Eqs. 17 and 18 into Eq. 6 and taking into account Eq. 12 the following result is obtained

$$U_p = \tfrac{1}{2}\left[9K_1\epsilon^{(0)2} - \frac{p^2v_2}{K_2 - K_1} - \frac{p^2v_1v_2}{\frac{4}{3}G_1 + K_1} + 6p\epsilon^{(0)}v_2\right] \leq U^*. \quad (19)$$

The third term in Eq. 19, which corresponds to the third term in Eq. 6, requires some comment. It can be derived by solving Eq. 12 subject to Eq. 9 by Fourier methods as in an analogous magnetic problem (6). Introducing Eq. 16 into Eq. 19, a lower bound on K^* is obtained. The highest lower bound is found when U_p in Eq. 19 is maximized with respect to p. The result is

$$K^* \geq K_1 + \frac{v_2}{\dfrac{1}{K_2 - K_1} + \dfrac{3v_1}{3K_1 + 4G_1}} = K_1^*. \quad (20)$$

To find an upper bound it is assumed that

$$\begin{aligned} K_0 &= K_2 \\ K &= K_1 \end{aligned} \quad (21)$$

$$\begin{aligned} p_{ij}^{(1)} &= p\delta_{ij} \\ p_{ij}^{(2)} &= 0. \end{aligned} \quad (22)$$

It follows by the same procedure that the lowest upper bound is given by

$$K^* \leq K_2 + \frac{v_1}{\dfrac{1}{K_1 - K_2} + \dfrac{3v_2}{3K_2 + 4G_2}} = K_2^*. \quad (23)$$

By a similar procedure it is possible to obtain bounds on the effective shear modulus. In this case a shear displacement of the form

$$\begin{aligned} u_1^{(0)} &= \tfrac{1}{2}\gamma^{(0)}x_2 \\ u_2^{(0)} &= \tfrac{1}{2}\gamma^{(0)}x_1 \\ u_3^{(0)} &= 0 \end{aligned} \quad (24)$$

is applied to the boundary, where $\gamma^{(0)}$ is a constant. The effective shear modulus G^* is then defined by the strain energy expression

$$U^* = \tfrac{1}{2}G^*\gamma^{(0)2}V. \quad (25)$$

In this case the non-zero stress polarization components are chosen in the form of a shear stress in the 1, 2 directions. Continuing as for the bulk modulus the following bounds are obtained.

$$G_1^* = G_1 + \frac{v_2}{\dfrac{1}{G_2 - G_1} + \dfrac{6\,(K_1 + 2G_1)v_1}{5\,(3K_1 + 4G_1)G_1}} \tag{26}$$

$$G_2^* = G_2 + \frac{v_1}{\dfrac{1}{G_1 - G_2} + \dfrac{6\,(K_2 + 2G_2)v_2}{5\,(3K_2 + 4G_2)G_2}} \tag{27}$$

$$G_1^* \leq G^* \leq G_2^*. \tag{28}$$

It should be emphasized that the bounds for the moduli do not depend on the geometry of structure of the composite material, the only assumptions being isotropy and quasi-homogeneity.

It can furthermore be shown that the bounds for the bulk modulus are the most restrictive ones that can be obtained in terms of phase constants and fractional volumes. This is done by proving that for certain phase configurations, K_1^* and K_2^* given in Eqs. 20 and 23 are exact expressions for K^*.

For this purpose consider composite spheres each of which consists of an inner sphere of one phase surrounded by a concentric spherical shell of the second phase, the volume ratio of the two phases being fixed in all spheres. Let a body be completely filled with composite spheres (this is possible if no size restriction is imposed). In the case when the inner spheres are of phase two and the shells of phase one, then

$$K^* = K_1^*. \tag{29}$$

If the materials are interchanged, then

$$K^* = K_2^*. \tag{30}$$

This follows by a method used by Hashin (1) employing the minimum potential energy and minimum complementary energy principles of the theory of elasticity.

The difference between the bounds on the moduli given here increases with the difference between the phase moduli. However, for quite a number of cases of practical interest the difference between them is small. Good agreement has been obtained with experimental results of Nishimatsu and Gurland for a cobalt-tungsten carbide alloy (7). In this case

$$\frac{K_2}{K_1} = 2.4 \qquad \frac{G_2}{G_1} = 3.6.$$

The maximum difference between the bounds was found to be 6 per cent of the average for the bulk modulus and 7 per cent for the shear modulus.

REFERENCES

(1) For references to earlier work see for example: Z. HASHIN, "The Elastic Moduli of Heterogeneous Materials," Office of Naval Research, Nonr 1866(02) TR9 Div. Engng. Appl. Phys. Harvard University, 1960.

(2) W. F. BROWN, JR., "Solid Mixture Permittivities," *J. Chem. Phys.*, Vol. 23, No. 8, pp. 1514–1517 (1955).

(3) Analogous principles have been formulated by the authors for magnetostatic fields. These are an extension of a variational theorem formulated by W. F. Brown, Jr., in a private communication.

(4) J. D. ESHELBY, "The Determination of the Elastic Field of an Ellipsoidal Inclusion and Related Problems," *Proc. Roy. Soc.* (*London*), Ser. A, Vol. 241, pp. 376–396 (1957).

(5) E. KROENER, "Berechnung der elastischen Konstanten des Vielkristalls aus den Konstanten des Einkristalls," *Z. f. Physik*, Vol. 151, pp. 504–518 (1958).

(6) L. NEEL, "La loi d'approche an $a:H$," *J. de Physique*, Vol. 9, pp. 184–192 (1948).

(7) C. NISHIMATSU AND J. GURLAND, "Experimental Survey of the Deformation of the Hard-Ductile Two Phase Alloy System WC-Co," Preprint No. 155, 41st Ann. Convention Am. Soc. Metals, Chicago, 1959.

THE FRANKLIN INSTITUTE LABORATORIES
J. G. RICHARD HECKSCHER, ACTING DIRECTOR

COOK-OFF IN AIRCRAFT GUNS*

BY

GUNTHER COHN[1]

Cook-off is the explosion of ammunition caused by absorption of heat from its surroundings. Whereas it was once a vexing problem in aircraft guns, it is now on the brink of control. The solution: a new seal, called a ring seal, which seals the propellant gases effectively and prevents excessive heating of the gun.

The Air Force constantly strives to have its fighter planes carry more rounds per mission and deliver them at higher rates of firing. When a rapid firing burst ceases, the live round, already in place for the next shot, will absorb heat from the chamber walls and transmit this heat to propellant and explosives. Too high a temperature, for too long, for a given quantity of explosive will cause cook-off. Cook-off is a serious accident that may damage not only the weapon but also aircraft and personnel.

Among its latest aircraft guns, the Air Force employs two high-rate-of-fire 20 mm weapons. The M39A2 (Fig. 1) is an automatic gun of

U. S. Army Photograph, Springfield Armory, Ordnance Corps

FIG. 1. The automatic aircraft gun, 20 mm M39A2, achieves high fire power with a drum of five chambers.

the revolver type firing about 25 rounds per second from a single barrel. The M61 automatic gun, Vulcan, firing up to 100 rounds per second, is a power-driven refinement of the Civil War Gatling gun, having six barrels arranged in a circle. Of the hazardous materials in the round, propellant and fuze detonator are the most critical in that they have the lowest cook-off threshold.

It is an oversimplification to think of the occurrence of cook-off as a simple function of the maximum temperature of the gun. On the other hand, the primary mechanism of cook-off is fairly well understood. Cook-off is affected by many factors: composition of propellant and explosives, firing schedule, gun age, climate, and altitude.

* This is a summary of a state-of-the-art survey compiled by The Franklin Institute under contract with Springfield Armory. It covers six-years' research and development by five Government agencies and four principal companies.

[1] Senior Staff Engineer, Applied Physics Laboratory.

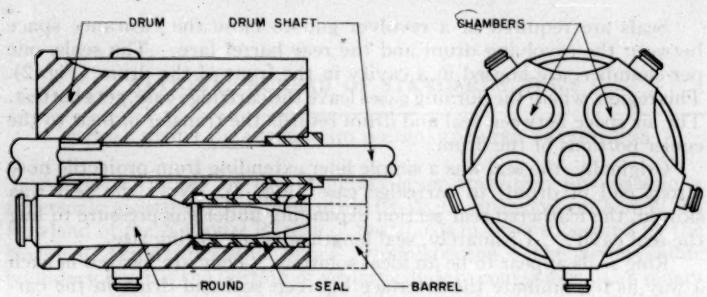

FIG. 2. In the drum of the M39A gun, the bottom chamber contains the round that is ready to fire. Each of the five chambers carries its own seal.

Three different approaches have been used to prevent cook-off: use of propellants and explosives with a high cook-off threshold; use of a device that will clear the gun; or use of some means to prevent the temperature from reaching the cook-off threshold. The first pertains to improving the high-temperature performance of explosives while the second makes use of one of the gun safety systems. Several such systems and several means for activating them were tried but found to be awkward.

Anti-cook-off systems of the third type get at the root of the trouble, heat. They either provide means for cooling the gun or for preventing excessive heat from flowing into it in the first place. While methods of blowing air over the gun or refrigerating the drum worked well, they carried with them a penalty in weight, space, cost, complexity, or difficulty in retrofit (adaption to existing weapons). During subsequent efforts in search for a simpler solution, gun seals were examined.

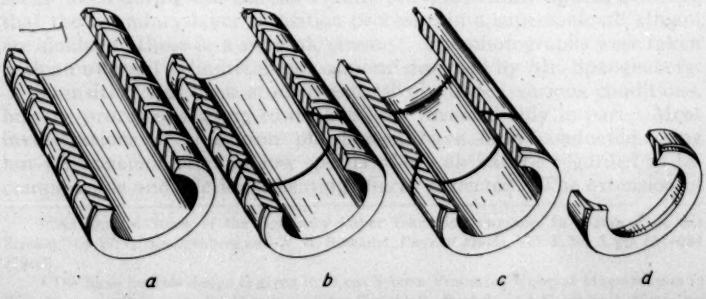

FIG. 3. The evolution of drum seals for the M39A2 is shown left to right. Ball-joint *b* improved alignment over one-piece liner *a*. Promising anti-cook-off models, full-length skirted *c* and ring *d*, make grooves unnecessary.

Seals are required in a revolver gun to close the clearance space between the revolving drum and the rear barrel face. The seals, one per chamber, are housed in a cavity in the front of the drum (Fig. 2). This region, where the burning gases leave the cartridge case, gets hottest. The air space between seal and drum retards the transfer of heat to the cooler portions of the drum.

Originally, the seal was a simple liner extending from projectile nose (front end of drum) to cartridge case (Fig. 3). Next the seal was skirted, the feathered rear section expanding under gas pressure to hug the seal cavity. Ultimately, seal length was cut to ring size.

Ring seals appear to be an ideal solution. They are located in such a way as to eliminate the interface between seal and drum in the cartridge case region so as not to hamper cooling. Because ring seals have a smaller mass than full-length seals, they have less heat capacity and, because of their smaller weight, they have less slap on the barrel face. They have eliminated drum erosion by sealing effectively against drum and barrel, both seals and drum lasting over 10,000 rounds. They permit the firing of over 400 rounds without cook-off. This ingeniously simple seal has become a standard gun part and has eliminated cook-off in the M39A2 gun.

NATIONAL BUREAU OF STANDARDS NEWS

OPTICAL STUDY OF SUPERSONIC BOUNDARY-LAYER TRANSITIONS

An optical study of the boundary-layer transition processes in a supersonic air stream[1] has been made by W. G. Spangenberg and W. R. Rowland of the National Bureau of Standards in work sponsored by the National Aeronautics and Space Administration. The aerodynamic boundary layer is the portion of air immediately contiguous to an object in an air stream. In the boundary-layer region, the velocity of the stream is affected by the presence of the object, and the frictional qualities of the air are important in determining the air flow.

In most instances of fluid flow near a smooth wall, such as the outer surface of a missile, the flow is laminar for some distance from the leading edge and then becomes turbulent because of instabilities resulting from variations in velocity throughout the boundary layer. This change of regime, called transition, increases the rate of transfer of properties such as momentum and aerodynamic heating between the wall and the stream, causing increased skin friction at all speeds and significantly increased wall temperatures at higher speeds where aerodynamic heating becomes important.

A better understanding of the physical role played by transition processes in boundary-layer behavior would aid in the design of longer-range, higher-speed aircraft and missiles. Some designs of re-entry vehicles also must take into account the heating effects of boundary layers.

Microsecond-exposure sequential schlieren photographs of transition areas taken during the Bureau's study provide definite optical evidence that the boundary-layer transition processes in a supersonic air stream are similar to those in a subsonic stream. The photographs were taken with an unusual cylindrical-lens camera[2] designed by Mr. Spangenberg.

Transition has been studied extensively under various conditions, but the processes leading to it have been revealed only in part. Most investigations of transition phenomena have been conducted using hot-wire anemometers at low speeds where air can be regarded as incompressible and frictional heating effects neglected. The extension of

[1] "An Optical Study of the Boundary Layer Transition Processes in a Supersonic Air Stream," by W. G. Spangenberg and W. R. Rowland, *Phys. of Fluids*, Vol. 3, No. 5, pp. 667–684 (1960).

[2] The basis for this design is given in "Lens System Producing Unequal Magnification in Two Mutually Perpendicular Directions," by Donald R. Buchele and Herman R. Goossens, *Rev. Sci. Inst.*, Vol. 25, No. 3, pp. 262–263 (1954).

their use to supersonic flow has been limited. Previous experiments[3] have established that in the absence of naturally large disturbances transition is initiated by the self-amplification of the small disturbances within the stream.

The localized breakdown of these disturbed regions and the subsequent growth of turbulent "spots" so clearly evident from observations at low speeds[4] have been observed sporadically at supersonic speeds, but have never been recognized as an inherent part of the transition process. The purpose of the Bureau's study was to obtain detailed information on the history of transition from laminar to turbulent flow in the boundary layer on a hollow cylindrical model in a supersonic air stream to learn whether the processes occurring at supersonic speeds are similar to those observed in low-speed flow. A particular objective of the investigation was to find whether there is any correlation between local breakdown of laminar flow to turbulent spots and the transition process.

Since use of the hot-wire anemometer in supersonic and transonic air streams[5] involved extreme difficulties, schlieren photography was utilized to determine the nature of the transition region with the hope of possibly correlating these observations with hot-wire information in the future to obtain a more detailed description of transition phenomena.

Optical System

A schlieren system can be used to view the variations in refractive index within a boundary layer which are associated with differences in frictional heating. At all supersonic speeds, these variations are sufficient to supply information pertinent to transition—a transient process of short duration.

In schlieren photographs taken with the Bureau's cylindrical-lens camera, the image of the viewed area is recorded three times full size in the vertical dimension and 3/20 full size in the 6-in. horizontal dimension. The magnification ratio of the depth of the extremely thin boundary layer to its length permits close inspection of the areas of turbulent "spot" eruption and of their movements as shown by se-

[3] "Laminar-Boundary-Layer Oscillations and Transition on a Flat Plate," by G. B. Schubauer and H. K. Skramstad, NACA Rep. 909 (1948); "Stability of a Supersonic Laminar Boundary Layer on a Flat Plate," by J. Laufer and T. Vrebalovich, Jet Prop. Lab., Cal. Inst. Tech., Rep. 20-116; (1958).

[4] "Contributions on the Mechanics of Boundary-Layer Transition," by G. B. Schubauer and P. S. Klebanoff, NACA TN 3489 (1955); "Evolution of Amplified Waves Leading to Transition in a Boundary Layer with Zero Pressure Gradient," by P. S. Klebanoff and K. D. Tidstrom, NASA TN D-195 (1959).

[5] "Turbulence in Supersonic Flow," by L. S. G. Kovasznay, *Jour. Aero. Sci.*, Vol. 20, No. 10, pp. 657–674 (Oct. 1953); "Heat-Loss Characteristics of Hot-Wire Anemometers at Various Densities in Transonic and Supersonic Flow," by W. G. Spangenberg, NACA TN 3381 (1955); "Fluctuations and Hot-Wire Anemometry in Compressible Flows," by M. V. Morkovin, AGARDograph 24, NATO Adv. Group for Aero. Res., Paris (1956).

quential photographs. The particular values of magnification were so chosen that the lens can be used with a standard camera. All the elements of the camera lens except the condensing mirror of the schlieren system are contained within a tube $2\frac{1}{4}$ in. in diamerer and about 4 ft. in length to make it easily adjustable.

Both flash and continuous light sources are provided. The schlieren image obtained using either source may be recorded by either a standard camera or with a 20:1 magnification ratio by the cylindrical-lens camera. The light source and the camera are selected through the use of auxiliary prisms.

The spark light source for the flash photographs is installed in duplicate so that two independent pictures of the test section may be taken in rapid sequence. Knowing the time delay (as measured with a rotating-mirror camera designed by the Bureau) between two sequential photographs, one can compute the velocity, growth rate, and frequency of turbulent spots. The continuous arc light source and the standard camera aid in visual examination of the transition region.

The effect of refraction of light passing through the boundary layers on the test section windows is prominent in spark photographs taken with a standard camera-lens combination and detracts from their quality. Direct photography of the boundary layer on the test body with the cylindrical-lens camera produces pictures that are not so adversely affected by this refraction because the depth of focus of this lens in the magnified plane is only a small fraction of the width of the tunnel.

Results

Results of the Bureau's study show that transition in a supersonic stream starts with high-frequency disturbances in the laminar boundary layer which degenerate into areas of turbulent flow. These "spots" of turbulence erupt independently near the trailing face of the turbulent flow region, which is constantly moving downstream. The addition of newly turbulent areas of finite size to the trailing face of the region causes it to jump upstream discontinuously. These spots are traveling at about 0.25 to 0.5 free-stream velocity at the time that they first become visible, and as they continue downstream accelerate to a velocity about 0.7 free-stream speed at their trailing face.

The origin of fresh areas of breakdown to turbulence apparently is in amplified Tollmein-Schlichting waves. Turbulent spots are most frequently produced within the region in which one can predict, using stability theory, that disturbances within the boundary layer will be amplified. It can be concluded from these results that transition mechanisms in supersonic flow are similar to those in a subsonic air stream.

Continuously-Operating Optical Maser.—The first continuously operating optical maser—a device potentially capable of carrying vast numbers of telephone calls and television programs—has been demonstrated by Bell Telephone Laboratories.

The new optical maser, operating on less power than an ordinary light bulb, continuously generates a coherent beam of infrared light. This beam, several hundred thousand times narrower in frequency, or purer in color, than any other coherent light source, promises to be one of the most efficient information carriers ever conceived.

Even with existing communication techniques, large amounts of information can be carried by the beam. With improved techniques under investigation, its capacity could be increased many, many times.

In addition, the new maser will provide scientists with a powerful tool for the study of the atom and its structure.

The optical gas maser—an approach to light amplification entirely different from solid state masers—was the result of a "planned scientific discovery." It was invented by Bell scientist, A. Javan, and described in a scientific publication in July, 1959. W. R. Bennett, Jr., and Donald R. Herriott collaborated with Mr. Javan in the development of this proposal which led to the device Bell demonstrated recently.

The new maser uses a mixture of helium and neon gas to achieve continuous operation. Previous optical masers—built around crystals—required thousands, even millions of watts of power to transmit large bursts of visible light of very short duration.

The term "maser" is an acronym for "microwave amplification by simulated emission of radiation." Basically, a maser is a highly effective device for amplifying electromagnetic waves like light and radio signals.

Light waves vibrate millions of times faster than radio waves. Because these "optical" frequencies are so high, light beams should be capable of handling enormous amounts of information—telephone calls, TV programs, data messages . . . by the millions.

But the light must be coherent. It is the coherence of radio waves, for example, that enables them to carry voice, music, television and other forms of intelligence efficiently. Radio waves move like disciplined soldiers and can be controlled, directed and made to carry information. Ordinary light waves—the kind thrown off by light bulbs—are highly incoherent and move like an unruly mob.

Bell Laboratories' maser brings communication systems that can exploit the fantastic data-handling capabilities of coherent light a giant step closer to realization. It has already carried messages. On December 14, 1960, scientists responsible for the maser's development first succeeded in impressing a voice signal on the infrared beam.

This beam—of an almost absolutely pure color—was slightly under one-half an inch wide. It is so directional that if aimed at a wall one mile away, it would show up as a spot of light only a foot in diameter. With a suitable telescope used as an antenna,

the spot would be only one-foot wide even 100 miles away.

Bell scientists visualize the possibility of using the gas maser for communications through outer space, between air and space craft and—on the ground—through long pipes or conduits.

Applying the gas maser to communications is actually an important by-product of an achievement that provides scientists with a remarkably precise tool for investigating atomic structure. Since the gas maser generates a light beam several hundred thousand times narrower in frequency than heretofore available, scientists will be able to study the atom in much greater detail.

From a scientific point of view, one of the outstanding accomplishments made possible for the first time by the new optical maser was the extraction of radio signals from the difference between two light waves.

The maser also will allow precise measurement of distance over many miles, with accuracies unobtainable by older techniques.

The principles of optical masers were described by A. L. Schawlow of Bell Laboratories and Professor C. H. Townes of Columbia University as early as 1958. During the year 1960, Bell Laboratories and a number of other research organizations introduced optical masers made of crystalline solids.

All of these, however, are so far capable of only pulse-type operation at huge expenditures of power. They are sometimes called "brute force masers."

Since the optical maser under discussion used a radically new approach to light generation, considerable time was spent working out the complex physical principles underlying the gas maser, and on the exact structural form the device would take. When the completed maser was plugged in—literally—it performed precisely as predicted.

In greatly simplified terms, the gas maser achieves its effect through interactions between helium and neon atoms enclosed in a glass tube about 40 inches long.

The helium atoms are excited to a highly energetic state by a continuous electrical discharge at radio frequencies. The excited helium atoms transfer their energy to the neon atoms by colliding with them. The neon atoms, now "stimulated," radiate this energy —on demand—as a highly coherent stream of infrared light.

The invention of Bell Laboratories' gas maser has opened up a new era of research in gas discharges. It is expected that within the next few years, large numbers of scientists will exploit other maser possibilities in this field.

Self-Regulating, Solid-State Data-Processing System.—Burroughs Corporation has announced a new solid-state electronic information processing system—a self-regulating, problem-oriented data-processing system that makes flexible multi-processing and system expansion without reprogramming practical for the first time.

Departing from traditional concepts of electronic computer design, the system—called the B5000—is the first computer designed especially for automatic programming.

Ray R. Eppert, Burroughs president, said the medium-priced system will provide large-scale performance for both business and scientific problems "with an ease of operation some computer experts predicted would not be forthcoming for another decade."

In spite of their sometimes spectacular progress, computers have en-

countered some special problems of their own creation. Chief among these have been the difficulties of man-machine communication and the inefficient use of high-speed electronic systems capabilities.

For example, it has been difficult, if not impossible, accurately to assess the time and costs of initial programming requirements. It has been even harder to predict the costs of reprogramming if a system was expanded or changed. The object of the new system is to solve problems without creating even bigger ones.

The B5000, like other large-scale electronic systems, is fast (execution time for the add operation is three microseconds or more than 250,000 additions per second), but Burroughs designers have found a way to use this speed efficiently and close the communications gap at the same time. They developed the hardware and "software"—automatic programming and operating systems—concurrently, making sure that the software should help dictate equipment specifications.

The result was a problem-oriented system, operating in common algebraic and business languages, so that high speed computations would no longer be preceded by painfully slow computer programming, problem translation and debugging.

A complete "software" package—including ALGOL (Algorithmic Language) and COBOL (Common Business Oriented Language) compilers, as well as powerful extensions of each, and a *comprehensive* master control program—will be standard with each system, the Burroughs executive said.

This will enable users to communicate efficiently with the machine in the language of the problem, both for initial programming and subsequent symbolic debugging, rather than in complex numerical codes. Efficient object machine language programs will be compiled automatically 20 to 50 times faster than the most advanced automatic programming techniques employed thus far on conventional computers.

The master control program will permit maximum, efficient operation with minimum human intervention. Virtually self-regulating, the system schedules and keeps track of its own workload, automatically by-passes certain units if they malfunction, and advises its operator when he makes a mistake, Eppert declared.

The computer automatically performs diagnostic maintenance routines to assure maximum up-time—either during processing or at the conclusion of all processing.

For the first time, users will be spared the massive and costly job of re-programming when a system is expanded or changed. Any size program can be run on any B5000 system. The no re-programming feature will also make it possible for computer users to exchange programs as well as ideas—a goal long sought by computer organizations.

Multi-processing—the key to maximum use of all elements of the system—will not only be possible, but practical. Any two or more completely independent programs can be run simultaneously.

Additional features which contribute to the B5000's efficient operation are: the ability of the processor to operate in fixed-point (integer) and exponential (floating-point) representation interchangeably; the facility of the system to operate in either word-length or in individual character logic modes; and generalized, flexible subroutine handling abilities. These features, in particular, permit processing of both scientific and data-processing problems with equal facility.

Programs and data are completely independent of memory location within the processor and are automatically segmented during compilation into logical divisions. Thus, the system can efficiently accommodate programs which exceed the core memory capacity of a particular hardware configuration as well as process several programs simultaneously.

In summary, the Burroughs president declared, the B5000 represents a new total systems approach that will (1) permit easier, faster and far less costly programming; (2) result in higher productivity because of its new standard of automatic operation; (3) make multiple and parallel processing of independent programs practical for the first time, and (4) permit expansion or contraction of a system without reprogramming through a new concept of program-independent modularity.

Distillation Process for De-Salting Sea Water.—Tests recently completed at General Electric Company prove the "thorough feasibility" of a radical new distillation process for desalting sea water. The new system has as one of its key features an assembly of revolving blades which operate much like an automobile's windshield wipers. Also unusual is vaporization of the water without either boiling or bubbling.

G. E. said more than 1,000 hours of tests, including one continuous run of approximately 130 hours, at its General Engineering Laboratory in Schenectady, demonstrate the system can extract high volumes of pure water from the sea. The fresh water produced is salt-free to within one part of salt per million parts of water.

More than 175,000 gallons of sea water used in the tests were trucked 200 miles to the engineering laboratory from Rockport, Mass.

The tests were conducted at the direction of the Company's operation in Burlington, Vt., under contract with the Navy's Bureau of Ships and the Department of Interior's Office of Saline Water.

The system's clean tube heat-transfer rate, a critical factor in the process, is at least four times higher than that achieved by any other distillation unit now in commercial use, the Company said.

How to transfer heat from its source in the system to where it is used for evaporation—without large heat loss—has been a difficult problem in the distillation approach to salt water purification, it was explained.

Boiling of the salt water, which could seriously diminish purity, has been eliminated—due to the fact that the films of water spread by the revolving wipers are so thin they will not support bubble formation. The bubble-free distillation produces fresh water of exceptionally high purity by avoiding carry-over of mineral particles.

The system can extract 42 lb. of fresh water from each 100 lb. of sea water used. It is applicable to salt, brackish, or polluted water.

The evaporator in the system consists of two vertical tubes, one inside the other. Sea water is fed into the wiper assembly where the slowly revolving blades spread the salt water on the inner surface of the inside tube in a film scarcely one-thousandth of an inch thick.

Heat, produced by steam, is transferred through the walls of the inside tube—causing the salt water to evaporate. Pure water leaves the evaporating chamber as vapor, and the concentrated brine is drained off.

Most of the Company's develop-

ment work up to now has been slanted to marine needs for fresh water—in which it is believed the new system may offer a 60 per cent space saving and a 40 per cent weight saving, over conventional systems.

Other application possibilities, G.E. said, seem limited only by the world's needs for fresh water. For non-marine use, the Company added, the system could be designed with low-cost operation as the key feature.

Nuclear Generator Converts Heat Directly into Electrical Power.—A new lightweight nuclear generator which converts heat directly into electrical power is undergoing performance testing at the Air Research and Development Command's Air Force Special Weapons Center in Albuquerque, New Mexico.

The completely portable nuclear auxiliary power device, which weighs considerably less than 40 lb., was designed and constructed by the Westinghouse New Products Laboratory in Pittsburgh, Pennsylvania.

It was developed under Air Force contract to provide a reliable and long-life power source for facilities such as small unmanned surface radio beacons and weather stations.

The generator produces approximately 150 watts of electrical power and was designed for one year of continuous unattended operation. It is designed to use radioactive isotopes, such as Curium 242 as its heat source. The generator's 144 small semi-conductive elements are heated by the heat source to a temperature of about 1,000 degrees F. Finned heat exchangers, which cover the generator like the quills on a porcupine, keep the ends of the elements farthest from the heat source at a temperature of 300 degrees F. This temperature difference produces a flow of electrical current in the elements.

Only 10 in. high, with a diameter of 16 in., the generator has the highest efficiency of any direct-conversion electrical power device of comparable size. It also produces more power per pound of generator weight than any similar device.

Designated the NAP-100, it is another step in a series of developments by the Air Research and Development Command which will lead to increasing Air Force utilization of thermoelectric devices for converting nuclear energy directly into electrical power. Such devices are dependable and durable. They have no moveable parts, are easy to install and require a minimum of maintenance.

"Speed-of-Light" Computer Circuitry.—Basic circuitry operating at speeds approaching that of light has been devised by the Radio Corporation of America as the first big step toward an ultra swift electronic computer for the U. S. Navy.

"The new circuitry can do its job 100 times faster than any system in existence and up to 1,000 times faster than the circuits in most-data processors now in use," Donald H. Kunsman, Vice President and General Manager, RCA Electronic Data Processing Division, announced. "This means electronic action can take place at a pace approximating 186,300 miles per second—the speed of light."

This major advance in computer circuitry design was achieved through use of the tiny tunnel diode. The new circuitry is a part of a development program sponsored by the Navy Bureau of Ships looking toward ultra high speed computer systems of the future of truly miniature size and unbelievable speeds.

The tunnel diodes employed in the

RCA circuitry design are solid state devices no larger than a small pill. They were developed through the joint efforts of the RCA David Sarnoff Research Center at Princeton, New Jersey, and the RCA Semiconductor and Materials Division, Somerville, New Jersey. The Research Center also developed the basic concepts for the circuitry design portion of the project.

In approaching the operating limits imposed by the speed of light, the new circuitry will have the capability of handling problems too complex for solution within a reasonable time under previous techniques. The end result will be a broadening of electronic computer applications, with an accompanying impact on industry, science and defense.

Inter-Computer Magnetic Tape Conversion Equipment.—A family of magnetic tape translation devices has been developed to provide computers with lower-cost on-line input conversion of foreign tape formats and signals. Auerbach Electronics Corporation, Philadelphia, has developed custom equipment, highly tailored to the needs of individual computers and tape transports.

The Auerbach approach is to translate tapes by making use of the reading computer's ability to edit the information, converting pulse shapes, format, and timing into a form exactly equal to that normally supplied by the computer's own magnetic tape readers. The computer edits the information by means of a special routine which transforms the symbols into meaningful language.

A sizeable group of computers has been analyzed to be coupled with such tape transports as Uniservo II, IBM 727 and 729, Ampex FR-300, and others.

World's Mightiest Radio Station.—What will be the world's mightiest radio station, broadcasting with 40 times the power of any existing commercial broadcasting installation, is being outfitted by Republic Steel Corporation with special stainless steel grading or corona rings, believed to be the largest ever fabricated, for use on antenna insulator strings. This station is now being erected on a peninsula on Machias Bay, Maine, for the U. S. Naval Communications System, as a component of the Polaris FBM System.

The antenna system of the station consists of 26 supporting towers interconnected by a virtual spider web of antennae. Each antenna panel is insulated and supported from the towers at each of four points by a chain of insulator links 74 in. long. In turn each of these long strings of porcelain insulators is fitted with a pair of the giant grading rings; the rings with supporting frame work for attaching to the ends of the insularor strings straddle the insulating units like funnels strung on a washline. The rings form a safe gradient for 400,000 volts so that the station's power is not dissipated in corona losses or arcing.

Looking like frames for mammoth funnels, the grading rings are fabricated in two sizes from Republic Steel's stainless steel tubing to give the needed non-magnetic properties, strength and corrosion resistance to salt sea air.

The larger of the two corona rings has a 20-ft. diameter mouth pyramided to a steel plate at the other end by six 15-ft. legs. The smaller of the two rings is similar in construction with a 15-ft. diameter mouth. The open end of the rings is made from Type 304 4-½-inch O.D., 0.165-inch wall stainless steel tubing in three sections. Three attachment fittings

to which turnbuckles and legs are attached are welded to each section of the tubular circle. The end of each section is flared for the insertion of a section of the circle to the next.

Completed, a ring is mounted at each end of every insulator string requiring some 96 corona rings in all. The mouth ends of the rings face each other on the insulator string and are fastened to the insulator links by six shielded barrel turnbuckles. The insulators are necessarily located close to the towers where the voltage gradient is the greatest and where corona losses and arcing would certainly occur if the grading rings were not used.

The antennae are spread out in two arrays, each having a center tower 980 ft. high, an inner circle of six towers 875 ft. high and an outer circle of six towers 800 ft. high. The two antenna arrays that link these towers cover an area of more than 1200 acres. The towers were fabricated by Republic Steel's Truscon Division, Youngstown, Ohio.

Generally, the station will broadcast with an input power of two million watts. The power house will be able to generate 12 million watts so that deicing operations may be carried on simultaneously with the powerful Very Low Frequency transmission. When completed early next year, the station will be capable of sending signals throughout the world as well as to our submarines anywhere under the sea.

New Environment Simulator.—A 240-cu.-ft. environment test chamber which can simulate the living conditions encountered by human occupants of submarines and space vehicles, was demonstrated recently by Ionics, Incorporated, Cambridge, Mass. The firm is best known for its development of electric membrane plants for water desalting and other industrial applications.

Shown to the public for the first time at the annual meeting of American Research and Development Corporation, the environment control simulator will be used in the design and testing of life support equipment now being developed by the company under government contract and on its own sponsorship.

According to Wayne A. McRae, Ionics' vice president of research, medical and technical personnel will be sealed in the chamber for periods of several days or weeks. They will evaluate, under simulated operating conditions, the effectiveness of various components which remove waste carbon dioxide from the atmosphere, generate life-giving oxygen and reclaim pure water from waste water in a closed system.

Tests will be conducted under the direction of Ionics' medical director, Dr. Leonard W. Cronkhite, Jr., of Massachusetts General Hospital. During the initial tests, the only utility to be supplied from outside the chamber will be electric power. Later, Ionics plans to install one of its newly-developed fuel cells to generate needed power within the chamber.

Initially, a solid state electrolytic device which removes carbon dioxide from air and generates oxygen has been installed in the chamber for thorough performance evaluation. This new device is gravity-independent and is potentially useful in manned space vehicles and possibly submarines.